VS-99-007
JANUARY 1999
M8A01
REVISED

Sponsor: Mr. J. R. Ryan
Air Transport Association
1301 Pennsylvania Avenue N.W. #1100
Washington, DC 20004-1707

GPS RISK ASSESSMENT STUDY

FINAL REPORT

THE JOHNS HOPKINS UNIVERSITY • APPLIED PHYSICS LABORATORY
11100 Johns Hopkins Road, Laurel, Maryland 20723-6099

Operating Under Contract 98-JHU-01 With the Air Transport Association

VS-99-007
JANUARY 1999
REVISED

GPS RISK ASSESSMENT STUDY

FINAL REPORT

By: T. M. Corrigan
J. F. Hartranft
L. J. Levy
K. E. Parker
J. E. Pritchett
A. J. Pue
S. Pullen (consultant)
T. Thompson

99-018

THE JOHNS HOPKINS UNIVERSITY • APPLIED PHYSICS LABORATORY
11100 Johns Hopkins Road, Laurel, Maryland 20723-6099
Operating Under Contract 98-JHU-01 With the Air Transport Association

ABSTRACT

The Federal Aviation Administration (FAA) has initiated plans to transition from its present ground-based navigation and landing system to a satellite-based system using signals provided by the Department of Defense's Global Positioning System (GPS). However, GPS alone will not meet all aviation positioning requirements. To meet the National Airspace System (NAS) requirements, the FAA has proposed two augmentations to GPS: a Wide Area Augmentation System (WAAS) and a Local Area Augmentation System (LAAS). There have been expressions of concern regarding the robustness of this plan and whether the risks to dependence upon GPS have been adequately addressed. In response to this concern, the FAA, with co-sponsorship from the Air Transport Association (ATA) and the Aircraft Owners and Pilots Association (AOPA), issued a request for an impartial study. The Johns Hopkins University Applied Physics Laboratory (JHU/APL) was selected to conduct that study, which is the subject of this report.

The report quantifies the ability of GPS, GPS/WAAS, and GPS/LAAS to satisfy Required Navigation Performance (RNP) as expressed by accuracy, integrity, continuity, and availability requirements. Additional navigation options that mitigate the identified risks were also evaluated. In particular, these options included potential improvements to the GPS Standard Positioning Service (SPS) and additional capabilities onboard the aircraft such as integration of additional sensors and application of GPS anti-jam technologies.

KEYWORDS: National Airspace System
Global Positioning System
Navigation

TABLE OF CONTENTS

CLICK ON THE ITEM IN THIS TABLE OF CONTENTS THAT YOU WANT TO READ ABOUT

TABLE OF CONTENTS (Continued)

LIST OF ILLUSTRATIONS

LIST OF TABLES

EXECUTIVE SUMMARY

ES.1 PERFORMANCE

An independent risk assessment was conducted by the Johns Hopkins University Applied Physics Laboratory (JHU/APL) to determine if the Global Positioning System (GPS) and augmented GPS can satisfy the performance requirements to be the only navigation system installed in an aircraft and the only service provided by the Federal Aviation Administration (FAA) for operations anywhere in the National Airspace System (NAS). This report quantifies the ability of GPS, GPS with the Local Area Augmentation System (LAAS), and GPS with the Wide-Area Augmentation System (WAAS) to satisfy navigation performance requirements as expressed by accuracy, integrity, continuity, and availability requirements. Oceanic through Category III Precision Approach operations were evaluated with risks that present both normal and abnormal degrees of performance degradations. The primary conclusion is that GPS must be augmented to meet these requirements and that WAAS/LAAS can provide the required navigation performance. The study considered all known risks and its primary conclusion assumes the identified mitigation actions are instituted, and specific WAAS/LAAS configurations are implemented. The main conclusions of the study are as follows:

a. GPS with appropriate WAAS/LAAS configurations can satisfy the required navigation performance as the only navigation system installed in the aircraft and the only navigation service provided by the FAA.

b. Risks to GPS signal reception can be managed, but steps must be taken to minimize the effects of intentional interference.

c. A definitive national GPS plan and management commitment is needed to establish system improvements with civil aviation users and to provide greater informational access to the civil aviation community.

In particular, the final conclusion points to the need to develop a combined GPS and augmentations system design based on cost and performance trades among GPS system improvements, GPS operational policies, and WAAS/LAAS capabilities. Study findings with regard to the three system configurations considered are summarized in the following subsections.

ES.1.1 SATELLITE CONSTELLATIONS

Currently, 27 GPS satellites are operating. They provide the minimum basic configuration of 24 satellites (6 orbit planes of 4 satellites each) and 3 active on-orbit spares. The number of operating satellites could slip to 24 before additional replacements are added. In this study, the current constellation is assumed to be the nominal basic 24-satellite constellation (i.e., 6 by 4). The next logical extension of this geometry would be a 30-satellite constellation (i.e., 6 by 5), and that geometry was considered to represent an expanded GPS constellation that might practically be implemented.

The current GPS/WAAS test configuration is based on the current GPS constellation supported by two geostationary satellites (GEOS). Therefore, the base constellation for GPS/WAAS analysis was 24 GPS satellites and the current 2 GEOS. Improvements considered expansions up to five GEOS. GPS/LAAS analyses were based on the minimum acceptable GPS/WAAS configuration—a 24-satellite and a 30-satellite GPS constellation. Airport pseudolites (APLs) were also included to improve local geometry.

ES.1.2 GPS WITHOUT AUGMENTATION

A 24-satellite GPS constellation without augmentation cannot meet oceanic, en route, terminal, and nonprecision approach service requirements of the NAS. The removal of selective availability and/or the addition of a second civil frequency did not alter this finding. The best performance was achieved with a 30-satellite constellation (with selective availability off and a second civil frequency available), and even that configuration met the required levels of service for only oceanic navigation.

ES.1.3 GPS/WAAS

A GPS/WAAS configuration with 24 GPS satellites and 4 GEOS can satisfy all NAS positioning requirements from oceanic through Category I approach. This result did not require any specific improvements to the GPS satellites. Performance is sensitive to the ionospheric correction methods and further analysis is recommended to better optimize the WAAS configuration (i.e., number of GEOS and number of ground stations). It must also be noted that the current GEOS establishment and replacement plan is not yet clearly identified; this plan must be defined to ensure the required capabilities are provided.

ES.1.4 GPS/LAAS

A GPS/LAAS configuration based on a 30-satellite GPS constellation or one with 24 GPS satellites and 4 GEOS can satisfy all precision approach requirements. Some airports will require ground transmitters that act like additional GPS satellites (APLs) and/or improved GPS antennas and extra receivers to achieve the highest availability levels (i.e., >0.99999). This level of performance will require no GPS satellite improvements.

ES.1.5 PENDING GPS SIGNAL IMPROVEMENTS

Because the current augmentation designs are responsive to the current GPS satellite signal conditions, the removal of selective availability and the addition of a second civil frequency did not have a major impact on the cases analyzed for this study. However, the pending GPS signal improvements are very important to system robustness and to eventual cost savings and/or performance improvements of the final system.

Removal of selective availability greatly reduces the information rate required for the corrections provided by WAAS and LAAS, which reduces the communications burden. More importantly, removal of selective availability could allow the system to maintain acceptable performance even with a brief interruption of communications. With GPS/LAAS, for example, the corrections provided at the start of an approach would be valid throughout the approach.

As announced by Vice President Al Gore in March 1998, the secondary military frequency (1227.6 MHz) would have an added signal modulation that could be used for civil applications. However, the second frequency referred to in this report is required to be in a portion of the spectrum that is internationally allocated for aeronautical radio-navigation services. A White House press release on 25 January 1999 announced that agreement has now been reached on the addition of a new GPS frequency (1176.45 MHz) that will provide the second frequency capability needed to serve the NAS requirements.

The impact of the second civil frequency will completely remove the requirement for ionospheric corrections for users equipped to take advantage of this feature, and it will improve the corrections provided by WAAS. If, at some future time, the full community were to shift to dual-frequency user equipment, the WAAS ground station requirements could be reduced significantly. The density of WAAS reference stations required for ionospheric correction is greater than that required for orbit determination or for integrity monitoring. Furthermore, the second civil frequency, and the proposed higher signal power, will mitigate interference concerns.

ES.2 RISKS

The only risks that proved significant are interference (unintentional and intentional) and ionospheric propagation effects (high sunspot cycle and scintillation); these risks are discussed in the following subsections.

ES.2.1 UNINTENTIONAL INTERFERENCE

Although there have been few reports of GPS receiver interference from the many Government and commercial transmitters currently operating in the NAS, a review of interference sources identified in RTCA DO-235 indicates that several have the potential for GPS signal disruption. Three potential interference sources were singled out for further analysis. The first and potentially most serious one is television broadcast. The current Federal Communications Commission (FCC) specifications allow out-of-band emissions of sufficiently high levels to interfere with GPS signal reception. A simulation effort, undertaken to evaluate television emissions, indicated that stations transmitting on channel 23 within line of sight of aircraft approach paths could readily deny GPS signal reception. However, this threat is easily managed by modifying television broadcast regulations to exclude unacceptable power levels in satellite radio-navigation bands, by testing for interference when FAA instrument approaches are first established, and by adding filtering to the television transmitter output that are found to interfere with GPS reception.

The second area of concern is commercial very high frequency (VHF) broadcast (e.g., taxi dispatch). The levels of power and typical antenna configurations restrict this threat to small regions near runways. VHF broadcast interference would also be managed by the same measures indicated for television broadcast.

The third possible threat is from over-the-horizon (OTH) military radar. OTH radar interference was not analyzed because insufficient information was available during this study. This threat is very restricted with regard to number and geography; therefore, it is not expected to be a significant risk. However, it is recommended that this emission source be further reviewed to ensure the risk is truly insignificant.

In summary, unintentional interference is not a major risk factor. Most interference difficulties reported by the aircraft community thus far have been the result of onboard interference, which is necessarily resolved during certification. While it is not possible to rule out future interference from offboard emitters, remedying such problems should not be difficult. The introduction of a second civil frequency will further reduce concerns about unintentional interference. Furthermore, the actions required to counter intentional interference will readily address this risk.

ES.2.2 INTENTIONAL INTERFERENCE

Intentional interference is by far the largest risk area; however, the planned avionics are designed to quickly recognize the onset of this threat. Assuming that sufficient resources are available to vector aircraft away from jammed regions, this threat will pose no safety risk. It can, however, create considerable disruption in traffic control and flight schedules. Methods to detect, locate, and prosecute those who intentionally jam GPS signals must be put in place to discourage such activities. Air traffic control procedures must also be established to manage affected aircraft. The study concludes that there is no credible spoofing threat and that, although real, jamming threats can be managed.

Further refinements of this analysis need to be based on specific threat definitions. The study was based on a threat the study team judged to be plausible with regard to economic and motivational characteristics. It is strongly recommended that the Department of Transportation (DOT), in cooperation with the intelligence community, establish specific threat definitions as a basis for further analysis.

Technologies are emerging that can greatly reduce vulnerability to GPS signal jamming. Techniques that can add 40 to 50 dB of additional rejection are possible; inclusion of such capabilities would virtually defeat the jamming threat considered in this study.

ES.2.3 LARGE IONOSPHERIC REFRACTION ERRORS

Considerable concern has been expressed about the impact of increased ionospheric refraction errors caused by spatial gradients during peaks of the sunspot cycle. A reasonable model of the ionosphere was created to evaluate this effect. It was found that errors produced did not significantly alter system performance for GPS only or LAAS, but did significantly degrade WAAS. It is important to note that the WAAS results regarding the larger ionospheric errors are sensitive to the ionospheric correction methodology. According to the definitions of the hazard risk index, its risk frequency is classified as "reasonably probable" and its consequence was considered "major" because of possible safety implications. With these classifications, the risk was determined to be "undesirable." This risk can be mitigated by increasing the density of the wide-area reference sites (WRSs) and/or grid points, as well as improving the ionospheric correction algorithm. This area of WAAS ionospheric correction methodology should receive further analysis, but it is JHU/APL's judgement that the WAAS configuration can be designed to meet the needed performance so that risk becomes "acceptable." However, note that when the second civil frequency becomes available, the risk is eliminated.

ES.2.4 IONOSPHERIC SCINTILLATION

Ionospheric scintillation is most severe in equatorial regions and in the auroral region. The most likely means by which ionospheric scintillation affects GPS users in the Continental United States (CONUS) is in viewing GPS satellites through these regions. The auroral region covers the northern part of Canada between 65° and 72° N *geomagnetic* latitude, and the equatorial region covers zones at 15° ± 10° N and at 15° ± 10° S geomagnetic latitude. Only the northern equatorial zone is seen from the United States and only by two of the locations included in the study.

A conservative model was used to test the overall impact of including this effect in the normal system availability analysis. Its impact was to drop the availability below requirements at a few locations. Therefore, ionospheric scintillation must be considered as a risk factor. According to the definitions of the hazard risk index, its risk frequency is classified as "reasonably probable" and its effect was judged to be "minor." With these classifications, the risk is determined to be "acceptable" with FAA approval.

ES.3 RECOMMENDATIONS

The following subsections offer recommendations in three areas: GPS, WAAS/LAAS, and risk mitigation.

ES.3.1 GPS

If civil aviation is to rely on GPS, greater access, cooperation, and agreement must exist on GPS operational control segment (OCS) procedures and future system performance. Specifically, the following must be addressed:

a. GPS operational procedures that support civil aviation policy need to be defined and implemented (e.g., signal monitoring, orbit management, and end-of-life operation and replacement strategies).

b. A means to convey full knowledge of failure rates and mechanisms that are essential to intelligent system design and operations must be established.

c. A process for Department of Defense (DOD) and DOT data collection and analysis must be established and sustained to characterize system performance and resolve incident reports (including international reports).

d. GPS specifications that reflect actual system performance and operational policies should be developed.

e. GPS coverage is currently limited by prediction of receiver autonomous integrity monitoring (RAIM) availability; current approaches are overly conservative by assuming all satellite failures are soft failures; and current algorithms are limited to "snapshot" position computations. These restrictions tend to increase reliance on the number of in-view satellites. Improvements to RAIM algorithms should be evaluated for possible cost reduction opportunities or performance improvements in the augmentation system structure.

These recommendations will allow sensible cost and performance trades between possible GPS system improvements and the implementation and operation of the augmentations supporting civil aviation. In support of these augmentations and to benefit the full domain of civil applications, a need exists to clearly define a national GPS plan that includes the following:

a. Establish a firm agreement on the size and characteristics of the satellite constellation and signal structures that will be maintained for all navigation services.

b. Specify the timetable for planned improvements (e.g., removal of selective availability and providing the second civil frequency).

ES.3.2 WAAS/LAAS

The following GPS/WAAS actions should also be taken to support development of a national GPS plan:

a. Establish the size and characteristics of the GEOS constellation that will be maintained to support civil aviation requirements. The plan will allow for the WAAS configuration to sensibly evolve and adapt in response to the availability of GPS satellite improvements. This study concluded that four GEOS are required to augment the current GPS satellite capabilities.

b. Further analyze, design, and validate the ionospheric correction methodology to support sizing of the ground reference station requirements and mitigation of the ionospheric risks discussed previously. Analyze possible robust receiver designs for mitigation of scintillation effects. Validate both analyses using National Satellite Test Bed (NTSB) and Phase 1 WRS data.

ES.3.3 INTERFERENCE RISKS

The following recommendations are directed at interference risks:

a. Develop regulations for all licensed transmitters that explicitly limit radio frequency (RF) emissions at satellite radio-navigation frequencies.

b. Require compliance monitoring of potential sources of satellite radio-navigation interference after maintenance or new construction.

c. Ensure that interference levels at satellite radio-navigation frequencies are measured during flight inspections at airports where GPS approaches are planned and where a potential unintentional interference threat exists.

d. Derive a DOT-authorized threat definition to support design of mitigation actions for intentional GPS signal interference.

e. Implement enforcement measures to discourage and remedy potential threats. Threat detection might be part of standard user aircraft reporting structure, but a separate airborne platform will be needed to locate the threat(s). This activity should naturally be coordinated with law enforcement agencies.

f. Develop traffic control procedures and provide training to overcome wide-area GPS signal outage caused by intentional interference.

g. Develop standards for onboard interference suppression system performance that address postulated threat(s), aircraft types, and postulated traffic control procedures.

h. Obtain measurements of underbody aircraft antenna gain and assess advantages of antenna locations to determine antenna pattern benefits.

i. Evaluate additional means for aircraft-based interference suppression. These might include antenna nulling and signal processing techniques and integration with inertial navigation instrumentation.

j. Review the risk of interference from military OTH radar.

ES.4 LIMITATIONS

The conclusions and recommendations offered here represent sound engineering judgements that are backed by considerable analysis. The timeframe for this study required that certain approximations be made in lieu of comprehensive simulations. The study results are believed to be conservative; margins were applied in those areas where the models and/or data sources were limited. The following limitations should be noted:

a. All performance analyses were based on snapshot measurement error statistics for an array of distributed geographic locations sampled every 5 min throughout one repeat cycle of the GPS constellation (i.e., one sidereal day). While this approach is believed adequate to estimate aggregate performance, verification of performance should be based on higher fidelity trajectory simulation.

b. Full aircraft trajectory simulations were restricted to evaluating interference effects using typical landing conditions with an antenna pattern derived from limited data sources. The television interference model was necessarily based on a very small data set.

c. No data were available to characterize high-definition television interference levels at the GPS frequencies.

d. Although the receiver model used to support this study is believed to be a good representation of typical receivers, the study did not explicitly account for actual receiver performance differences that may exist among users.

e. GPS/WAAS performance estimates were based on making adjustments to models derived from NSTB data. No detailed simulation was constructed for this analysis.

f. The ionospheric scintillation model used for this study was simplified, but the model used is believed to conservatively bound reality.

g. Time-to-alert analyses could not be explicitly included within the simulation structure used for these studies. The augmentation system's ability to meet these requirements was based on evaluations of the system design constraints provided by current descriptions and specifications.

Section 1

INTRODUCTION

The Federal Aviation Administration (FAA) has initiated plans to transition from its present ground-based navigation and landing system to a satellite-based system using signals generated by the Department of Defense's (DOD's) Global Positioning System (GPS). However, GPS will not meet all aviation positioning requirements. In particular, the requirement to be available virtually all of the time and to support precision landings will not be met with GPS alone. To meet the National Airspace System (NAS) requirements, the FAA has proposed two augmentations to GPS: a Wide Area Augmentation System (WAAS) and a Local Area Augmentation System (LAAS). GPS/WAAS is intended to support navigation for all phases of flight from oceanic through Category I precision approaches. GPS/LAAS is intended to support Category II and III precision approach requirements and to provide higher availability for Category I than the GPS/WAAS. However, concern has been expressed regarding the robustness of this plan and whether the risks to dependence on GPS have been adequately addressed. In response to this concern, the FAA, with co-sponsorship from the Air Transport Association (ATA) and the Aircraft Owners and Pilots Association (AOPA), issued a request for an impartial study. The Johns Hopkins University Applied Physics Laboratory (JHU/APL) was selected to conduct this study, which is the subject of this report.

The study was completed in 6 months using skilled JHU/APL investigators teamed with some uniquely qualified individuals from Stanford University, supported by an experienced panel of reviewers from industry, academia, and Government. The independent risk assessment was conducted to specifically determine if GPS and augmented GPS could be relied on to meet all navigation requirements within the NAS. The evaluation relied heavily on simulation analyses to assess performance of GPS, GPS/WAAS, and GPS/LAAS against requirements, and, thus, development of mathematical models was a key element of the study. Generally, models were based on historical data in those cases in which the team judged the data to be the best source. In cases in which data were lacking, specification values were applied. The developed simulation tools were also used to assess how major system parameters [e.g., number of geostationary satellites (GEOS) and number of airport pseudolites (APLs)] could be varied to meet NAS performance requirements. Additional navigation options that mitigate the identified risks were also evaluated. In particular, these options included potential improvements to the GPS Standard Positioning Service (SPS) and additional capabilities onboard the aircraft, such as integration of additional sensors and application of GPS antijam technologies.

The following sections describe requirements, analysis methodology, performance analysis results, and the impacts of risks. More detailed discussion of simulation models is provided in the Appendixes C through K in a separate volume.

Section 2

NATIONAL AIRSPACE SYSTEM REQUIREMENTS

Performance requirements for each operation are shown in Table 2-1. The same requirements apply to all system and aircraft configurations. They represent service requirements and, as such, the study performance analyses assume all equipment onboard the aircraft is functioning properly. Values typically represent the most stressing requirements found in GPS/WAAS and GPS/LAAS documentation. The defining service requirement is availability. It is location dependent and varies by region. The table shows International Civil Aviation Organization (ICAO) threshold and objective requirements and the acceptable value for the Continental United States (CONUS) as set for this study (i.e., the *FAA* column). Exceptions are made for Alaska and GPS/WAAS Category I service where the availability requirement was set to 0.999.

Table 2-1 NAS Performance Requirements (as Modified from Original Statement of Work)

Operation	Accuracy (95%)	Integrity			Availability			Continuity (Loss of Nav.)
		Time-to-Alert	Alert Limit	Probability of MI	Thres.	Obj.	FAA++	
Oceanic En route & Remote	12.4 nmi	2 min	12.4 nmi+	10^{-7}/hr	0.99	.99999	.999	$1x10^{-5}$/hr
Domestic En route	2.0 nmi	1 min	2.0 nmi+	10^{-7}/hr*	0.999	.99999	.99999	$1x10^{-6}$/hr
Terminal	0.4 nmi	30 sec	1.0 nmi+	10^{-7}/hr*	0.999	.99999	.99999	$1x10^{-6}$/hr
Non-precision	220 m	10 sec	0.3 nmi+	10^{-7}/hr*	0.99	.99999	.99999	$1x10^{-5}$/hr
Cat. I Precision	H – 16 m V – 7.7 m	6 sec	H-40 m** V-10-15 m++	$2x10^{-7}$/ approach*	0.99	.99999	.99999	$5x10^{-5}$/ approach
Cat. II Precision	H – 6.9 m V – 2.0 m	2 sec	H-17.3 m** V-5.3 m**	2×10^{-9}/ approach**	0.99	.99999	.99999	$4x10^{-6}$/ 15 sec
Cat. III Precision	H – 6.1 m V – 2.0 m	2 sec** 1 sec (goal)	H-15.5 m** V-5.3 m**	2×10^{-9}/ approach**	0.99	.99999	.99999	$2x10^{-6}$/last 15 sec $1x10^{-7}$/last 15 sec (vertical)

*FAA-E-2892C (draft) **RTCA/DO-245
+RTCA/DO-208 ++B. DeCleene

2.1 AVAILABILITY

The definition of availability used for this study was modified to recognize the unique nature of the operational procedures provided by GPS augmentations. In particular, all GPS-based operations include a predictive availability calculation before conducting the operation. For oceanic through Category I approach service, availability is defined as the probability that the predicted availability test is passed and that the actual accuracy and integrity requirements are met. Because continuity is not included within this definition, the requirement for acceptable service from oceanic through Category I approach is that both availability and continuity requirements are met. For Category II and III service, availability is defined as the probability that the predictive availability test is passed and that the actual accuracy, integrity, and continuity requirements are met. For these services, acceptable performance is assured when the availability requirement is met.

2.2 ACCURACY

Accuracy is the 95-percent radial horizontal navigation error and 95-percent vertical navigation error at the GPS antenna electrical center. The accuracy requirement must be met at all locations within the service volume at all times. Accuracy is only counted in cases where the system is predicted to be available before the start of an operation.

2.3 INTEGRITY

Integrity relates to the level of trust that can be placed in the information provided by the navigation system. As with accuracy, integrity is evaluated in cases where the system is predicted to be available before the start of an operation. Loss of integrity is defined as the occurrence of an unsafe condition without annunciation for a time longer than the time-to-alert limit. An unsafe condition is defined as the occurrence of misleading information, that is, when the true navigation error exceeds the alert limit specified for each phase of flight operation. Loss of integrity can happen in two ways. Either an onboard integrity alert algorithm does not detect the unsafe condition, or it is detected, but the annunciation takes longer than the time-to-alert limit. Integrity must be maintained throughout the operation.

Note that the integrity requirement is expressed in terms of three parameters shown Table 2-1. The integrity requirement includes a maximum time-to-alert requirement, a position error alert limit, and a probability of misleading information. The probability of misleading information is the probability that the navigation position error exceeds the position alert limit and this event is not detected.

2.4 CONTINUITY

The continuity requirement is expressed as a loss of continuity per unit of time. Given the system is predicted to be available before the start of an operation, a loss of continuity occurs when the onboard integrity alert algorithm raises an alarm that an unsafe condition exists. The probability that this event occurs at any time during the specified time interval during an operation must be less than the continuity requirement.

Section 3

ANALYSIS METHODOLOGY

3.1 GENERAL APPROACH

The general approach was to categorize the identified risk elements into those risks viewed as "normal" and those risks viewed as "abnormal." Normal risks are factors that cause performance degradations consistent with design specifications for the GPS system and augmentations. For example, normal risks include scheduled and unscheduled satellite downings, ionospheric compensation errors, and unintentional interference caused by television broadcast. Abnormal risks include satellite "soft" failures that result in significantly misleading information, excessive ionospheric error attributable to the solar cycle or solar storms, and interference owing to malicious intent.

Study results are based on simulation analyses using the approach illustrated in Figure 3-1. Simulation models were developed using measured data wherever possible to accurately reflect the observed, rather than specification, performance of system elements. Models were largely based on published data.

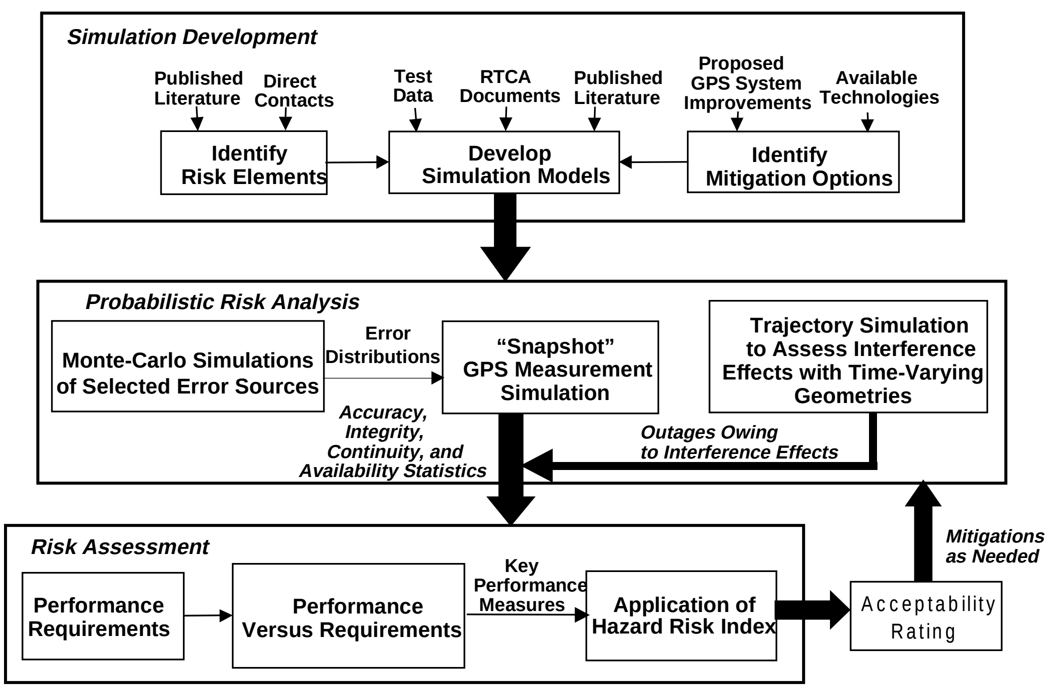

Figure 3-1 Risk Assessment Process

The probabilistic risk analyses were conducted in collaboration with Stanford University personnel. The principal tool to compute accuracy, integrity, continuity, and availability values was a GPS measurement "snapshot" simulation in which GPS performance is characterized in terms of the error statistics of single measurements taken at locations throughout the service volume and at times throughout the day. In addition, an aircraft trajectory simulation was used to assess GPS outage intervals owing to the time-varying interactions between aircraft motions, antenna pattern gain variation, and changing GPS satellite directions relative to the aircraft.

Availability was used as the key performance measure to evaluate the impact of each identified risk on system operation. A Hazard Risk Index was applied to rate the acceptability of each risk and determine the need for risk mitigation. The hazard risk characterization process is illustrated in Figure 3-2.

Judged Consequence of Failed Requirement

- **Reduction in Safety Margins or Functional Capabilities of Airplane**
- **Increase in Crew Workload**
- **Effects on Occupants**

Probability of Failed Requirement and Risk Occurrence

Consequence / Prob. of Occurrence	Catastrophic	Hazardous	Major	Minor	No Effect
Frequent ($>10^{-2}$)	1	3	6	10	21
Reasonably Probable (10^{-2} to 10^{-5})	2	5	9	14	22
Remote (10^{-5} to 10^{-7})	4	8	13	17	23
Extremely Remote (10^{-7} to 10^{-9})	7	12	16	19	24
Extremely Improbable ($<10^{-9}$)	11	15	18	20	25

Risk Index & Acceptability

1-6 = Unacceptable
7-10 = Undesirable
11-18 = Acceptable, but FAA Review Required
19-25 = Acceptable

Figure 3-2 Hazard Risk Index

Definitions to judge operational consequences (AC 25.1309-1A) are as follows:

a. Minor – Failure condition that would not significantly reduce airplane safety and which involve crew actions that are well within their capabilities

b. Major – Significant failure condition that would

(1) Reduce safety margins or functional capabilities of an airplane

(2) Increase crew workload or conditions impairing crew efficiency

(3) Produce some discomfort to occupants

c. Severe Major (Hazardous-ATA SOW, JAA) – Failure condition resulting in more severe consequences than major, such as

(1) Larger reduction in safety margins or functional airplane capabilities

(2) Higher workload or physical distress such that the crew could not be relied on to perform its tasks accurately or completely

(3) Adverse effects on occupants

d. Catastrophic – Failure conditions that would prevent continued safe flight and landing

Performance analysis was conducted by comparing computed performance with requirements at 5-minute sampling intervals throughout one sidereal day (the repeat cycle for GPS constellation geometry) and at geographically distributed locations. The sample locations used in the study are shown in Figure 3-3. The locations were chosen to uniformly sample the service volume with emphasis on the most heavily used routes. Note that Guam, North Pacific route, and Reykjavik locations were not included in GPS/WAAS analyses, except for oceanic requirements, because they are outside the WAAS service volume. Reykjavik, North Pacific route, and Bermuda were not used in GPS/LAAS analysis because they are not airports in the NAS.

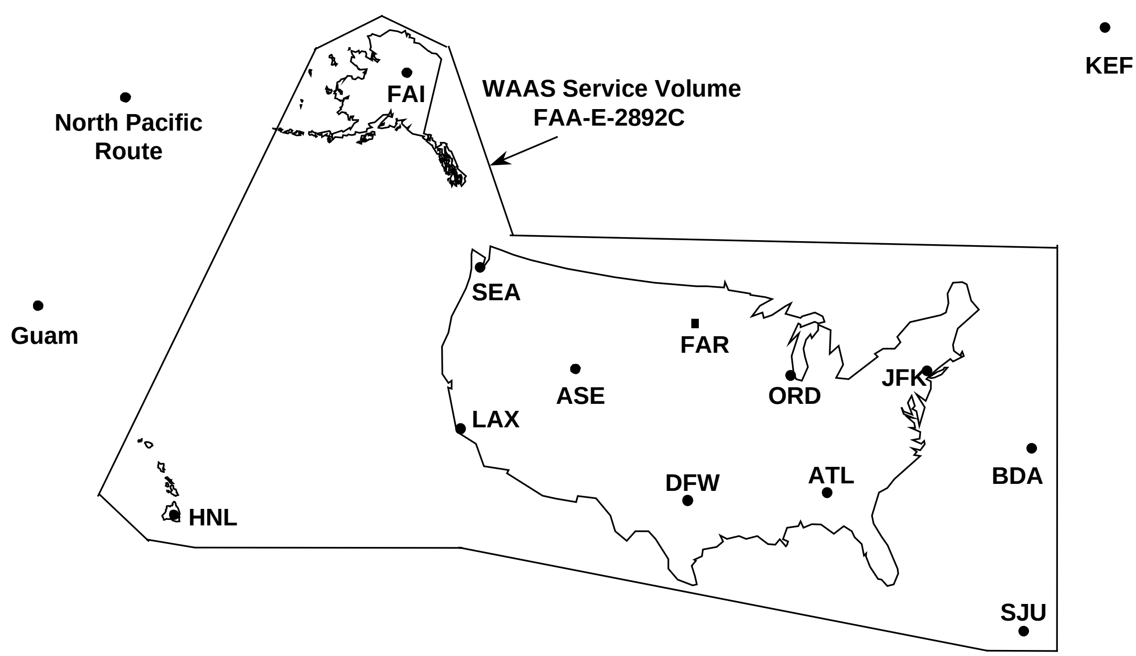

Figure 3-3 Locations Used for System Performance Analysis

3.2 KEY ASSUMPTIONS

The following key assumptions were used in this study:

a. The current GPS constellation results were based on a 24-satellite constellation rather than the 27 available today. GPS signal-in-space ranging accuracy and satellite downing probabilities were derived from GPS OCS Performance Analysis and Reporting (GOSPAR) project studies. GPS satellite end-of-life failure rates and replacement strategy were based on current specifications. Performance was also analyzed with a 30-satellite GPS constellation.

b. GPS/WAAS analysis baseline assumed the 24-satellite GPS constellation and 2 GEOS at the current locations. Ionospheric correction and orbit determination errors were based on analysis of National Satellite Test Bed (NSTB) data (19 reference stations and Stanford algorithms). Ground system reliability was based on specifications using 25 reference stations, 2 master stations, and 2 geostationary uplink stations per GEOS. GEOS reliability was taken from the FAA-E-2892C WAAS specifications, except the mean times to repair (MTTRs) were varied to reflect different replacement strategies. Performance was also analyzed with 3, 4, and 5 GEOS.

c. GPS/LAAS accuracy models were based on the specifications given in RTCA/ DO-245. Performance was analyzed with 24 and 30 GPS satellites, 4 GEOS, and 1 and 2 APLs.

The configuration variations considered in the study were generally set to represent the improvement timeline shown in Figure 3-4. It is understood that dates may not be accurate, but it was judged that the system capabilities shown in the figure represent realistic combinations of possible future improvements.

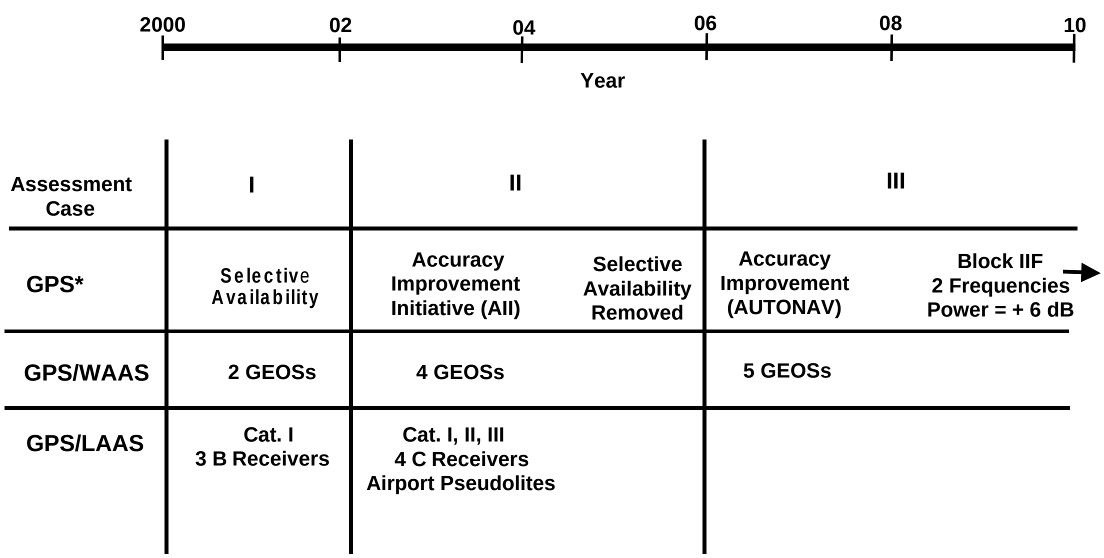

Figure 3-4 Notional Timeline for System Improvements

The initial evaluation timeframe (2000–2002) includes the current GPS with selective availability invoked, although the 24-satellite constellation discussed earlier was assumed rather than the actual 27-satellite constellation in place during late 1998. The current GPS Joint Project Office policy is to replace satellites on an as-needed basis, but there is no guarantee as to the number of satellites on orbit beyond the required 18. Current commitments, however, are that a minimum of 24 satellites will be maintained. The first timeframe also includes initial WAAS and LAAS capabilities.

The second evaluation timeframe (2002–2006) includes expected GPS improvements, the final LAAS configuration, and WAAS with 4 GEOS. The Accuracy Improvement Initiative (AII) will improve ranging accuracy by Master Control Station (MCS) filter improvements, inclusion of six additional ground stations, and an increased number of uploads per day. It is also expected that selective availability will be removed by 2006.

During the third evaluation timeframe (2006–2012), JHU/APL postulates a second civilian frequency and a 6-dB increase in satellite power. In addition, coded dual-frequency receivers will be available for WAAS. Finally, a 30-satellite GPS constellation was evaluated for timeframes II and III.

3.3 REQUIREMENTS EVALUATION

The diagram shown in Figure 3-5 illustrates the requirement evaluation process. Performance is conditionally evaluated for each measurement event. A measurement event is defined as a single GPS measurement of all satellites in view at a specific location and time. A measurement event may be further distinguished by, for example, the occurrence of a satellite downing and/or some other risk element. A given measurement event defines the set of available satellites, satellite geometry, and ranging accuracy.

Given the available satellites after scheduled and unscheduled downings, predictive availability is computed for an assumed ranging accuracy. The method used for each system configuration (GPS, GPS/WAAS, and GPS/LAAS) is detailed in Appendixes C through K. Note that it is also possible that a satellite will fail during the operation.

If the system is predicted to be available, accuracy, integrity, and continuity are then evaluated. Continuity depends on the integrity alert algorithm and estimated ranging errors. The probability that a loss of continuity occurs is computed as the probability that the alert threshold is exceeded.

As shown in Figure 3-5, a loss of integrity can occur only if either an alert is not declared or if the time-to-alert is exceeded. The loss of integrity is computed as the probability that the position error exceeds the alert limit, given one of these two events has occurred.

The probability distribution for true navigation error is computed, and the minimum value greater than 95 percent of all values is found. If this value is less than the required 95-percent accuracy, the accuracy requirement is passed. This is indicated by setting the conditional probability that accuracy is met equal to one.

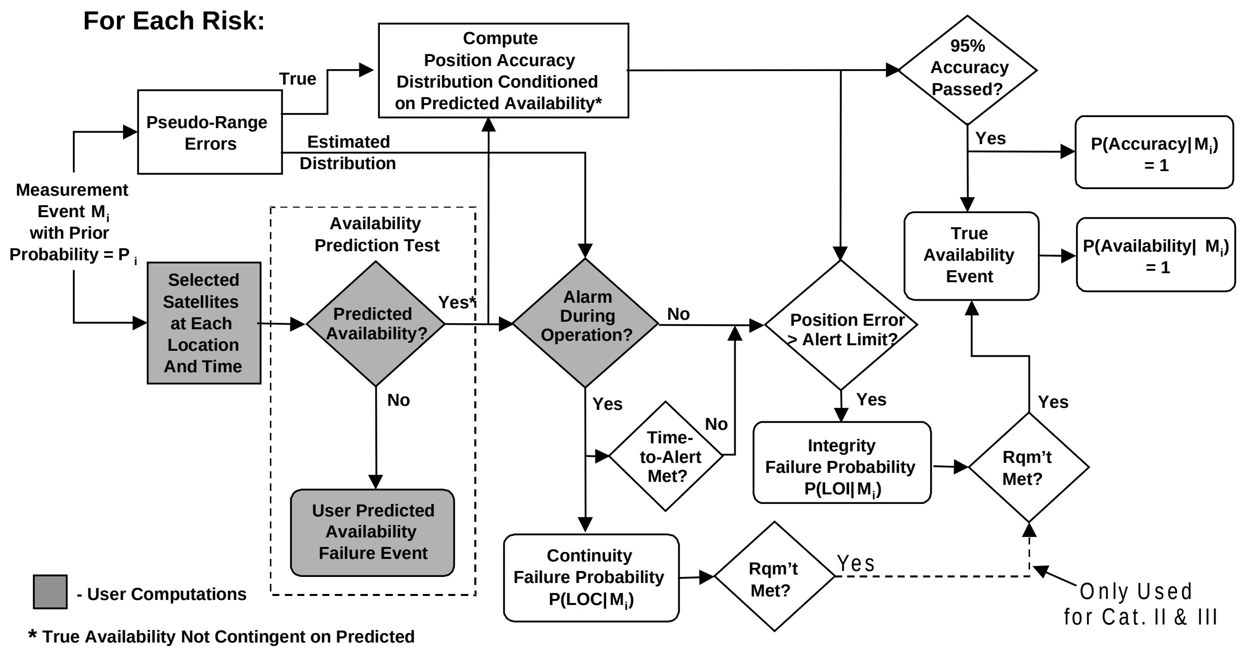

After All Measurement Cases for Each Risk Have Been Completed,

Accuracy Probability = Σ P(Accuracy| M_i)P_i Loss of Continuity Probability = Σ P(LOC| M_i)P_i

Loss of Integrity Probability = Σ P(LOI| M_i)P_i Availability Probability = Σ P(Availability| M_i)P_i

Figure 3-5 Requirement Evaluation Process

If the accuracy, integrity, and continuity requirements are all passed, a true availability event is declared. For each measurement event, the system is either truly available or not. This is also indicated by setting the conditional probability equal to one when availability is satisfied; otherwise, it is set equal to zero. Note that predicted availability is included in true availability because for any measurement event where predicted availability fails, the conditional true availability will be zero. As discussed earlier, true availability is also computed without continuity for oceanic through Category I service.

Finally, the total value of each performance measure is computed by summing the products of the prior probability of each measurement event, P(M_i), and the conditional probability for each performance measure.

Section 4

ANALYSIS RESULTS

The principal results are reported here for the most important configurations of the three systems: GPS without augmentation, GPS/WAAS, and GPS/LAAS,

4.1 GPS WITHOUT AUGMENTATION

GPS without augmentation is the SPS provided by the DOD. In addition, receiver autonomous integrity monitoring (RAIM), although an augmentation in the strict sense, is assumed to be an integral part of this system. GPS system performance models were mostly based on data provided by published GOSPAR analyses. User error models, including receiver noise, multipath effects, ionospheric compensation error and tropospheric compensation error, were also mostly derived from published literature. The simulation configuration, references, and models used to analyze this system are presented in Appendix C. The availability results for five GPS configurations are shown in Figure 4-1.

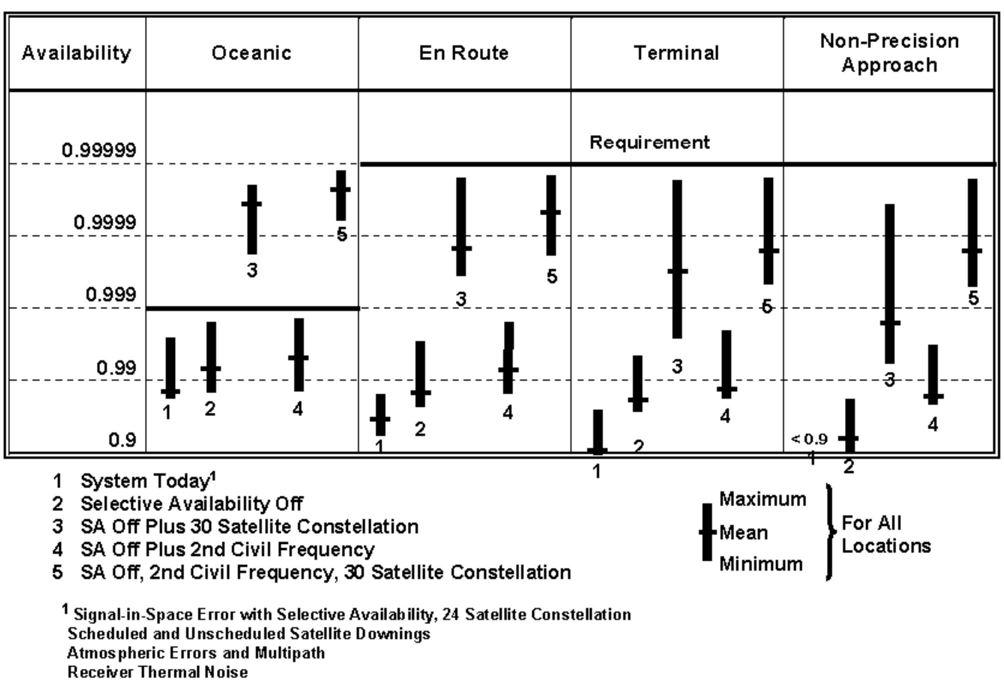

Figure 4-1 Analysis Results for GPS Without Augmentation

Each vertical bar represents the range of availability values determined for a specific service using a particular system configuration (number key below table). For example, the first bar within the oceanic column represents the range of availability considering all locations and times using the current GPS constellation (i.e., 24 satellites, selective availability on, no second frequency). The mean value is indicated by the horizontal line (i.e., the system's availability is less than 0.99). The performance of this system is seen to further degrade as more accurate service requirements are attempted (number 1 bar in successive columns). The number 2 bar represents the impact of turning selective availability off. While this definitely improves performance, the mean values continue to provide less than 0.99 availability (recall that the requirement for oceanic is 0.999 and for the other services it is 0.99999). The number 3 bars indicate the availability for a 30-satellite constellation with selective availability off. The numbers 4 and 5 bars indicate availability with selective availability off and with a second civil frequency for 24- and 30-satellite constellations, respectively. The analysis indicates that GPS without augmentation can only meet NAS oceanic requirements, and even then the constellation must be increased to 30 satellites. On the other hand, it should be noted that a considerable level of GPS service is already available to supplement existing capabilities, but it will not meet the availability objectives set for this study.

4.2 GPS/WAAS

A full "end-to-end" simulation was desirable with all the WAAS functions [Wide-Area Reference Sites (WRSs) functions, through the complex Wide-Area Master Site (WMS) processing and integrity functions, through the Geostationary Uplink Site (GUS) and GEOS links to the User], shown in Figure 4-2, being modeled. In principle, this model could be fully sensitive to all normal error sources and abnormal risks. Error distribution inputs could be validated by NSTB databases. However, the required extensive modeling/programming staffing was beyond the scope of this study.

A more efficient partial "middle-to-end" simulation was chosen, which models WMS estimation output errors developed from extensive NSTB databases as "satellite error models" to the existing GPS-only simulation, with added GEOS. User differential range error (UDRE) and grid ionospheric vertical error (GIVE) distributions were functionalized per satellite geometry with respect to WRS positions and abnormal conditions, such as peak solar sunspot activity. These models essentially replaced the detailed simulation of the WRSs and the WMS with less-extensive modifications to the GPS-only simulation. The UDRE and GIVE always produced horizontal and vertical upper bounds on the true position errors at the evaluation stations. Consequently, their use as truth models in the simulation will yield conservative results. The added value of this approach was that it was based on actual NSTB data experience using the Stanford orbit determination and ionospheric estimation algorithms. CONUS evaluations were produced from a 19-WRS database, while Alaska/Hawaii evaluations were based on an additional 5 WRSs in Alaska and 2 WRSs in Hawaii. Upper bounds for the reliability of the WAAS ground network were analytically calculated and the simulation results were modified, which modeled the GPS and GEOS geometry and reliability. These calculations assumed a full network of 25 WRSs, 2 WMSs, and 2 GUSs per GEOS. More details are included in Appendix D.

Figure 4-3 shows the main analysis results for GPS/WAAS. Availability is shown for six different system configurations (number key below table). Configuration #1 through #5 evaluations were at the eight CONUS sites plus Fairbanks (see Figure 3-3). Configuration #1 also was evaluated at the six non-CONUS sites for oceanic through nonprecision approach (NPA), resulting in better than 0.999 availability, except for Guam at NPA (0.998). Configurations #1, #2, and #3 represent the baseline results for GPS/WAAS. These results show that a GPS/WAAS configuration with 4 or 5 GEOS can meet the navigation performance requirements without any improvements to the 24 GPS satellites. The *IONO & OD* notation refers to assumed ionospheric and orbit determination processing algorithms at the WMS, those currently being used to support Stanford investigations and those being implemented by Raytheon (configurations #4 and #5). The bars labeled "Raytheon" in the figure were obtained by comparing Raytheon-published results (References 1 and 2) with corresponding Stanford results, yielding scaling factors on the NSTB/Stanford models. In both cases, however, the less conservative Stanford 15° restriction for valid ionospheric grid points [at least one WRS ionospheric pierce point (IPP) within a 15° great circle radius of the grid point] was assumed rather than the more conservative "three-of-four" restriction of the WAAS Specification (at least three out of four 5° quadrants surrounding the grid point must contain WRS IPPs). The three-of-four restriction significantly reduces availability and was not evaluated. JHU/APL believes that the NSTB database and Stanford processing results have tended to indicate adequate integrity of the Stanford processing and less conservative restriction (Reference 3). Further research is needed to validate this indication. If this is valid, the number of WRSs required for phase 2 may be reduced from the currently planned 48 stations.

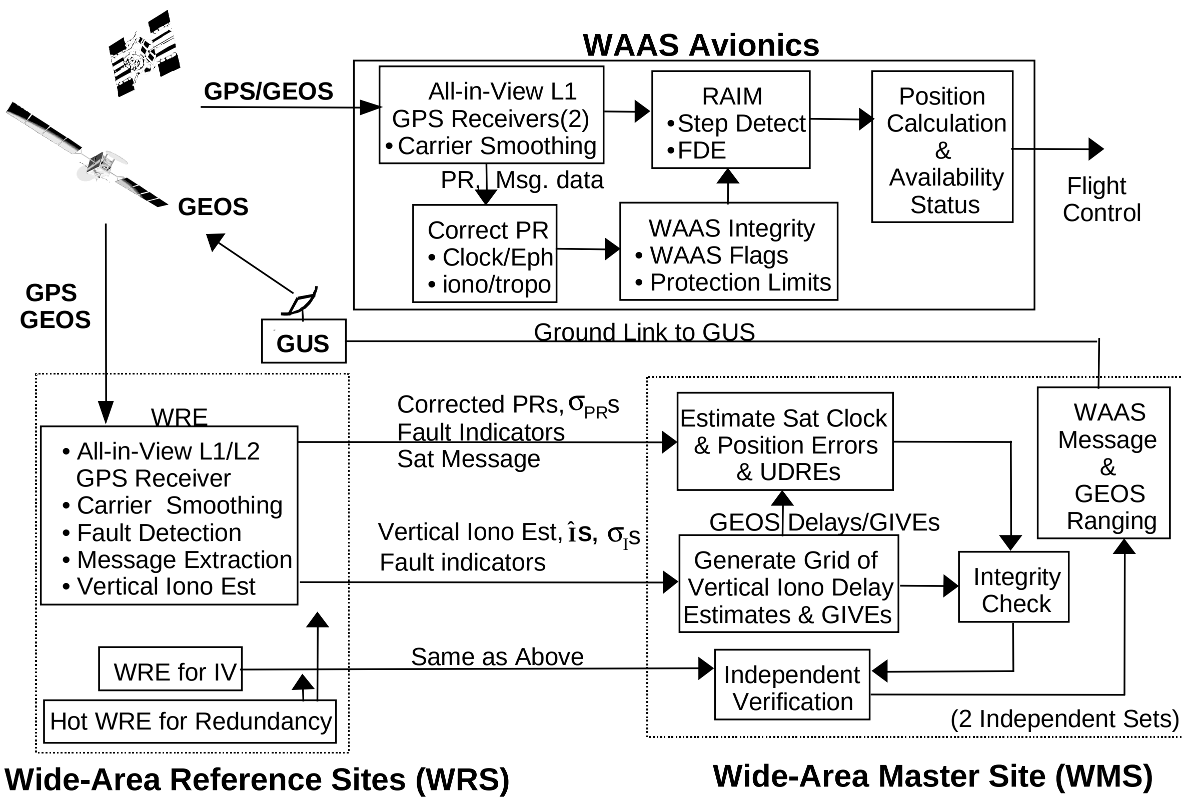

Figure 4-2 GPS/WAAS Functional Block Diagram

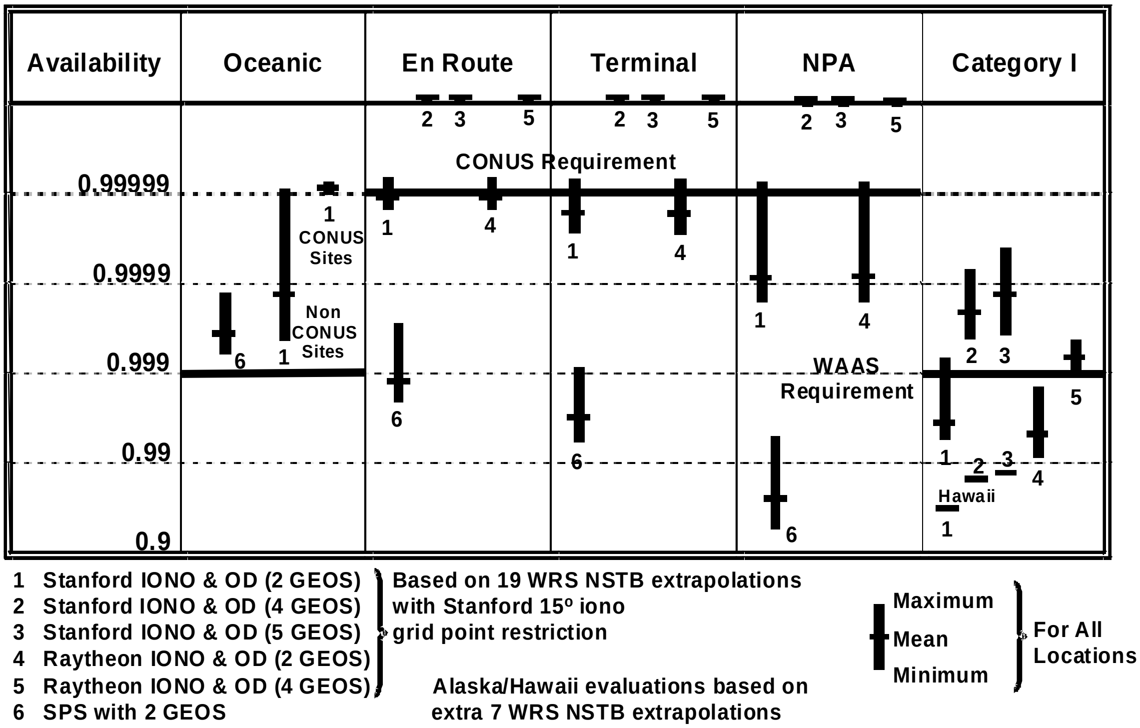

Figure 4-3 GPS/WAAS Analysis Results

The last configuration (#6) was added to evaluate if the oceanic requirement that was not met with the 24-satellite GPS constellation would be met by including ranging signal measurements from the current 2 GEOS. While this configuration does meet the necessary oceanic requirement, it can be seen that specifications for none of the other services can be met by this configuration. It can also be seen that the corresponding WAAS configuration (#1) can readily meet the oceanic requirements over CONUS and at all non-CONUS test sites. It will also be noted that none of the 2-GEOS configurations meet the 0.99999 requirement for en route through NPA or the 0.999 requirement for GPS/WAAS Category I service. The 4- and 5-GEOS configurations readily meet all service requirements except for Category I in Hawaii. The WRSs on CONUS and Alaska are too far from Hawaii to add much information to the essentially independent 2-WRS WAAS at Hawaii. GPS/LAAS must be used to achieve Category I availability greater than 0.999 at Hawaii. It should be noted that all requirements are met with a 24-satellite GPS constellation, without a second frequency, and with selective availability on (i.e., using the current GPS configuration).

The current WAAS GEOS implementation plan is unclear in that the number, location, suppliers, and replacement strategy have not been established. JHU/APL has assumed the following configuration placements: 2-GEOS configuration at Pacific Ocean Region (POR), Atlantic Ocean Region, West (AOR-W); 4-GEOS configuration at POR, AOR-W, 135W°, 75W°; 5-GEOS configuration at POR, AOR-W, 135W°, 75W°, 90W°; and 3-GEOS configuration at POR, AOR-W, 90W°. The importance of the replacement strategy is illustrated in Figure 4-4, by showing the availability for two different MTTR values. The 3-year GEOS MTTR (current WAAS specification in FAA-E-2892C) corresponds to having no spare in orbit, which would require procurement and launching. The 3-month MTTR assumes a more optimistic strategy and is clearly required to meet CONUS requirements.

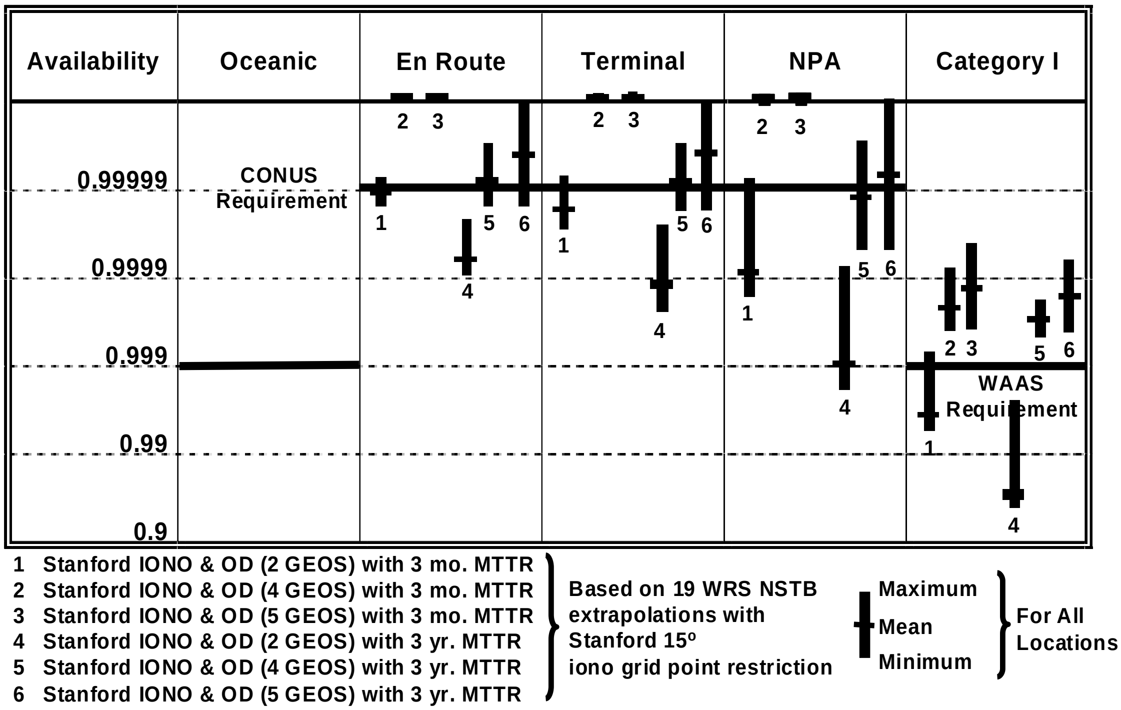

Figure 4-4 GPS/WAAS Results Versus Number of GEOS and Their MTTR

GPS/WAAS performance seems to be most sensitive to ionospheric processing (as indicated previously in the Stanford/Raytheon comparisons and the different grid point restrictions) and ionospheric phenomena, as shown in Figure 4-5. In all these cases, except for scintillation, the en route through NPA results were similar and passed the requirements. The solar maximum results were based on scaling the NSTB output ionospheric models, as suggested by Klobuchar, et al. (Reference 4). A conservative factor of 3 was used here. Clearly, the solar maximum results show serious degradation. An improvement in the ionospheric processing (such as tomography) and improvement in the measurements (more WRSs) will be needed to meet the WAAS specification for the solar maximum case. Further discussion appears in the WAAS risks section.

The scintillation results were based on Pullen, et al. (Reference 5) and Skone, et al. (Reference 6). Areas of moderate to strong scintillation were designated in the auroral region. IPPs that fell within these regions were checked to see if loss-of-lock occurred, affecting the availability of that measurement. As shown in Figure 4-5, scintillation will also degrade the nominal performance but not as seriously as solar max, affecting only the northern most sites, especially Fargo. Oceanic through NPA performance was minimally affected, with only Fargo dropping below the requirement at 0.99993 for NPA. The scintillation results and their implications are discussed more fully in the later section on WAAS risks.

The full spectrum of number of GEOS possibilities is explored in Figure 4-6. The 3-GEOS configuration meets the requirements. However, considering the potential degradation in performance due to abnormal ionospheric phenomena, as indicated previously, the 4-GEOS configuration represents the best choice for assured overall GPS/WAAS performance.

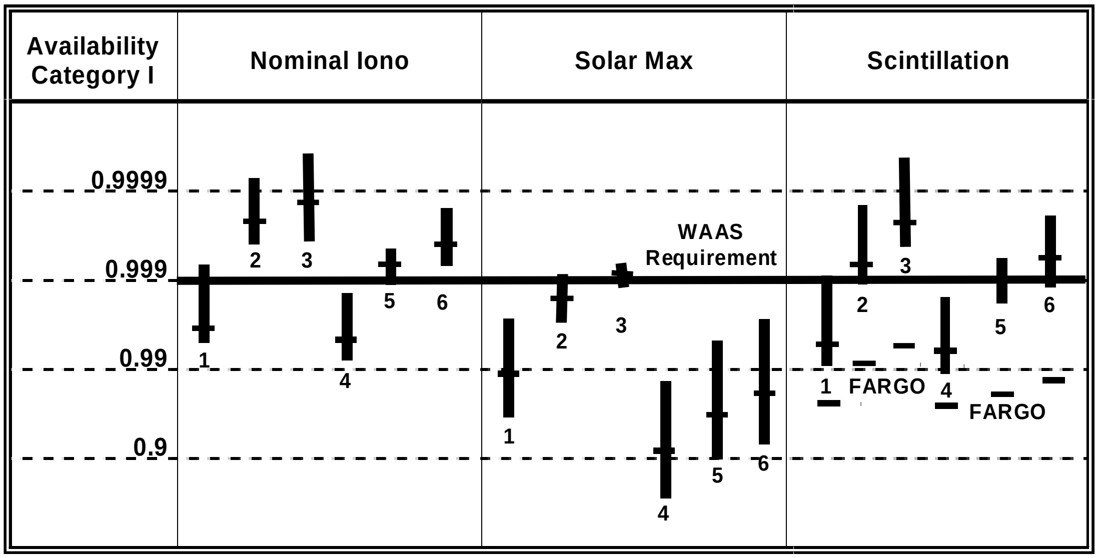

1 Stanford IONO & OD (2 GEOS)
2 Stanford IONO & OD (4 GEOS)
3 Stanford IONO & OD (5 GEOS)
4 Raytheon IONO & OD (2 GEOS)
5 Raytheon IONO & OD (4 GEOS)
6 Raytheon IONO & OD (5 GEOS)

Based on 19 WRS NSTB extrapolations with Stanford 15° iono grid point restriction

Maximum
Mean
Minimum
For All Locations

Figure 4-5 GPS/WAAS Results Versus Ionospheric and Orbit Determination Algorithms

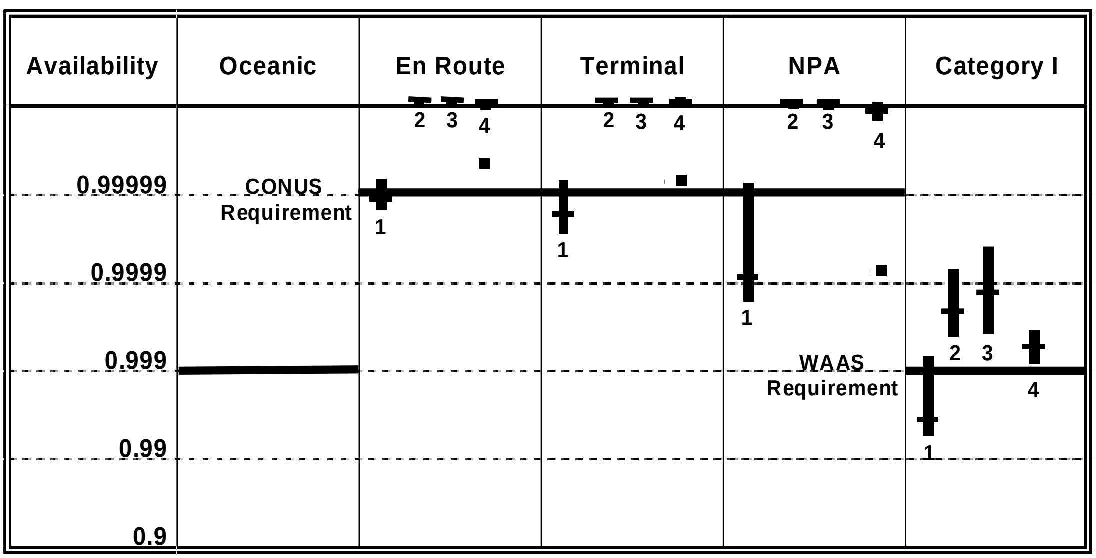

1 Stanford IONO & OD (2 GEOS)
2 Stanford IONO & OD (4 GEOS)
3 Stanford IONO & OD (5 GEOS)
4 Stanford IONO & OD (3 GEOS)
■ Alaska (requirement =.999)

Based on 19 WRS NSTB extrapolations with Stanford 15° iono grid point restriction

Maximum
Mean
Minimum
For All Locations

Figure 4-6 GPS/WAAS Results Versus GEOS Configuration Options

4.3 GPS/LAAS

System simulations and probabilistic risk assessments were conducted for a wide range of GPS/LAAS configuration options. Three classes of LAAS ground stations were considered. The first, referred to as a current LAAS station, was represented as having three ground antennas and receivers of the type commonly in use today for special Category I approach service. This is the type of station indicated for timeframe I (i.e., three modified choke-ring antennas with class B receivers). The second, referred to as an upgraded LAAS station, is based on the use of improved antennas and receivers to be used in timeframe II (i.e., four multipath limiting antennas and class C receivers). The third, referred to as a special LAAS station, includes an antenna configuration that further improves multipath performance and doubles the number of GPS receivers used in the upgraded station. This special configuration is expected to reduce the signal-in-space errors by a factor of 2. The analysis considered 24- and 30-GPS satellite constellations, with and without the 4 GEOS for additional ranging measurements, and 1 or 2 APLs. The results for six specific 24-satellite cases are shown in Figure 4-7.

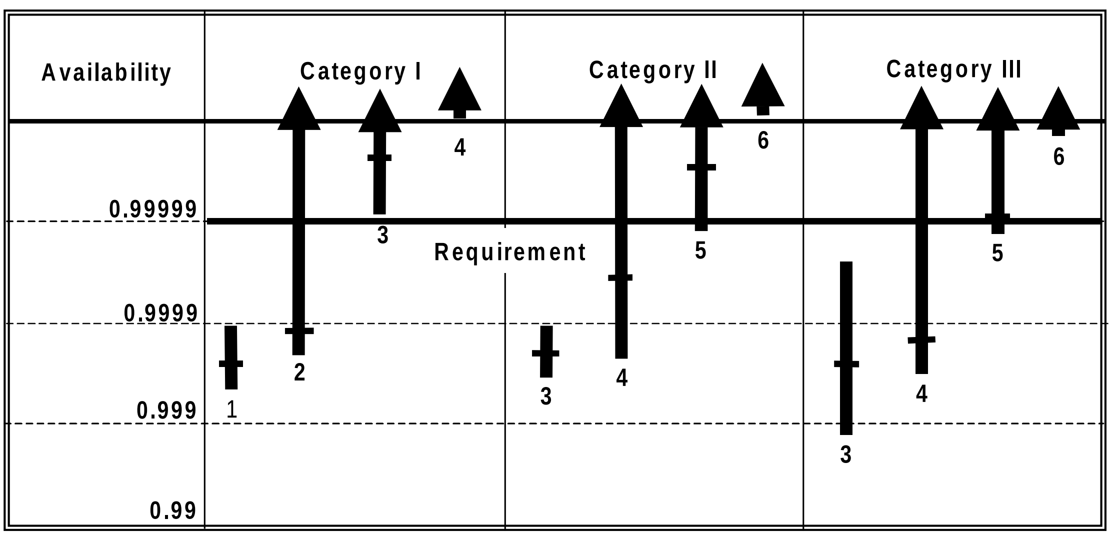

1 Current LAAS station, 24 GPS
2 Current LAAS station, 24 GPS, 2 APLs
3 Upgraded LAAS station, 24 GPS, 4 GEOS
4 Upgraded LAAS station, 24 GPS, 4 GEOS, 2 APLs
5 Special LAAS station, 24 GPS, 4 GEOS
6 Special LAAS station, 24 GPS, 4 GEOS, 2 APLs

Figure 4-7 Analysis Results for Several GPS/LAAS Configurations

The configuration #1 (i.e., current capability) will meet the minimum requirement set for GPS/WAAS Category I approaches, but it certainly cannot meet the 0.99999 availability requirement set for GPS/LAAS service. Configuration #2 shows the benefit of two APLs. While this provides considerable improvement, it will not meet all Category I requirements. The use of four

GEOS shown in configuration #3 meets the Category I requirements, and the addition of APLs (configuration #4) pushes the mean availability beyond 0.999999. However, none of these configurations can meet Category II and III requirements. A 30-satellite GPS constellation with 2 APLs based on the upgraded LAAS station (not shown in the figure) was just able to meet the Category II requirement, but fell short of meeting Category III. Because of the limited time, the next case considered (also not shown in the figure) used the maximum geometry case considered; 30 GPS satellites, 4 GEOS, 2 APLs, and the upgraded LAAS station. That case met the Category II and Category III requirements. The difficulty in meeting the high-availability numbers for Categories II and III is primarily because of measurement accuracy limitations of the upgraded LAAS station. With specialized equipment, it is expected that the station errors can be reduced by a factor of 2. The case using this special LAAS station with 24 GPS satellites and 4 GEOS (configuration #5) continued to fall short of meeting Category III requirements at some locations. However, all requirements can easily be met with 4 GEOS and 2 APLs (configuration #6) with the special station.

It was also determined that a special LAAS station used with a 30-satellite GPS constellation provided about the same performance as configuration #5 shown in the Figure 4-7. These results indicate that the GPS and GPS/WAAS configuration choices should influence the decisions on LAAS configuration options. If it is unlikely that GPS will be upgraded to a 30-satellite constellation, the LAAS will need to depend on special station improvements, four GEOS, and APLs. However, if a 30-satellite GPS constellation and the 4-GEOS configuration were assured, LAAS could meet its requirements without special station improvements. In any event, the study indicates that given either a 30-satellite GPS constellation or a 4-GEOS commitment, GPS/LAAS can meet all NAS precision approach requirements. Further details of the GPS/LAAS analysis are discussed in Appendix E.

Section 5

RISKS

Risks were considered for GPS and for the two augmentation systems. GPS risks are central to all operations considered and they will be discussed first, followed by the WAAS and LAAS risks.

5.1 GPS RISKS

All performance analyses of GPS positioning assumed conservative models with regard to receiver thermal noise; multipath; ionosphere; troposphere; satellite ephemerides; unscheduled satellite failures; and for satellites being unavailable because they were scheduled for maintenance, repair, repositioning, training, or testing. The loss of GPS ground support functions (i.e., health of the operational and master control stations and their associated communications functions) were considered, and because of the very low probability of significant performance impact, these risks were not considered further. Signal emissions from other normal and expected transmissions were evaluated with regard to their potential to interfere with GPS signal reception. Finally, abnormally high levels of ionospheric errors and scintillation were evaluated and intentional interference was investigated. Of these, only the ionosphere and interference risks were found to be significant.

5.1.1 UNINTENTIONAL INTERFERENCE

There have been very few reports of GPS outages caused by unintentional interference, so this portion of the study was based on evaluating the impact of potential interference sources listed in RTCA/DO-235. Of these, only commercial very high frequency (VHF) radio, over-the-horizon (OTH) military radar, and broadcast television were considered possible interference threats requiring further analysis. Detailed characterizations of the military radar signals were not available for analysis, but it was determined that there are only a few widely dispersed systems and they use relatively narrow antenna beams. For these reasons, and because there have been no reported problems from these emissions, they are not considered a significant risk. However, further review is required to confirm this expectation.

A simulation was developed and run to determine the potential impact of commercial VHF and television transmissions on GPS reception. A standard link budget equation was used along with models of typical transmit and receive antennas, assumed distributions of transmitter radiated harmonic levels, and aircraft trajectories for en route and approach phases of flight. Simulation results, in the form of predicted maximum interference level contours, were then compared to the WAAS-specified interference levels to determine the likelihood of outage that would be experienced by a GPS receiver just meeting the specification. A detailed description of the evaluation is presented in Appendix I.

Information on actual commercial VHF transmitter out-of-band emissions was not readily available, so analysis was based on maximum transmit power and out-of-band emissions permitted by regulation. This is expected to yield a worst-case result. Even so, because of the low power involved, VHF transmitters pose no threat to aircraft en route. They are of concern only to aircraft on approach, where transmitters can be relatively close, and interference can arrive from near (instead of far below) the horizon where the aircraft body provides less attenuation.

VHF interference was analyzed by considering an aircraft on a typical approach path. Two types of interference sites were examined: one was assumed to be a mobile unit with its antenna 10 feet above ground, and the second was a fixed site with its antenna 100 feet above the ground. For both, transmit power was set at the maximum authorized level with out-of-band emissions at the Federal Communications Commission (FCC) limit. Contours of transmitter site locations that cause interference for the two cases are shown in Figure 5-1. (The origin of the range scale is the aircraft touchdown point.) They are shown for a receiver that just meets current WAAS specifications and for receivers with 10 and 20 dB more suppression capability. It can be seen that the 20-dB suppression improvement removes the mobile threat and forces a fixed site to locate close to the runway, if it is to be a threat. For a receiver operating at the WAAS specification level, these results suggest a significant amount of interference over a reasonably sized area. However, this result is offset by several factors:

a. Several currently available GPS receivers outperform the WAAS specification (by as much as 20 dB) for this type of interference.

b. Transmitters often don't transmit at the maximum allowed power.

c. It is expected that typical transmitter output harmonic levels are far lower (20 dB or more) than FCC regulations require.

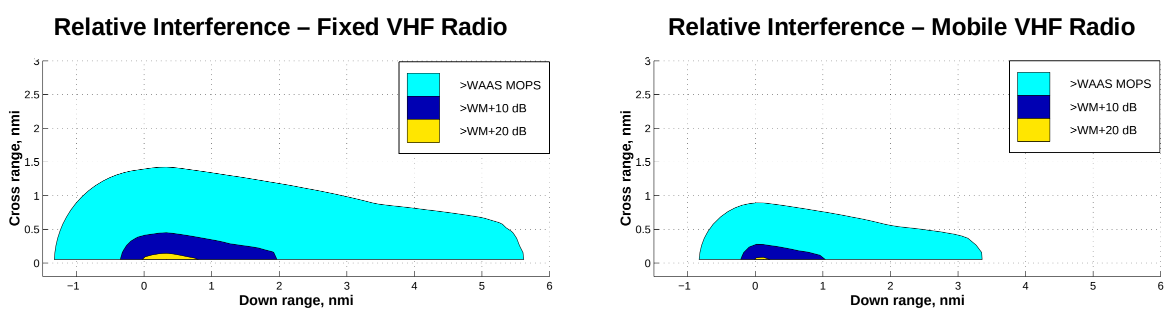

Figure 5-1 Interference Zones for VHF Radio Transmitters

For these reasons, commercial VHF transmissions probably do not pose an operationally significant threat. However, consideration should be given to reducing the allowed out-of-band emission power (from 60 to 80 dB below carrier power) and on restricting siting of fixed VHF transmit antennas near runways. These two actions would eliminate the risk without requiring increased interference mitigation in GPS receivers.

Television stations can use very high power transmitters. This and the relatively lenient out-of-band suppression requirement makes television harmonic emissions a significant threat to GPS. The FCC requires out-of-band emissions be limited to levels 60 dB below the carrier power. This could allow, for example, a 5-MW transmitter operating within specifications to radiate 5 W in the L_1 band. Three television channels have harmonics that fall in the GPS L_1 band: channel 23 (second harmonic) and channels 66 and 67 (third harmonic). Field measurements made by JHU/APL and others indicate that out-of-band emissions of many stations are far lower than the permitted maximum level. However, some have been observed to do worse.

Not only are the harmonic levels a potential threat, no mechanism is in place for monitoring compliance. While stations operate nearly continuously, events do cause out-of-band emissions to change over time, such as degradation of transmit tubes with age and occasional maintenance (especially when it involves replacing the transmit tube, which occurs every couple of years).

We ran simulations of approach and en route scenarios using television transmit power distributions and antenna heights from the FCC database, distribution of carrier-harmonic power ratios from JHU/APL-collected field data, a typical television transmit antenna pattern, and a typical GPS receive antenna pattern. Figure 5-2 shows the probability of interference level that can be assumed whenever an en route general aviation aircraft is within radio line of sight of a channel 23, 66, or 67 television station (for a typical commercial flight at 30,000 feet, the risk of interference is zero). The two vertical lines indicate the current WAAS specification levels for interference from high-definition television (HDTV) (left applies to channel 66, right applies to channels 23 and 67). It can be seen that only channel 23 exceeds levels that receivers are designed to be tolerant of, and that occurs less than 1 percent of the time. It should be noted that only 4 dB of additional interference suppression would overcome this interference. Because the analysis is conservative and the WAAS specification is conservative, television emissions are not expected to be a problem for any en route aircraft.

The conditions possible during approach are shown in Figure 5-3, again based on HDTV transmissions. Two cases are shown: a worst case transmitter [i.e., one whose transmitted harmonic levels are in the top 1 percent (99 percentile) represented by the FCC database combined with the carrier-harmonic data we measured] and one that is in the 90 percentile. Contour levels are shown for interference levels relative to the WAAS requirement for non-precision approach (these levels are 3 dB higher than those used for the en route case).

The figure shows that if the worst-case transmitter were located inside the interference zone contour, it would cause interference at or above the level indicated by the depicted area. To avoid interference above the WAAS specification, the worst-case channel 23 transmitter would have to be located over 72 nmi away from the airport. However, for all but the worst 10 percent transmitters, the radius of the interference zone is reduced to 8 nmi. This suggests a combination of mitigation strategies.

By itself, television transmitter siting is not a practical means for preventing outages. However, adding only a modest amount (10 dB) of interference suppression (by increasing the WAAS specification levels and/or adding AJ processing in the receiver) reduces the threat radius down to a range where siting restrictions are easily enforceable for most (say, 90 percent) of the transmitters. The highest power transmitters can be handled by radio frequency interference (RFI) monitoring, both initially (during GPS approach certification) and after transmitter maintenance periods that can change out-of-band emissions levels (e.g., transmit tube replacement).

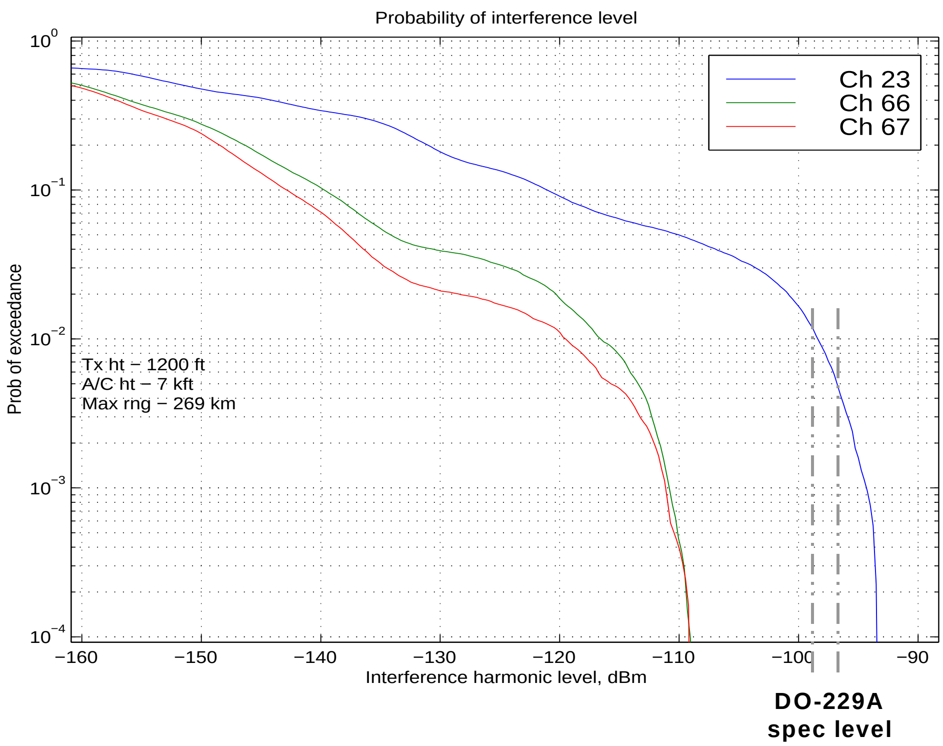

Figure 5-2 Probability of Receiving Interference Power at the Indicated Level

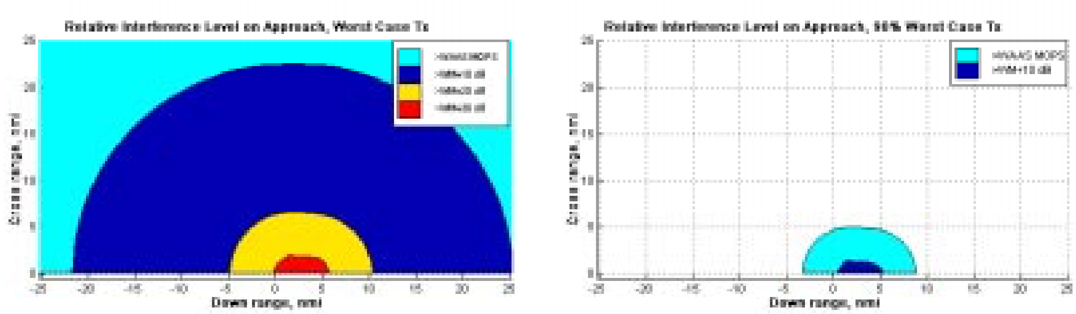

	All of TV Tx		90% of All TV Tx	
	Ch 23	Ch 66	Ch 23	Ch 66
Interference tolerance re WAAS MOPS	37 dB	24 dB	15 dB	1 dB

Notes for figures:

1. **Assumes worst (highest) 1 percent transmitted harmonic level. That is, 99 percent of channel 23 stations would not have this much impact.**
2. **Aircraft on standard approach.**
3. **TV station antenna at 600, 900, 1200 ft**
4. **Only 1 station considered here.**
5. **WAAS MOPS levels for non-precision approach.**

Figure 5-3 Computed Channels 23 and 66 Interference Zones

Note that the contours presented are based on a limited data set. Although they represent our best judgement with the available data, actual interference zones could be larger or smaller. In either case, television harmonics could deny GPS to aircraft on approach. Fortunately, it is clear that the risk of television interference can be made operationally insignificant by taking the simple mitigation steps described previously.

Acceptability of the unintentional interference risks was derived for the VHF radio and television broadcast. VHF radio interference was found to have no significant impact for en route operations and was therefore rated as acceptable for that case. In the terminal area there are no data characterizing the likelihood of occurrence, but an assumption was made it would be "reasonably probable." The impact of the risk was judged to be "minor" due to the intermittent and localized nature of outages caused by this source. As a result, application of the Hazard Risk Index shows the VHF interference risk is "acceptable but requires FAA review."

The risk due to television broadcast harmonics is "reasonably probable" en route but the impact is no effect because of the short duration of any outage. Thus, the television broadcast risk is acceptable for en route operations. In the terminal area, the impact was judged as "major" because of the significant outages that could occur. The television broadcast risk is therefore undesirable for terminal area operations. Recommended mitigations, however, would make this risk acceptable.

5.1.2 INTENTIONAL INTERFERENCE

Among potential risks to the GPS signal, the most problematic is that because of intentional interference. While the likelihood of such an event is impossible to predict, it can not be easily dismissed. It is well known that the GPS signal is very weak, and, assuming a standard GPS receiver, a small level of noise in the GPS band can disrupt reception over tens or even hundreds of miles. A modest level of jamming power can essentially stop GPS operations within a large area surrounding an airport. The result would be simultaneous loss of navigation by all aircraft and, therefore, a substantial increase in workload and a possible compromise of safety. To date the Department of Transportation (DOT) has not defined an intentional GPS interference threat to civil aviation nor specific circumstances that permit tolerable GPS outages. Thus, the approach taken in this study was to first define a plausible threat and then determine the level of interference suppression that eliminates GPS outage caused by that threat.

First, it was judged that the occurrence of a widespread GPS outage caused by intentional interference does not pose any direct safety risk because no flight operation is wholly dependent on GPS navigation. For example, if we consider the most critical case of a Category III precision approach, a sudden loss of the GPS signal would be known to the navigation system and might necessitate an abort, or in the final critical moments, use of the altimeter and possibly an inertial measurement unit (IMU). Thus, GPS outage because of jamming could have continuity impact, but loss of integrity is not an issue because accuracy degradation is relatively small before the signal is completely lost. The only potential risk to safety would result if the air traffic control system were not able to accommodate the disruption caused by interference. However, with validated procedures and proper training, this risk should be manageable. The only possible threat to integrity is spoofing where a phantom GPS satellite signal is generated to significantly increase navigation error, but this would require considerably greater expense and effort.

The possible sources of intentional GPS interference are (1) individuals or small groups ("hackers") who seek to create a nuisance by exploitation of a technological weakness or (2) a hostile organization or government that views the reliance of civil aviation on GPS as an opportunity for terrorist actions. It was the conclusion of this study that the latter source of interference is improbable because of the lack of incentive given the very low safety risk cited above. The hacker, on the other hand, may be satisfied with the more limited nuisance that is created. Interest could be expected to dwindle as the cost and difficulty increase.

To derive the hacker threat, estimates of jammer cost and size were developed versus jammer power. It was assumed that parts are the only cost, and the jammer is constructed of an inexpensive frequency source, solid-state transmitter, battery power supply, and an omni-directional antenna. The frequency source, in particular, is not readily obtainable, but must be specifically ordered from a manufacturer. Table 5-1 illustrates the relative size and costs. Note that cost increases proportionally with power output and depends on operating time. A 100-W jammer would cost approximately $300 and is about the size of a shoe box, while a 1000-W jammer would cost approximately $3000 and is approximately the size of a small suitcase. Volume and weight increase significantly as operating time is increased to 1 day. Based on these data, it was judged that a hacker threat might reasonably obtain a 100-W jammer and a 1000-W jammer becomes much less likely because of cost. Thus, a single 100-W broadband jammer was chosen as the baseline jammer type for this study. As shown below, interference suppression that is completely effective against a 100-W jammer would also provide reasonable protection against a 1000-W jammer. In addition, a broadband jammer would be simpler to construct than the narrowband jammer because of the less stringent requirement on frequency control. Depending on specific receiver design, the broadband jammer may also be more effective.

Table 5-1 Estimated Jammer Characteristics

Power (W)	Operating Time					
	1 Hour			1 Day		
	Cost ($)	Weight (lb)	Volume (cu. in.)	Cost ($)	Weight (lb)	Volume (cu. in.)
10	50	1	50	60	11	250
100	300	3	500	409	112	2500
1000	3000	10	5000	4090	1100	25000

To illustrate the impact of a 100-W jammer on GPS signal reception, Figure 5-4 shows the area over which a 100-W jammer would cause a GPS receiver to lose track of the GPS signal. In this analysis, it was assumed the receiver could track a GPS signal up to a jammer-to-signal ratio of 30 dB. This value is typical of current technology and is consistent with the WAAS RTCA/DO-229 specification for broadband noise. The left portion of the figure shows the effect if the aircraft antenna gain were unity in all directions. In fact, an aircraft antenna pattern would have some decreased gain in the direction of the jammer because the jammer is expected to be below the aircraft and the aircraft provides some degree of shading. The right portion of the figure illustrates the reduction in effective area if the antenna gain were –10 dB (one-tenth) in the direction of the jammer. Circles are also shown to represent the horizon line-of-sight limits for aircraft operating at 30,000, 15,000, and 3000 feet. Thus, the jammer would not affect an aircraft flying at 30,000 feet until it is within the horizon circle, a radius of approximately 215 nmi from the jammer.

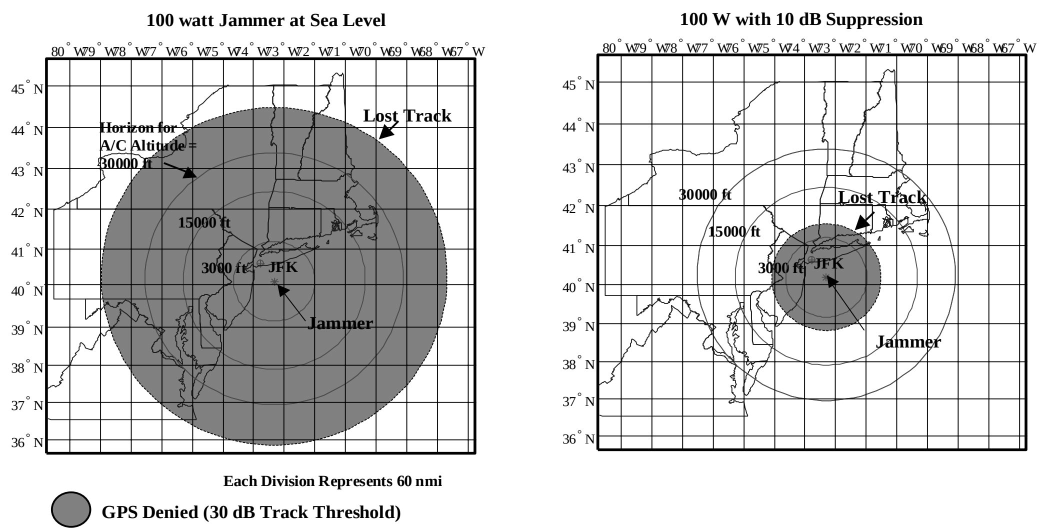

Figure 5-4 Outage Area Caused by 100-W Jammer

The effect of a further reduction in jamming signal because of either aircraft antenna pattern or other interference suppression is shown in Figure 5-5. The left portion of the figure shows the impact of 20 dB of additional suppression, and the right side shows a plot of jammer power versus corresponding denial range. Thus, for example, if the effectiveness of a 100-W jammer is to be reduced to less than a 1-nmi radius an additional 50 dB of interference suppression is required.

To analyze the potential impact of jamming in the terminal area, a scenario illustrated in Figure 5-6 was developed. A nominal aircraft trajectory was assumed, and a 100-W jammer was randomly placed at ground level within a 30-nmi radius of the landing point. Other maximum jammer distances were evaluated, but the 30 nmi value was found to be an approximate “worst case” after accounting for line-of-sight limits because of the horizon and range effects. The scenario also assumed a smooth Earth so that the benefit of terrain masking was not included. A baseline aircraft GPS antenna pattern was also included in the simulation model. The antenna pattern is discussed further in Appendix I.

An example trajectory is shown in Figure 5-7 where jammer-to-signal power ratio (J/S) is plotted as a function of range to touchdown for an aircraft making an approach and landing at JFK airport. The jammer is located approximately 20 nmi from the airport under the flight path. The plot illustrates that the J/S value after attenuation by the antenna is always greater than a typical receiver tracking threshold value of 30 dB. Thus, in this example, GPS would not be available throughout the entire approach and landing trajectory. The plot also serves to illustrate that an additional 32 dB of interference suppression would eliminate the GPS outage.

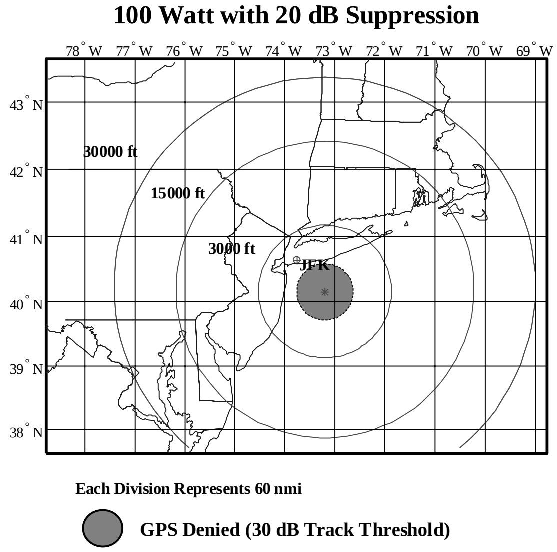

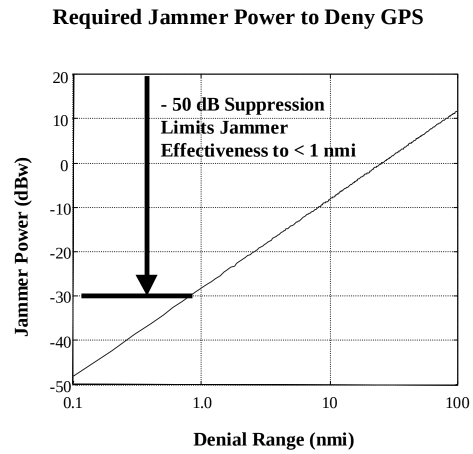

Figure 5-5 A 100-W Jammer with Additional Interference Suppression

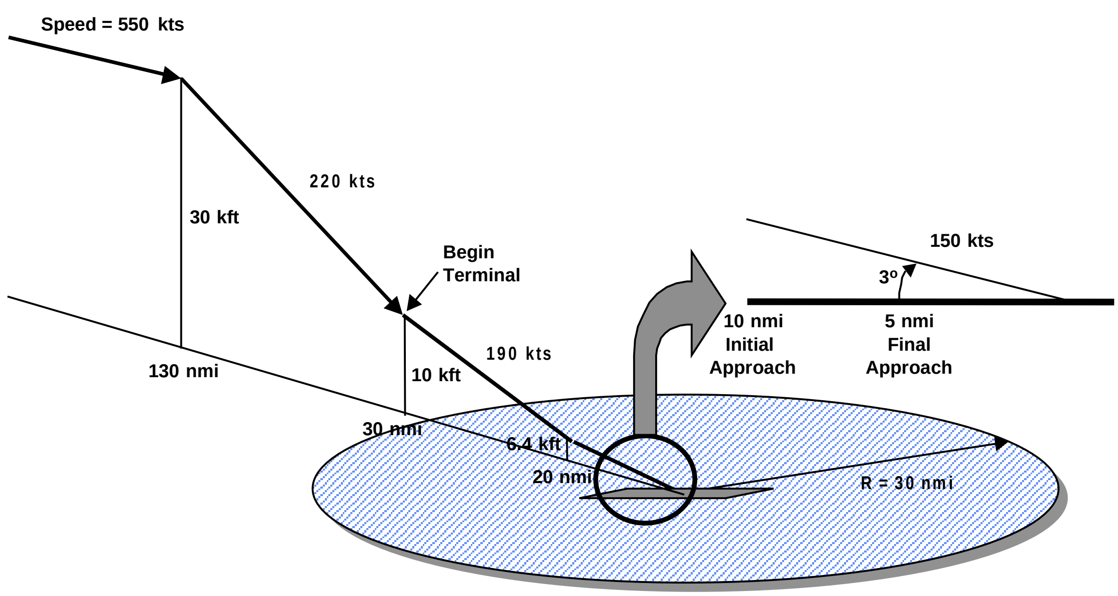

Figure 5-6 Terminal Area Scenario

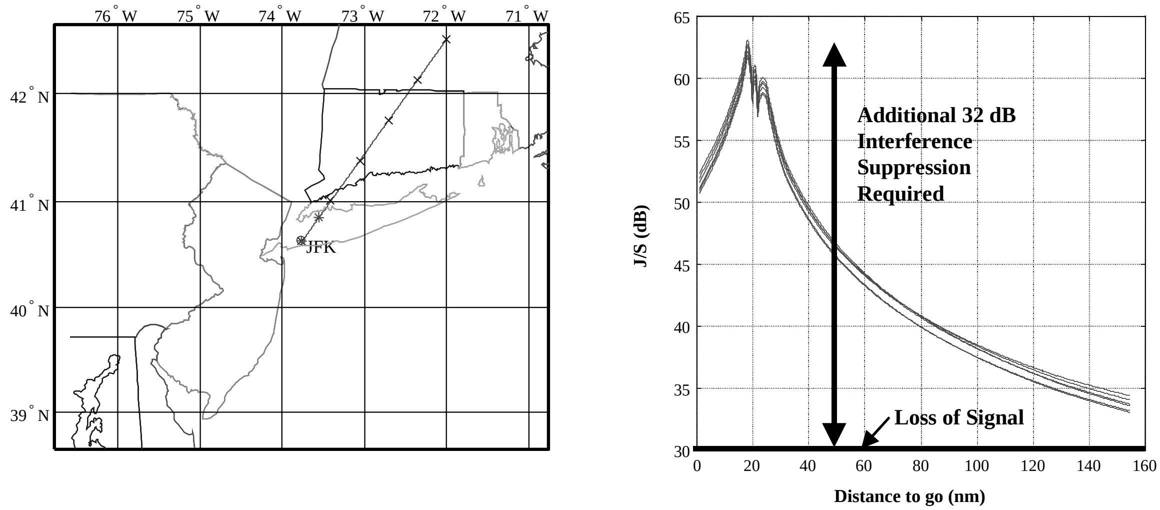

Figure 5-7 Example Jammer-to-Signal Ratio During Approach

Given the more general scenario defined by Figure 5-6 in which the jammer is randomly located, the probability of GPS outage versus distance to the landing point was computed using Monte-Carlo simulation. GPS outage was defined as the tracking of less than five satellites. Figure 5-8 shows the resulting probability values for different levels of interference suppression beyond that provided by the assumed baseline antenna pattern. In addition, the right-hand plot shows the result of placing a jammer detector at the airport and then making the assumption that all jammer locations are forced to be outside the line-of-sight horizon limit for a jammer located at ground level. For a detector at 200 feet, this limit is 17.4 nmi. Appendix J contains further discussion of the jammer detection option. Note that without the jammer detector, 50 dB of interference suppression eliminates GPS outage, and with the jammer detector 40 dB is sufficient. Also note that if the jammer power were 1000 W instead of 100 W, this would effectively reduce the interference suppression by 10 dB, so the 40-dB curve would apply if 50 dB of suppression were being used. Figure 5-9 indicates the impact of a 1000-W jammer would be relatively minor.

The impact of an airborne emitter in the airport area is shown in Figure 5-9 for a jammer located at 5000 and 20,000 feet. It can be seen that the jamming effectiveness is not largely enhanced relative to the levels shown in Figure 5-8. On the other hand, a jammer at altitude can be detected from a much greater range, which implies that the jamming detection process benefits more than the jammer.

Acceptability of the intentional interference risk was derived by judging the likelihood to be "reasonably probable," given the study threat scenario. The impact of this risk was conservatively judged to be "hazardous" because of the very widespread outage that can result and the potential impact on safety without appropriate air traffic control procedures. As a result, application of the Hazard Risk Index shows this risk is rated as "unacceptable" or at least, undesirable if the impact were judged to be only major. The recommended mitigations would make the risk acceptable.

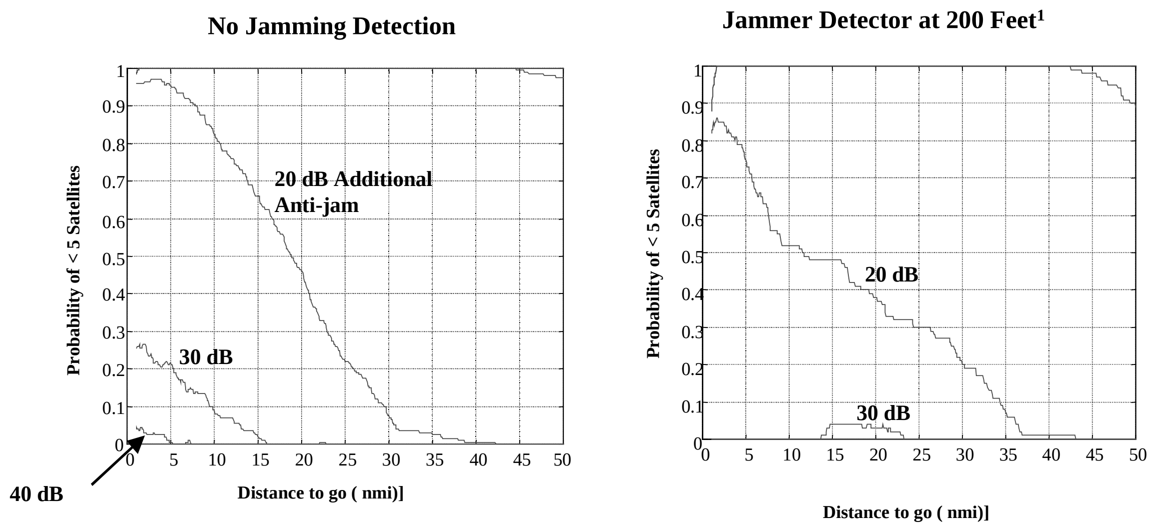

[1] Plot Shows Impact of Jammer Beyond 17.4 nmi Detection Range

Figure 5-8 GPS Outage Due to 100-W Jammer at Ground Level

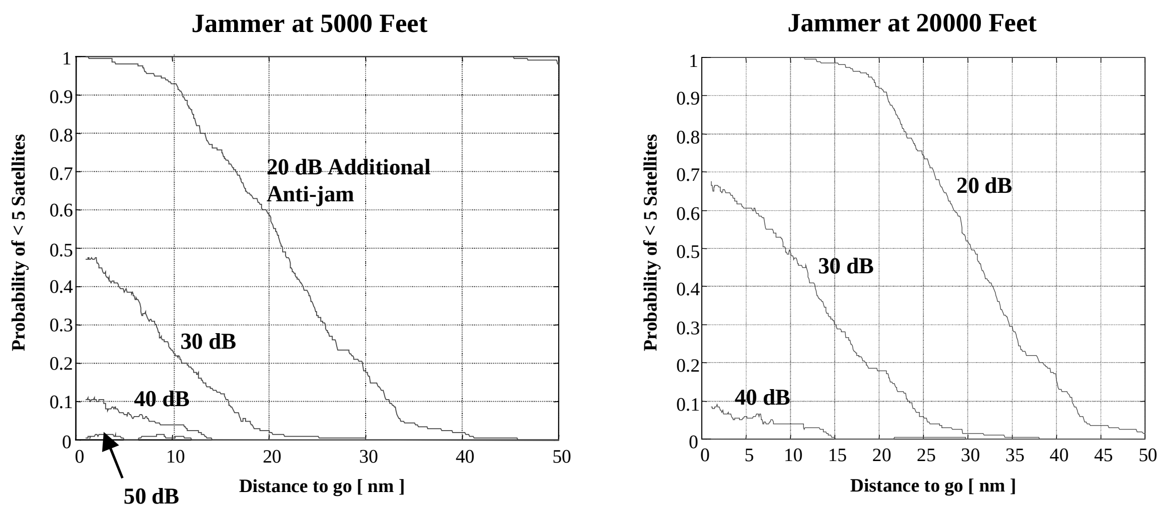

Figure 5-9 GPS Outage Caused by 100-W Airborne Emitter

5.1.3 INTERFERENCE MITIGATION

It will be necessary to establish methods and procedures for interference detection and location as discussed in Appendix J. Unintentional interference will need to be monitored and corrected, and persons maliciously producing intentional interference will need to be rigorously pursued and prosecuted. Beyond that, numerous technology options exist that provide additional GPS interference suppression to mitigate the risks of both unintentional and intentional interference. They fall into the general categories of GPS signal-in-space improvements, user antenna design and installation, coupling of the GPS receiver with other sensors, and receiver signal processing. Examples of user based techniques are given in Table 5-2. Estimated component costs are used to indicate relative complexity. They do not include the impact of nonrecurring engineering or the cost of integration.

Table 5-2 Example GPS Interference Suppression Technologies

Technology	Max Gain[1]	Number of Emitters	Estimated Cost	Remarks
IMU Receiver Code Loop Aiding	10 dB	N/A	$10 – 40 K	Cost depends on accuracy; higher cost represents 1 nmi/hr quality
Adaptive Controlled Radiation Pattern Antennas (CRPA)	35 dB	~(# elements –1), but Depends on geometry	$2 – 20 K	Less capable systems available now; higher end systems not in production for a few years
Low-Elevation Antenna Nuller (LEAN)	35 dB	Any Number Near Horizon	$3 K	Still in development; need to assess impact on satellite tracking
Signal Polarization Cancellation Antenna	31 dB	14 dB for 4 Broadband	$3 – 5 K	L1 C/A available
Reference Canceller	50 dB	Any Number Near Horizon	-	In development; need to assess impact on satellite tracking
Adaptive Filtering or Narrowband Frequency Excision (FX)	50 dB	3-20 Narrowband	<$100	Ineffective against broadband interference
Combined FX & Nonlinear Adaptive Processing (FXNONAP)	40 dB	20 Narrowband, up to 3 Broadband	<$100	NONAP deployed in sub fleet; FXNONAP still in development
Direct Measurement Processing	20 dB	N/A	-	In development

[1] **Actual performance highly dependent on scenario**

The most beneficial signal-in-space improvement with regard to intentional interference is an increase in satellite power. Recent proposals have suggested an increase of 6 dB. While this increase falls far short of that needed to counter the scenario examined in this report, any increase benefits the user because J/S would be lowered independent of user-interferer geometry and the specific suppression techniques applied by the user. Furthermore, the performance of some AJ techniques is improved with increased satellite power. A second civil frequency would provide additional benefit in the case of unintentional interference, because the likelihood of unintentional interferers appearing at both frequencies simultaneously should be considerably less than occurrence of interference at one frequency.

The interference suppression approach that has been most actively pursued in the GPS community is design of the user GPS antenna. As already noted, a standard antenna provides a degree of interference suppression in cases where the interferer is below the aircraft body, a situation that is most commonly expected. Appropriate selection of antenna location on the aircraft body and inclusion of additional treatments such as a skin embedded choke ring might further enhance interference suppression because of body masking. These techniques, however, must at the same time ensure visibility of GPS satellites to a 5° mask angle. It should also be noted that too little antenna gain below an aircraft could preclude the use of APLs for GPS/LAAS operations. These requirements will need to be considered together.

The potentially most effective antenna technique is adaptive nulling of interfering signals by use of multiple antenna elements. A number of manufacturers have developed systems of this type, mostly for military application. These antennas can also be used to increase gain in a satellite direction. There are, however, several limitations to these systems. The most fundamental is that the number of nulls is limited to one less than the number of antenna elements. Packaging and cost limit the number of elements. Systems have been developed that have from two to seven antenna elements. Thus, the performance of a nulling antenna will typically degrade as the number of interference sources increases and, moreover, can degrade as a function of the geometric relationship between the antenna and interferer locations. Another factor to consider is the possibility that the antenna not only nulls interference, but might also null the GPS signals because of both "sympathetic" nulls[1] and in satellite directions close to interferer directions. When installed on wide-body aircraft, the effectiveness of these antennas against sources beneath the aircraft body also needs to be assessed. The dynamic response of the nulling antenna must also be considered because the null direction must rotate to counter the relative motion between the aircraft and interference source.

The integration of other sensors with the GPS receiver is another technique that is commonly pursued by military systems to provide additional interference mitigation. In particular, an IMU can be used to provide aiding signals to the GPS signal carrier and code tracking loops in the receiver, allowing tracking bandwidth to be lowered. As a result, received noise is filtered to add approximately 10 to 15 dB of additional suppression. In the event GPS is jammed, the IMU continues to provide a navigation solution for a time period determined by the quality of the IMU and the accuracy requirement. Integration with an altimeter also provides benefit because, in effect, another ranging source is available.

The most basic signal processing techniques are only effective against narrowband sources and must be directly integrated with the receiver hardware. More advanced techniques that are under development have some additional capability against broadband sources. One promising approach is sometimes referred to as direct measurement processing where the traditional cascaded receiver tracking loops are replaced with a vector measurement process that more directly couples the IMU and the navigation Kalman filter with the fundamental GPS signal measurements.

It is clear that no single technique will achieve the recommended interference suppression value of 50 dB using current technology. An example combination of techniques is as follows. First, optimize the effectiveness of body shading. This will require the direct measurement of

[1] By virtue of the adaptive nulling algorithm, a null might be placed in a direction other than the direction of the interference source

underbody antenna patterns. This might increase the assumed baseline value by 5 to 20 dB. Second, the greatest gain will come from nulling antenna technology, which could provide another 25 to 35 dB of suppression. Finally, integration with an IMU, where available, would add another 10 to 15 dB. Thus, a possible total is 40 to 70 dB, although the upper value is subject to verification of the combined effects of body shading and the operation of the nulling antenna. Advanced signal processing could be included to further increase gain, if needed.

5.1.4 IONOSPHERIC PROPAGATION

Naturally, ionospheric signal refraction acts on all GPS signals. Current authorized users can correct for this effect by using the two signal frequencies provided for the precise positioning service (PPS), and eventually a dual frequency capability will be provided for the current SPS. Because the refraction effect is inversely proportional to the square of the transmit frequency, a two-frequency user can compute the first order refraction from the difference in time of arrival of the two signals. The process used virtually eliminates the refraction error, because higher order terms are exceedingly small at the GPS frequencies. Current civil use is based on the single-frequency SPS service now provided by GPS. These users make a correction to the GPS measurement data that is based on a model that considers location, time of day, approximate time within the solar cycle (i.e., the total effect varies with solar activity with an approximate 11-year cycle), and line-of-sight elevation angle (i.e., length of the refraction path). The experienced based model for this error indicates that the model corrections have an uncertainty equal to half the total delay.

For this study, a statistical distribution was developed to match the large historical database available for this error term. This distribution was used with the above noted model parameters to determine the errors used in the performance simulations. For the GPS-only runs, where only oceanic through non-precision approach flight phases were evaluated, two separate cases were tested. The baseline case considered the total distribution (i.e., looked at the long-term statistical nature of this error over the full solar activity cycle). The second case was restricted to the high solar activity period (i.e., to characterize the short-term worst-case condition). In either case, the impact for the phases of flight considered was not significant. The GPS/WAAS and GPS/LAAS implications are discussed later.

5.1.5 IONOSPHERIC SCINTILLATION

Ionospheric scintillation is the result of nonuniform electron distributions trapped by and moving in the Earth's magnetic field. The general model for ionospheric refraction is based on a model that assumes a relatively smooth distribution with no particularly dense regions. However, at certain times and locations the densities can be high enough or the temporal and spatial gradients large enough to diminish GPS signals below receiver thresholds. When that happens, some satellite signals will be lost to the user with the corresponding reduction in positioning accuracy. Ionospheric scintillation is most severe in equatorial regions and in the auroral region. The most likely means by which ionospheric scintillation affects GPS users in the continental United States is in viewing GPS satellites through these regions. The auroral region covers the northern part of Canada between 65° and 72° N *geomagnetic* latitude and the equatorial region covers zones at 15° ± 10° N and at 15° ± 10° S geomagnetic latitude. Only the northern equatorial zone is seen from the United States and only by two of the locations included in the study. Scintillation will most likely coincide with auroral storms (known as "Auroral-E ionization," or AEI), and, in these conditions, the southern edge of the auroral oval may dip down into continental United States. AEI is most likely to occur during evening hours (1900–2400 local time). Within this disturbed region, pierce points with a local time between 2000–2200 are considered to be susceptible to "strong" scintillation, whereas pierce points with local times between 1900–2000 or 2200–2400 are considered to be susceptible to "moderate" scintillation. Within both of these zones, scintillation is "patchy," such that an average of 30 percent of the pierce points are affected.

A conservative model was used to test the overall impact of including this effect in the normal system availability analysis. The best SPS case considered in this study (i.e., 30 GPS satellites, SA off, and dual frequency available) was tested with this model. The oceanic availability dropped from 0.999996 to 0.988; en route availability dropped from 0.99994 to 0.988; terminal availability dropped from 0.9999 to 0.988; and NPA availability dropped from 0.9998 to 0.998. The availability numbers with scintillation were only different beyond the third significant figure. Because this effect seriously degrades availability, it is a risk factor. Occurrence of the risk was determined to be "reasonably probable" (i.e., between 10^{-2} and 10^{-5}) and our assessment of consequences is that it is "minor." Using the hazard risk index, this risk is characterized as "acceptable with FAA review." The GPS/WAAS and GPS/LAAS implications are discussed later.

5.2 WAAS RISKS

The set of potential risks affecting WAAS are the same as for GPS, except for additional risks associated with the WAAS ground system and the GEOS. Most of these are statistically characterized in the GPS/WAAS simulation model and results discussed previously. Intentional and unintentional interference on the WAAS user avionics is the same as discussed in the previous section for GPS only. However, interference to the WAAS (ground system and GEOS) and ionospheric abnormalities are unique to WAAS and will be discussed in the following subsections.

5.2.1 INTERFERENCE (Reference 7)

Unintentional interference to the ground system is less likely than for the user avionics because of ground shielding. Intentional interference at a WRS would be detected in the integrity checks, with no safety effects. Losing an entire WRS has no impact on en route performance and minor impact on precision approach performance. Geographic dispersion of the WRSs mitigates any attack via WRS jamming. Data communications between the WRSs, WMSs, and GUSs is by a ground-based system, with integrity checks to assure data validity. The timing signal from the U.S. Naval Observatory (USNO) can be jammed but the WMS cesium reference keeps accurate time for extended periods. This, along with geographic dispersion of redundant WMSs minimizes any effects of WMS jamming. The GUS uplink to the GEO is difficult to overpower (16-m dish), and the GUS signal-in-space monitor would instantly recognize the difference between the transmitted and received signals. This, along with geographic dispersion of redundant GUSs and GEOS, minimizes any effects of GUS and/or GEOS jamming. Consequently, the probability of interference to the WAAS infrastructure is judged to be insignificant and would not result in an integrity failure.

5.2.2 IONOSPHERIC PROPAGATION (Reference 8)

Because WAAS accuracy for Category I precision approach is considerably higher than for NPA through Oceanic operations, the effects of ionospheric abnormalities on WAAS are potentially more significant than described in the GPS-only section. Three types of resulting phenomena will be considered (increased total electron content, increased geomagnetic storms, and increased scintillation), which are all related to the peak of the 11-year solar cycle (next peak in 2000–2001). First, the general increase in the total electron content (TEC) over nominal conditions is well modeled and should be corrected out. This would correspond to the largely prevailing “quiet conditions” at the solar maximum part of the cycle. However, geomagnetic storms become more frequent and intense during the solar maximum period with about two medium-to-severe storms expected per month. About half of these will produce ionospheric disturbances (large temporal and spatial gradients) over CONUS that will last for 2 to 3 hours. Consequently, no more than 36 hours per year (about 0.4 percent of a solar maximum year) will present solar maximum disturbance problems, which was modeled in the simulation evaluations labeled “solar max” in Figure 4-5. In that case, only the Category I performance failed the requirement. Because this could result in integrity failures, it was deemed a “major” consequence with a “reasonably probable” occurrence, resulting in an “undesirable” risk assessment. Mitigation of this risk is being accomplished by an extensive research program conducted by the FAA over the next few years using NSTB and Phase I WRS site data to validate the severity of this effect and develop better modeling and processing techniques [such as tomography (Reference 9)] with more WRSs, if needed.

5.2.3 IONOSPHERIC SCINTILLATION

The third phenomenon that increases near the peak of the solar cycle is the “flickering” effect, called scintillation, described in the previous section. Not only is the WAAS user affected as in the GPS-only case, but the WRS receivers as well (especially the less robust L_2 channel; this was not simulated in our WAAS simulation) (Reference 5). Using the simulation model as described in the GPS/WAAS performance section, the results in Figure 4-5 show some degradation for the northern most CONUS sites, but not as serious as the solar maximum case. Because serious scintillation occurrence for CONUS is a few tens of hours in every 11-year cycle (~$2x10^{-4}$; “reasonably probable”), with a “minor” consequence (no safety factor), this risk was judged “acceptable,” with FAA review. The main mitigation of these effects is to use more robust receivers at the WRSs and especially in the user avionics.

5.3 LAAS RISKS

Naturally, all the signal risks that impact GPS signals will affect LAAS performance. In particular, the interference as experienced at the aircraft will impact GPS/LAAS performance. The only additional interference potential is with the VHF data link between the ground station and the aircraft. Also, because the ground station and the data link represent single points of failure, their reliabilities must meet the LAAS ground station specifications. Assuming careful design, station reliability should not present a significant risk. The ionospheric propagation issues that apply to GPS and GPS/WAAS performance are not a factor for GPS/LAAS. The residual ionospheric errors in the local area differential processing of the GPS/LAAS are not a significant factor at any time in the solar activity cycle. The only ionospheric issue for GPS/LAAS is scintillation.

5.3.1 IONOSPHERIC SCINTILLATION

The same model conditions used for the GPS simulations were applied to GPS/LAAS simulations. The case that was selected for evaluating the scintillation effect was the 24-satellite

GPS constellation with 4 GEOS and 2 APLs. With the scintillation applied, the mean availability for Category I service dropped from above 0.99999 to 0.991; it dropped from above 0.99999 to 0.989 for both Category II and III service. This is again, by the hazard risk process, defined as "acceptable with FAA review."

Appendix A

LIST OF REFERENCES

1. Amadi, et al., “Validation Analysis of the WAAS GIVE and UIVE Algorithms,” ION Proceedings, 53rd Annual Meeting, July 1997.

2. Peck, et al., “User Differential Range Error Algorithms for the Wide-Area Augmentation System," ION Proceedings, 53rd Annual Meeting, July 1997.

3. Walter, et al., “Comparison of Stanford Grid Point Monitoring Algorithms to 3 out of 4 Monitoring,” Stanford University WAAS Laboratory, Unpublished Memorandum, December 1998.

4. Klobuchar, et al., “Potential Ionospheric Limitations to Wide-Area Differential GPS”, ION GPS-93 in Salt Lake City, UT., Sept. 1993.

5. S. Pullen, et al., “A Preliminary Study of the Effect of Ionospheric Scintillation on WAAS User Availability in Equatorial Regions,” ION GPS-98, pp.687-699, Nashville, TN, September 1998.

6. Skone, et al., “Detailed Analysis of Auroral Zone WADGPS Ionospheric Grid Accuracies During Magnetospheric Substorm Event,” ION GPS-98, pp. 701-710, Nashville, TN, September 1998.

7. Peterson, D., “Satellite Navigation Program Update,” presentation to the Space-Based Navigation Industry 1998 Conference, London, England, June 11-12, 1998.

8. Mannucci, A. J., “The Impact of Solar Maximum on WAAS Ionosphere Corrections,” White Paper at JPL, California Inst. Of Tech., February 13, 1998.

9. Hansen, A. J., “Real-Time Ionospheric Tomography Using Terrestrial GPS Sensors,” ION GPS-98, Nashville, TN, pp.717-727, September 1998.

Appendix B

LIST OF ACRONYMS AND ABBREVIATIONS

AC	Advisory Circular
AEI	Auroral-E Ionization
AII	Accuracy Improvement Initiative
AOPA	Aircraft Owners and Pilots Association
AOR-W	Atlantic Ocean Region, West
APL	Airport Pseudolites
ATA	Air Transport Association
CONUS	Continental United States
CRPA	Controlled Radiation Pattern Antennas
DOD	Department of Defense
DOT	Department of Transportation
FAA	Federal Aviation Administration
FCC	Federal Communications Commission
FM	Frequency Modulation
FX	Frequency Excision
FXNONAP	FX and Nonlinear Adaptive Processing
GEOS	Geostationary Satellite
GIVE	Grid Ionospheric Vertical Error
GOSPAR	GPS OCS Performance Analysis and Reporting
GPS	Global Positioning System
GUS	Geostationary Uplink Site

HDTV	High Definition Television
HRI	Hazard Risk Index
ICAO	International Civil Aviation Organization
IMU	Inertial Measurement Unit
IONO	Ionospheric Determination Processing Algorithm
IPP	Ionospheric Pierce Point
JHU/APL	Johns Hopkins University Applied Physics Laboratory
J/S	Jammer-to-Signal Power Ratio
LAAS	Local Area Augmentation System
LEAN	Low-Elevation Antenna Nuller
MASPS	Minimum Aviation System Performance Standards
MCS	Master Control Station
MOPS	Minimum Operational Performance Standards
MTTR	Mean Time to Repair
NAS	National Airspace System
NPA	Nonprecision Approach
NSTB	National Satellite Test Bed
OCS	Operational Control Segment
OD	Orbit Determination Processing Algorithms
OTH	Over the Horizon
POR	Pacific Ocean Region
PPS	Precision Positioning Service
RAIM	Receiver Autonomous Integrity Monitoring
RF	Radio Frequency
RFI	Radio Frequency Interference
RTCA	Requirements and Technical Concepts for Aviation

RTCA, Inc.	A not-for profit organization
SOW	Statement of Work
SPS	Standard Positioning Service
TEC	Total Electron Content
UDRE	User Differential Range Error
UHF	Ultra-High Frequency
USNO	U.S. Naval Observatory
VHF	Very High Frequency
WAAS	Wide Area Augmentation System
WMS	Wide-Area Master Site
WRE	Wide-Area Reference Equipment
WRS	Wide-Area Reference Sites

Appendix C

SPS SIMULATION DESCRIPTION

The simulation used to assess GPS SPS with RAIM computes GPS measurement error statistics for each location and at 5-minute intervals throughout a sidereal day. Both a denser grid of locations and 1-minute interval cases were analyzed and found to not alter results in any significant way. Thus, the baseline locations shown in the report and the 5-minute interval were selected for most of the analyses. Given the computed measurement error statistics, the simulation also evaluates navigation performance represented by accuracy, integrity, continuity, and availability measures.

C.1 MEASUREMENT ERROR STATISTICS

The general structure of the measurement error portion of the simulation is illustrated in Figure C-1.

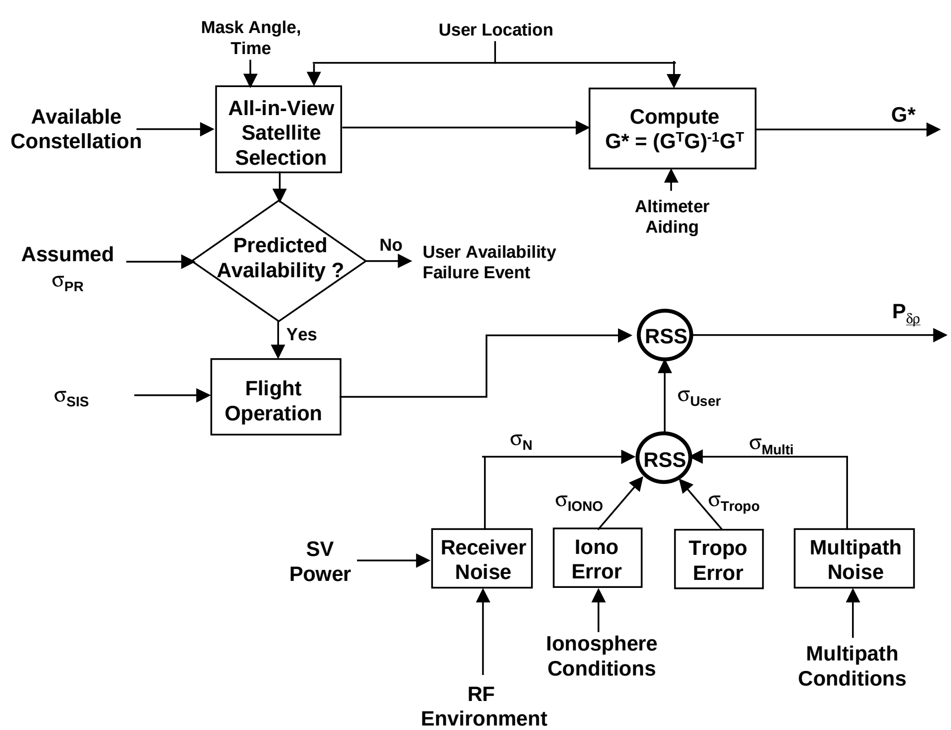

Figure C-1 GPS Measurement Error Simulation Structure

The available constellation defines the satellites in view to a user after accounting for both scheduled and unscheduled downings. The assumed mask angle throughout the study was 5 degrees. The resulting satellites in view and associated directions from the user location are used to form a geometry matrix, G, that provides the least squares solution for position error, $\delta\mathbf{x}$, in terms of pseudo-range error, $\delta\rho$:

$$\delta\mathbf{x} = \mathbf{G}^*\delta\rho, \ \mathbf{G}^* = (\mathbf{G}^T\mathbf{G})^{-1}\mathbf{G}^T$$

The geometry associated with the satellites in view is also the basis for the predictive availability test described in the following sections. Note that additional downings could occur during the operation, and this was taken into account when evaluating continuity. The covariance matrix for pseudo-range error was computed as a function of the signal-in-space ranging error statistics and receiver contributions due to thermal noise, ionospheric compensation error, tropospheric compensation error, and multipath error. Satellite power as a function of elevation angle was based on the combination of satellite signal power given the SPS signal specification and the aircraft antenna gain. The gain above 0-degree elevation angle is specified in RTCA DO-228 and shown in Figure C-2. The simulated value was the average of the minimum and maximum specified values. For negative elevation angles, the study relied on a limited set of measured data taken at the Patuxent River Naval Air Weapons Center (NAWC). This portion of the antenna pattern was needed for analyses of interference effects. Values plotted in Figure C-3 are taken from RTCA DO-235. A plot of the total antenna pattern simulated is shown in Appendix I. Each error component is discussed in the following sections.

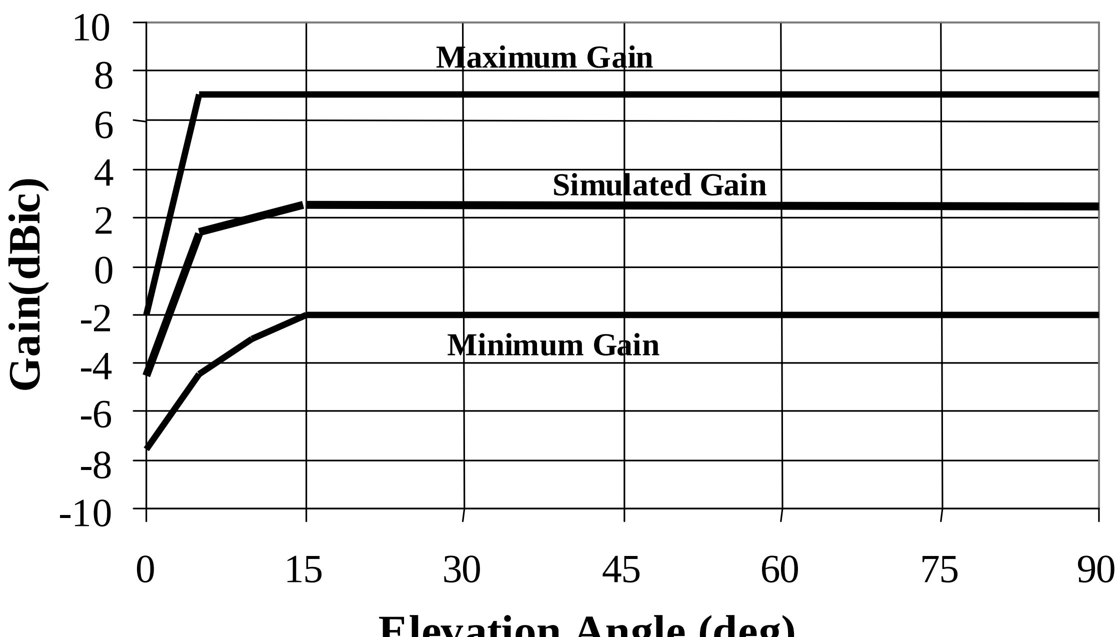

Figure C-2 Simulated Aircraft Antenna Gain

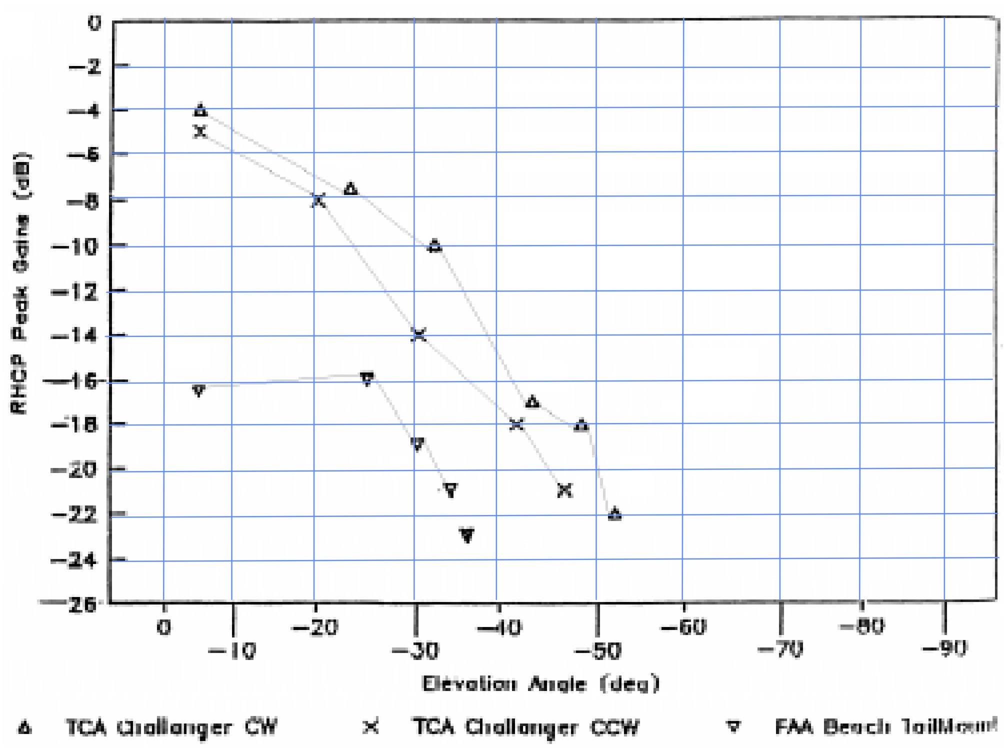

Figure C-3 Measured Antenna Pattern Data

C.1.1 SATELLITE RELIABILITY

Satellite reliability values were based on data gathered as part of the GOSPAR project. Table C-1 summarizes reliability data that have been published. Reference 1 [Phlong and Elrod] presents estimated values that have been used in the past by researchers. The values used in this study were the observed values given in Reference 2. Note the wide disparity between the observed and design values. More recent data (Reference 3) show some additional improvement except in MTTR for scheduled events (note that MTTR for unscheduled events dropped significantly at the same time).

Satellite downings were simulated as follows: Assuming that only one scheduled downing could occur at any time, the probabilities of either none, one, two, three, or four satellites in view being down were computed. Beyond four, the probability is insignificant. For each of those cases, all possible combinations were simulated as measurement events and weighted by the appropriate prior probability. The probability of a scheduled downing is given by:

$$\text{Probability(Scheduled Downing)} = \text{MTTR}/(\text{MTBF}+\text{MTTR}) = 0.124$$

where MTBF=3394/24 was used because only one scheduled downing at a time is assumed. For end-of-life failure, the study assumed a mean time to replacement of 1 month, which is more consistent with specification than the demonstrated values of only a few hours. The more conservative assumption was taken in this case because of the relatively little data available and the dependency on operational policy for which there is presently no guarantee. Sensitivity of performance to this value was run for several cases, but was found to not alter conclusions. Using a Block IIR mean lifetime of 101 months, the overall probability of unscheduled downing is 0.0127.

Table C-1 GPS Satellite Reliability

Satellite Downing Parameter	Ref [1]	Ref [2] *1 Jan 95 – 31 Jul 97*		Ref [3] *1 Jan 95 – 30 Apr 98*	
		Design	Observed	Observed	W/EOL
Unscheduled Events/Satellite/Yr	1.2	3.7	1.0	0.9	-
MTBF (hrs)	7300	2346	11698	13601	12684
MTTR (hrs)	36	17	31	13	13
Scheduled Events/Satellite/Yr	2.0	2.0	1.6	1.6	-
MTBF (hrs)	4380	1529	3394	5120	3239
MTTR (hrs)	4	15.4	20	30.5	-
Total Average Events/Satellite/Yr	3.2	5.7	2.6	2.5	

C.1.2 RECEIVER MODEL

The receiver modeled in this study was assumed to have all-in-view capability with a 5-degree mask angle, narrow gate correlation, an early-late gate correlator, and dot-product discriminator. As a result, the receiver thermal noise contribution to pseudo-range error is modeled in Reference 4.

$$\sigma^2 = 293.25^2 \left[\frac{Bd}{2(C/N_0)}\left(1 + \frac{1}{T(C/N_0)}\right)\right]$$

where T = integration time = 20 msec
B = code loop bandwidth = 0.5 Hz
D = correlator spacing = 0.1
C/N_0 = carrier-to-noise ratio.

The carrier tracking loop noise is modeled by

$$\sigma^2 = \left(\frac{.1903}{2\pi}\right)^2 \left[\frac{B_n}{C/N_0}\left(1 + \frac{1}{2T(C/N_0)}\right)\right]$$

$$B_n = \text{Carrier Loop Noise Bandwidth}$$
$$= 5.8\text{Hz}$$

A noise floor of 0.02 m in delta range due to quantization error was used.

The use of carrier phase smoothing was assumed where the blending filter has the form

$$\hat{PR}(k+1) = \left(\frac{W-1}{W}\right)(\hat{PR}(k) + \Delta PR) + \frac{1}{W} PR$$
$$PR = \text{Measured Pseudo} - \text{Range}$$
$$\Delta PR = \text{Measured Delta Pseudo} - \text{Range}$$
$$\hat{PR} = \text{Smoothed Pseudo} - \text{Range}$$

The smoothing time constant, W, is 100 seconds.

C.1.3 IONOSPHERIC COMPENSATION ERROR

The error due to compensation of delay through the ionosphere is a function of TEC. To form TEC statistics, a gamma distribution was fit to monthly variations of TEC as shown in Figure C-3 (1 nanosecond at L1 = 1.848 TEC units = 0.3-m delay)

A bounding Gaussian distribution has zero mean and δ_{base} = 24 ns. To derive the compensation error, it was assumed that the error is 50 percent of the total delay (Reference 5). Applying diurnal variation, obliquity factor, and location dependent scale factors results in a total standard deviation of the compensation error given by

$$\delta_{err}(t) = 0.5 \text{x } F \text{x } DM(t) \text{x} L_m \text{x } \delta_{base}$$

where

$DM(t)$	= diurnal multiplier	
	= 0.21 ($t < 7$, $t > 21$ hr)	
	= 0.21 + 1.57 cos[$2\pi(t$-14)/28], ($7 < t < 21$ hr)	
L_m	= location multiplier	
F	= obliquity factor	
t	= local time at ionosphere pierce point	
δ_{base}	= 24 ns	

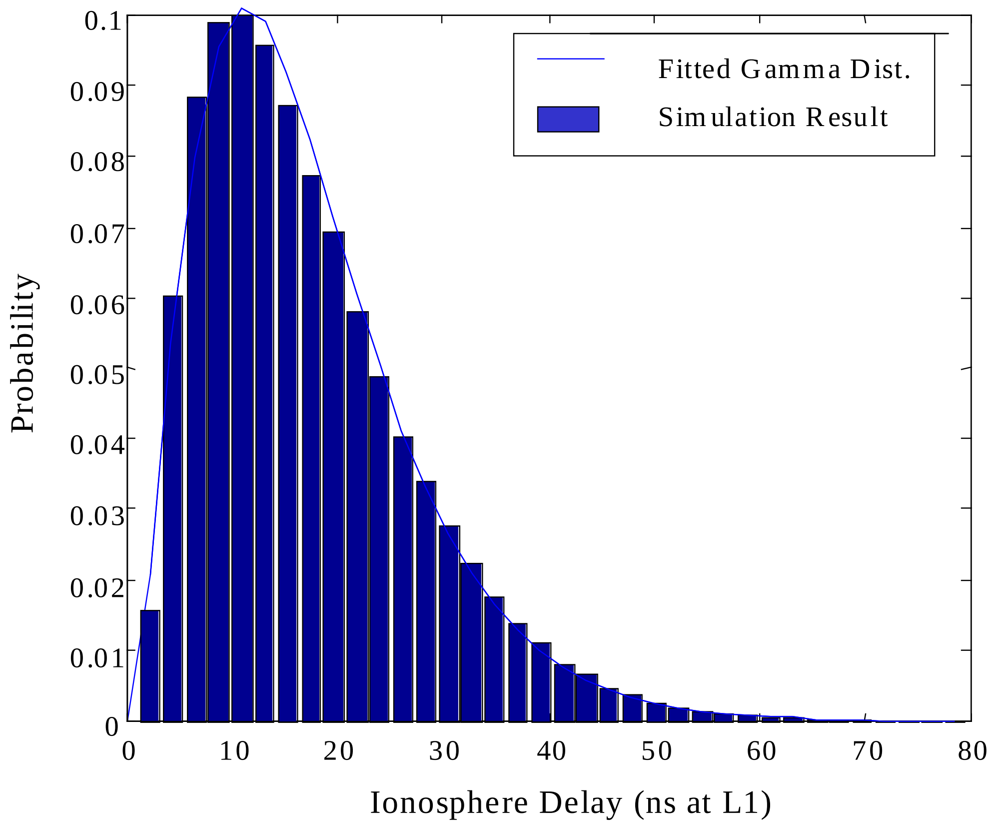

Figure C-3 Gamma Distribution Fit to Simulated Monthly TEC Variation

For the dual-frequency case, the error in the applied refraction correction becomes a function of thermal noise only and is given by:

$$\sigma_{\text{Iono}} = \sqrt{2}\left(\frac{L_2^2}{L_2^2 - L_1^2}\right)\sigma_{\text{Noise}}$$
$$= 2.19\,\sigma_{\text{Noise}}$$

C.1.4 IONOSPHERIC SCINTILLATION

Ionospheric scintillation can degrade GPS signal reception when a satellite's line of sight pierces a scintillation region of the ionosphere. CONUS GPS users are most likely to be affected by scintillation in the auroral region that covers the northern part of Canada. Auroral scintillation is a rare event that was included as one of the anomalous simulation cases and was implemented by approximate means in the JHU/APL SPS simulations.

Although auroral scintillation is assumed to be present only during a limited time, a normal 1-day SPS simulation was run with following scintillation effects procedure added:

a. After resolving removals due to satellite health at a given universal time code (UTC) time and user location, all ionospheric pierce point locations were checked for all usable GPS satellites (and GEOS).

b. For each ionospheric pierce point within the auroral oval, the local time at that pierce point was checked. (Note that locations are at *geomagnetic*, not *geographic*, latitudes.)

c. If at least one ionospheric pierce point was found within the auroral zone with a local time between 1900 and 2400, that satellite might be unusable and must be removed from the user geometry. If the pierce point had a local time between 2000 and 2200, *strong* scintillation was assumed and that satellite is eligible for removal if the C/N_0 is less than 48 dB-Hz. If the pierce point had a local time between 1900 and 2000 or between 2200 and 2400, *moderate* scintillation was assumed, and the satellite is eligible for removal if the C/N_0 for the affected satellite is less than 38 dB-Hz.

d. Given a satellite is eligible for removal because of scintillation, the probability that the satellite signal is lost was assumed equal to 0.3.

The prior probability of this scintillation scenario was based on an estimate that only 1 day in the 11-year solar cycle would have an auroral scintillation event this severe, giving it an approximate probability of $1/[(365.25)(11)] \cong 0.00025$.

C.1.5 TROPOSPHERIC COMPENSATION ERROR

The error due to troposphere delay may be approximated (Reference 6) by

$$\text{Delay (m)} \sim 2.47e^{-0.133h}/(\sin E + 0.012)$$

where h = altitude in km above sea level
E = elevation angle

Based on data given in Reference 6, a conservative estimate of the corresponding compensation error is up to 8 percent of this value. Assuming this to be a 2σ value, the simulated error was

$$\text{Error } (1\sigma, \text{m}) = 0.1e^{-0.133h}/(\sin E + 0.012)$$

C.1.6 MULTIPATH ERROR

The model of multipath error was based on data reported in Reference 7. Because these data were taken for wide-body aircraft, they most likely represent a conservative assumption when applied to all aircraft. A bounding standard deviation value of $\sigma = 0.5$ m was simulated.

C.1.7 SIGNAL-IN-SPACE ERROR

The signal-in-space error was based on reported data (Reference 8) and expected accuracies of future GPS upgrades as estimated by the GPS/Joint Project Office (JPO) (Reference 9). Current performance assumes selective availability is on. If selective availability were removed today, the signal-in-space error would approximately be 2.3 m. If selective availability were removed at the time when benefits of the AII are fully in place, the signal-in-space error would be approximately 1.5 m. Ultimately, signal-in-space error could be less than 1.0 m. Table C-2 illustrates the potential improvement in overall user equivalent range error (UERE) as selective availability is removed, AII is in place, and a second civil frequency is provided. Average values are used in the table where error sources are a function of satellite elevation angle.

Table C-2 Total Ranging Error versus System Improvement

Error Source	GPS System Improvement			
	SA	NO SA	NO SA AII	NO SA Dual Freq
Signal-in-Space	24	2.3	1.5	1.0
Ionospheric Compensation	7	7	7	2
Tropospheric Compensation	0.2	0.2	0.2	0.2
Multipath	0.5	0.5	0.5	0.5
Airborne Receiver Noise	.17	.17	.17	.17
Total UERE (m)	25	7.4	7.2	2.3

C.1.8 RECEIVER AUTONOMOUS INTEGRITY MONITORING

The algorithm simulated to represent receiver autonomous integrity monitoring was based on the algorithm derived by Brown (Reference 10). The algorithm used to determine predictive availability is summarized as follows:

Check > 5 SVs in View

For each N-1 subset of satellites:

$$S = I - GA, \quad A = (G^T G)^{-1} G^T$$

$$\text{Slope}(i) = \sqrt{a_{1i}^2 + a_{2i}^2} / \sqrt{S_{ii}}, \quad i = 1,2,\ldots, N-1$$

$$\text{Slope}_{max} = \max(\text{Slope}(i))$$

Select RAIM threshold, T, based on σ^2 distribution to satisfy false-alarm rate using:

$$p^T p > T$$
$$E[p^T p] = \sigma^2 I$$

$$\sigma = \begin{cases} 25 \text{ m, selective availability On} \\ 7.5 \text{ m, selective availability Off} \end{cases}$$

Given RAIM threshold, compute minimum range bias (p_{bias}) that can be detected to satisfy missed detection rate = 0.0001.

$HPL_{Max} = \text{Max}(Slope_{Max} \times p_{bias})$ Over All N-1 Subsets
Test HPL_{Max} < Alert Limit

The false-alarm rates used, corresponding to the 10^{-5} or 10^{-6} continuity requirement, were 1.67×10^{-7} or $1.67\text{x}10^{-8}$ for selective availability ON and 5×10^{-7} or $5\text{x}10^{-8}$ with selective availability OFF. These values were derived by allocating half of the continuity requirement to false alarms and the other half to faults not isolated. In addition, it was assumed that with selective availability ON, the measurements become decorrelated at 2-minute intervals. Thus, to satisfy the continuity requirement on a per-hour basis, the continuity requirement was divided by 30. Without selective availability, it was conservatively assumed that there are 10 independent measurements in 1 hour. Under normal conditions, it is expected the measurements would be highly correlated, but this more conservative assumption was made to allow for off nominal variations due to multipath or ionosphere.

The actual RAIM test during the operation is given by a test of the least-squares residual magnitude squared (or equivalently, parity vector magnitude squared) against the derived threshold.

$$D = \underline{\delta\rho}^T (I - GG^*) \underline{\delta\rho}$$

$$D < T$$

C.2 PERFORMANCE EVALUATION

Evaluation of the requirements given the measurement error statistics computed was based on the general diagram discussed in the main report. A diagram specific to SPS is shown in Figure C-4.

Given that the predictive availability test was passed, position error statistics are used to determine if the accuracy requirement is passed; pseudo-range statistics are used to determine if the continuity requirement is passed. The joint statistics between satisfaction of the RAIM threshold and accuracy is used to determine the probability of loss of integrity. If both the accuracy and integrity requirements are met, that is flagged as a true availability event. For each location, the total accuracy, integrity, continuity, and availability are computed by summing the products of the prior probability and the conditional probability for each performance measure.

Recall measurement events are associated with time of day and the combination of satellites that are downed.

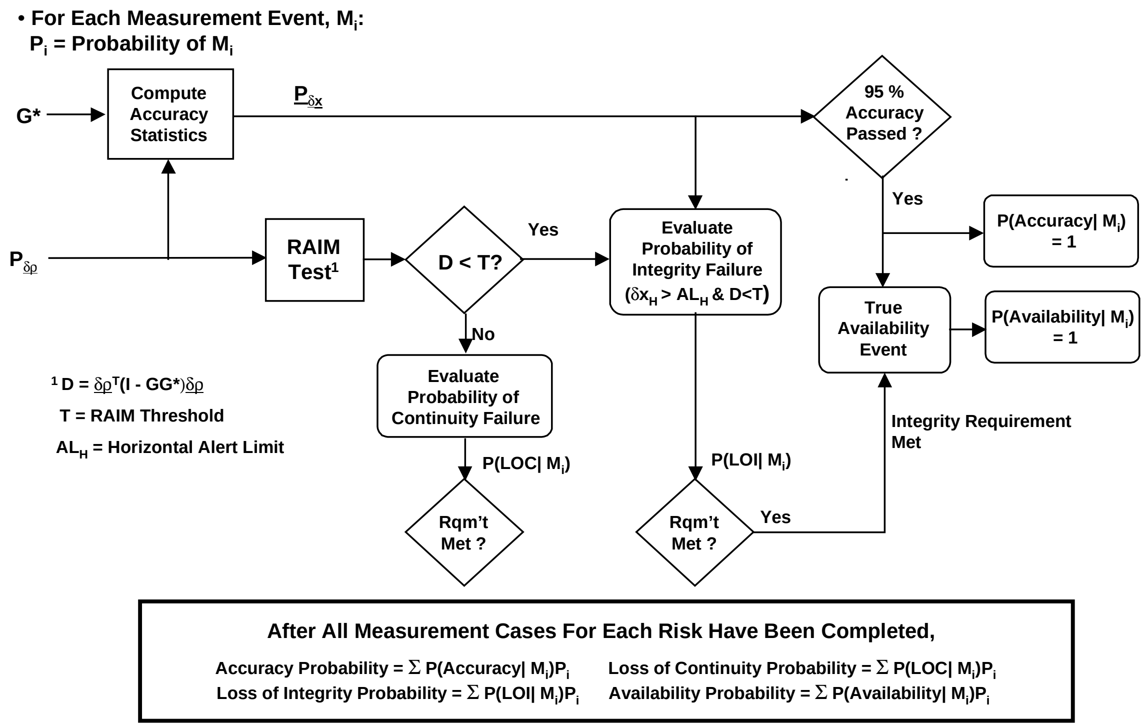

Figure C-4 Performance Evaluation

C.3 REFERENCES

1. W. S. Phlong and B. D. Elrod, "Availability Characteristics of GPS and Augmentation Alternatives," *Navigation,* Vol. 40, No. 4 Winter 1993-94, pp. 409-428.

2. R. Conley, "Results of the GPS JPO's GPS Performance Baseline Analysis: The GOSPAR Project," *Navigation,* Vol. 45, No.1, Spring 1998, pp.1-15. Data based on 1 January 1995 to 31 July 1997.

3. R. Conley, "Long-Term Trending of GPS Performance Characteristics," *Proceedings of the 54th Annual Meeting*

4. A. J. Van Dierendonck, "GPS Receivers," *Global Positioning System: Theory and Applications*, Vol. I, AIAA.

5. J. A. Klobuchar, "Ionospheric Effects on GPS," *Global Positioning System: Theory and Applications*, Vol. I, AIAA.

6. J. J. Spilker, “Tropospheric Effects on GPS,” *Global Positioning System: Theory and Applications*, Vol. I, *AIAA*.

7. T. Murphy and R. Snow, “GPS Multipath on Large Commercial Air Transport Airframes,” *Navigation*, Vol. 43, No.4, Winter 1996–1997.

8. R. Conley, “GPS Performance Characteristics and Trends,” ION-GPS 95.

9. Brown, K., “Dynamic Uploading for GPS Accuracy,” *Navigation*, Vol. 45, No. 1, Spring 1998.

10. R. G. Brown, ”Receiver Autonomous Integrity Monitoring,” *Global Positioning System: Theory and Applications*, Vol. II, AIAA.

Appendix D

GPS/WAAS SIMULATION DESCRIPTION

The simulation for GPS/WAAS is provided through modification of the GPS-SPS simulation. The primary differences are associated with the signal-in-space characteristics (due to the WAAS-unique corrections), and the computational details related to predictive availability, integrity, and continuity. GPS satellite downings and aircraft equipment models are the same as in the GPS-SPS simulation. The modified simulation computes GPS measurement error statistics for each location (defined in Figure 3-3 in the main body of the report) at 5-minute intervals throughout a sidereal day. Given the computed measurement error statistics, the simulation then evaluates navigation performance represented by accuracy, integrity, continuity, and availability measures. This appendix first briefly describes the WAAS from which the simulation approach to modeling the WAAS errors is developed. Errors specific to WAAS are described, along with the process of determining the performance measures.

D.1 WAAS ERROR MODEL

The architecture in Figure D-1 (same as Figure 4-2 of the main report) shows all the functions that need to be modeled for proper assessment of WAAS performance. The WRS, WMS, GUS, GEOS all provide the added WAAS capability as well as the WAAS-unique integrity checks in the user avionics. A complete end-to-end simulation would require a significant modification to the SPS simulation that would dwarf the SPS-only portion. Modeling all of the WRS measurement functions feeding the WMS estimation and integrity functions would correspond to modeling the GPS ground-tracking network feeding the MCS orbit determination and upload functions. Of course, this type of simulation is desirable from the standpoint of being, in principle, fully sensitive to all normal error sources and abnormal risks. Error distribution inputs could be validated by NSTB databases. However, the required extensive modeling and programming staff was beyond the scope of this study.

A more efficient partial middle-to-end simulation was chosen, which models WMS estimation output errors developed from extensive NSTB databases as satellite error models to the existing GPS-only simulation (with added GEOS) as shown in Figure D-2. Raw NSTB WRS CONUS output were collected at a 1-Hz rate over a 2-day period from 5–6 May and processed at the Stanford WMS using Stanford orbit determination and ionospheric processing. UDRE and GIVE distributions were spatially functionalized per satellite geometry with respect to WRS positions. Specifically, UDRE values were functionalized per satellite geometry with respect to the earth by averaging all values in a 5° x 5° box about a grid-point with 5° grid spacing on a sphere at GPS satellite altitude. GIVE values were similarly functionalized per 5° grid point on an ellipsoid at 350-km altitude. Several other sets of NSTB data were taken on 21 May, 3 June, 14 June, and 23 July to validate that the original 2-day results were representative. Variability of individual UDREs and GIVEs over time was minimal. These models essentially replaced the detailed simulation of the WRSs and the WMS with less-extensive modifications to the GPS-SPS simulation. NSTB data collected at several static user sites in 1997 and 1998 show that the UDRE and GIVE values give an upper bound to actual user vertical and horizontal position errors. Therefore, for this period at least, use of the sigmas related to the UDREs and GIVEs (UDRE or GIVE = 3.29σ) as the predictive WAAS statistical model will produce conservative results. The added value of this approach is that it is based on actual NSTB data experience using the Stanford orbit determination and ionospheric estimation algorithms. CONUS evaluations were produced from a 19-WRS CONUS database, while Alaska and Hawaii evaluations were based on an additional five WRSs in Alaska and two in Hawaii.

Models of Raytheon orbit determination and ionospheric processing at the WMS were obtained by comparing Raytheon-published GIVEs and UDREs (References 1 and 2) with corresponding Stanford results over the same geographic area, yielding scaling factors on the NSTB/Stanford models. In both cases, however, the less conservative Stanford 15° restriction for valid ionospheric grid points (see Figure D-3) was assumed rather than the more conservative three-of-four restriction of the WAAS Specification and Raytheon processing. The three-of-four restriction significantly reduces availability and was not evaluated. To evaluate the three-of-four restriction in the context of this simulation would have required many more WRSs (estimated to be about 40 to 50) providing real raw data to WMS processing. JHU/APL believes that the NSTB database and Stanford processing results have tended to indicate adequate integrity of the Stanford processing and less conservative restriction (Reference 3). Further research is needed to validate this indication.

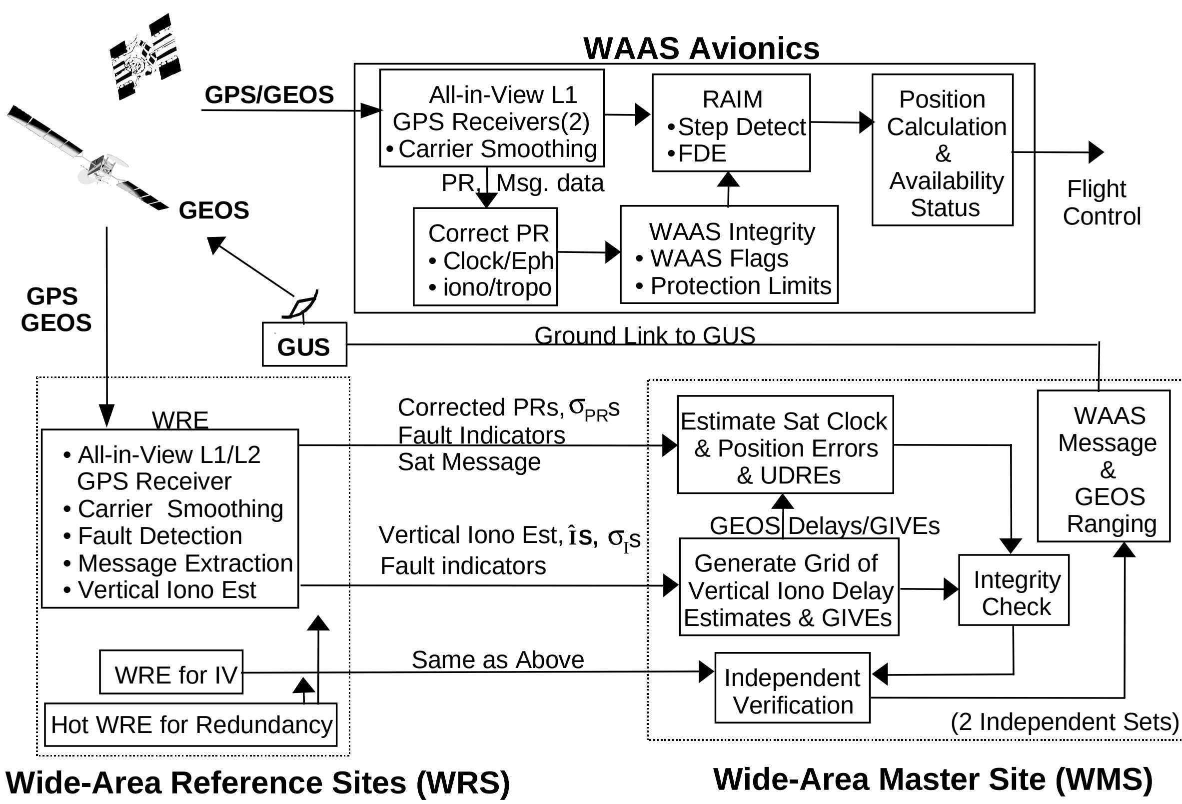

Figure D-1 GPS/WAAS Architecture

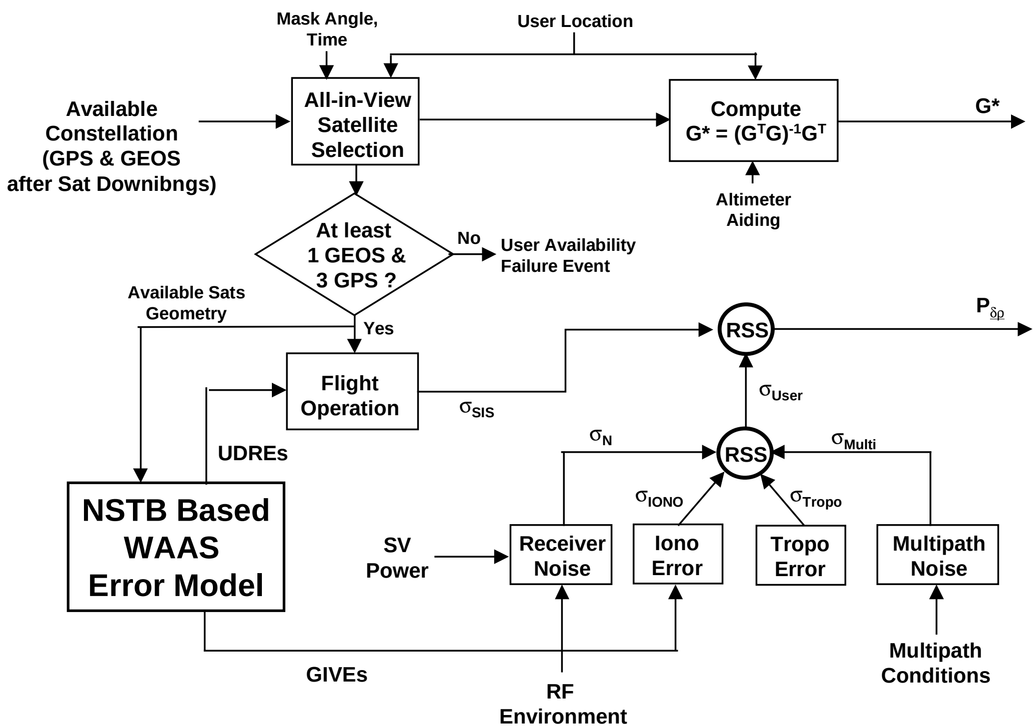

Figure D-2 WAAS Measurement Error Simulation Structure

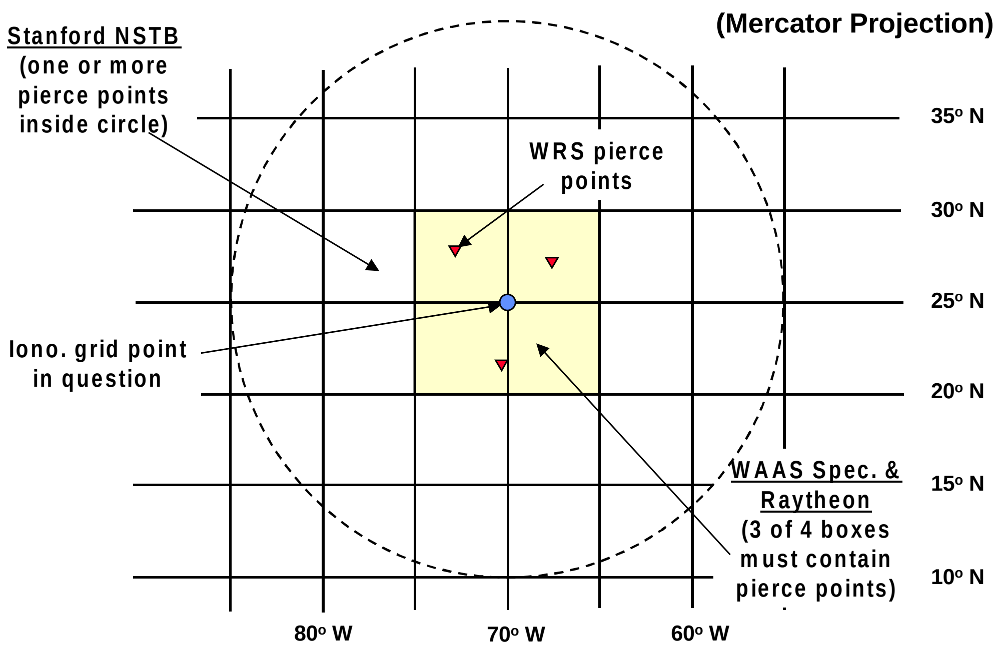

Figure D-3 Comparison of Proposed Ionospheric Gridpoint Validity Constraints

The modifications to the model used to simulate solar maximum results were based on scaling up the NSTB functionalized GIVE model, as suggested by Klobuchar, et al. (Reference 4). A conservative factor of 3 was used to model the decorrelation effects due to the large spatial gradients during geomagnetic storms. The scintillation model was similar to that described for the SPS case in Appendix C and was based on Pullen, et al. (Reference 5) and Skone, et al. (Reference 6). Areas of moderate to strong scintillation were designated in the auroral region. User ionospheric pierce points that fell within these regions were checked to see if loss-of-lock occurred, affecting the availability of that measurement.

The error models used to determine the covariance matrix of slant range measurement errors, $\mathbf{P}_{\underline{\delta\rho}}$ (shown in Figure D-2), are the same as the SPS models described in Appendix C, except that σ_{SIS} and σ_{IONO} are defined as:

$$\sigma_{SIS} = \sqrt{\left(\frac{UDRE}{3.29}\right)^2 + \sigma_{SAL}^2}$$

where σ_{SIS} is the ephemeris/clock pseudo-range error sigma for each satellite-to-user link and σ_{SAL} is the 1-sigma error resulting from quadratic error growth caused by the 7-second latency in correcting for selective availability (Reference 7), which is 11.3 cm (Reference 8).

$$\sigma_{IONO} = F(el)\sum_{i=1}^{n} W_i(x_{pp}, y_{pp})\frac{GIVE_i}{3.29}$$

where σ_{IONO} is the ionospheric pseudo-range error sigma for each satellite-to-user link, $F(el)$ is the obliquity factor as a function of the user elevation angle to each satellite, and n is 3 or 4 because each user ionosphere pierce point must be surrounded by valid GIVEs on at least three of the four neighboring 5° x 5° grid-points. The weights $W_i(x_{pp},y_{pp})$ and computation of $F(el)$ are defined in the WAAS MOPS RTCA/DO-229A. The rest of the computations of the WAAS simulation in Figure D-2 are as described in Appendix C for the GPS-SPS simulation.

D.2 WAAS RELIABILITY

GPS reliability was the same as modeled in Appendix C. GEOS reliability was modeled in the same way and is defined in Table D-1, along with the reliability parameters for the WAAS ground segment. Because the output of the WAAS ground segment (WRS to WMS to GUS) is being simulated using representative real-world test data, estimate its availability and consider it in series with the simulation's availability. Each GEOS availability is appropriately handled in the satellite geometry/accuracy simulation. Note also that the portion of the total WAAS/GPS availability due to GPS downings and improved accuracy (due to WAAS) will be carried on in the user avionics part of the simulation, as before in the GPS-SPS simulation. These calculations assumed a full network of 25 WRSs, 2 WMSs, and 2 GUSs per GEOS as shown in Figure D-4. The failure rate calculations were based on the reliability parameters of Table D-1. The WAAS ground segment availability can be estimated from the WAAS hardware diagram in Figure D-4. This is the a priori probability of at least N (of 25) WRSs (with communications to WMSs), at least 1 WMS (with communications to GUSs), and at least 1 of 2 GUSs (with communications to its GEOS) all operating for each GEOS in the program phase of interest (GEOS outages are counted separately). The results are shown in Table D-2. The NSTB database has shown acceptable accuracy for 19 WRSs. Therefore, the N >= 23 probabilities were used as multipliers on the availability values obtained from the GPS/WAAS simulation.

Table D-1 WAAS Reliability

Site Health Per WRS, WMS & GUS

	MTBF	MTTR
Unscheduled Outage*	2190 hours	45 min.
Scheduled Outage*	2190 hours	8 hours
WRS site (experienced)+	15,600 hours	25.2 min.
WMS site (experienced)+	1248 hours	52.3 min.
GUS(SGS)+	3328 hours	31.3 min.
GUS(RFU) & Com link+	2310 hours	4.2 hours

* FAA-E-2892C WAAS draft spec
\+ Brian Mahoney e-mails of 11/18/98, 11/24/98 12/01/98, 12/02/98 includes preventive maintenance that disrupts normal operation

Communications Availability

	Availability
WRS to WMS+	.99999
WMS to GUS+	.99999
GUS to GEO	GUS site health

\+ Brian Mahoney e-mails of 11/18/98 , 11/24/98, 12/01/98

GEOS Sat Outage Rates and Duration*

	Outage Rate	Mean Duration
Short Outage Mode*	0.083/year	19.8 hours
Long Duration Mode(build/launch new sat)*	0.014/year	3 years
Long Duration Mode(use on-orbit sats)**	0.014/year	3 months

* FAA-E-2892C WAAS draft spec ** Sam Pullen e-mail of 12/18/98

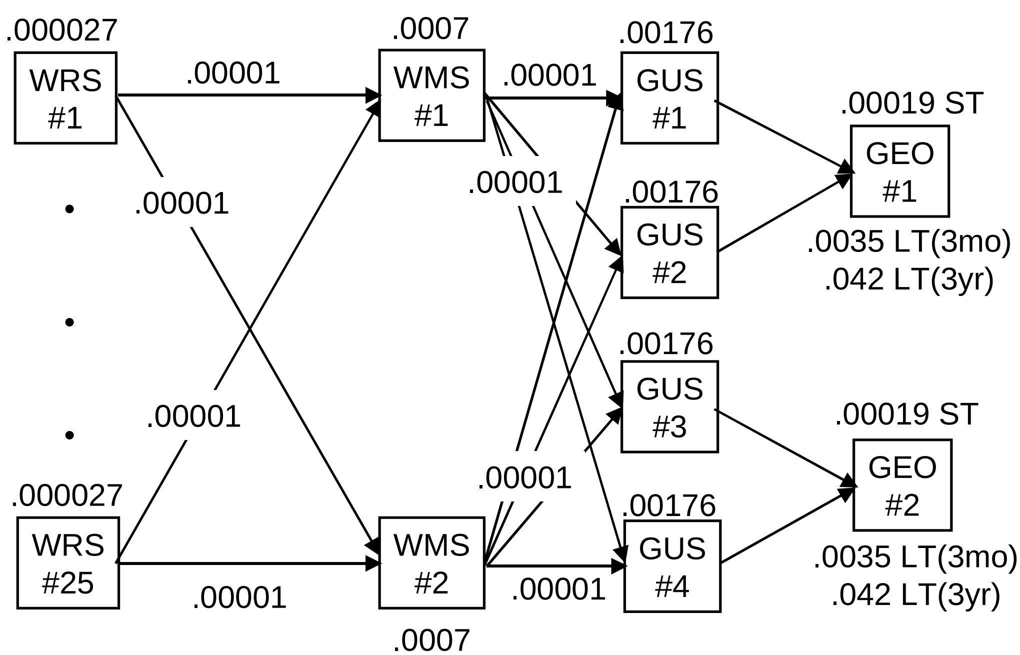

Figure D-4 WAAS Hardware Availability

Table D-2 WAAS Ground Segment Availability

Using	N=25	N>=24	N>=23
2 GEOS	.999068742083	.999992914863	.999993325211
3 GEOS	.999074906931	.999999085414	.999999495765
4 GEOS	.999074906950	.999999085433	.999999495784
5 GEOS	.999074906950	.999999085433	.999999495784

The continuity of the WAAS ground segment must also be handled in an analogous manner as for availability. Continuity is expressed as the probability of failure per time period of interest, dt, computed as $1 - e^{-\lambda dt}$, where $\lambda = 1/MTBF$. Consequently, continuity failure rates can be determined from Table D-1 for each WAAS ground site, and a continuity failure diagram analogous to Figure D-4 can be made. This was then used to calculate WAAS ground segment continuity probabilities in the same manner as done for Table D-2. These results are shown in Table D-3. As with availability, the N >= 23 column was chosen to add the continuity failure rate to the simulation calculated failure rate. These numbers will decrease by a factor of 24 to obtain the failure rates for Category I (150-second mission time).

Table D-3 WAAS Ground Segment Continuity Failure Rates per Hour

Using	N=25	N>=24	N>=23
2 GEOS	.001602981	.000002948	.000001717
3 GEOS	.001601909	.000001874	.000000643
4 GEOS	.001601909	.000001874	.000000643
5 GEOS	.001601909	.000001874	.000000643

D.3 PERFORMANCE EVALUATION PROCESS

Evaluation of the requirements given the measurement error statistics computed in Figure D-2 is based on the diagram specific to GPS/WAAS as shown in Figure D-5. Lookup tables of NSTB-derived UDREs and GIVEs are read into the simulation. The simulation cycles through one repeatable day of GPS geometries with GEOS added. All-in-view GPS + GEO satellite geometry is computed for each user location (assuming all satellites are healthy). For each user and nominal geometry, the simulation cycles through all possible no-SV-out, 1-SV-out, 2-SV-out, 3-SV-out, and 4-SV-out cases (outage case probabilities add to > 0.999999 to ensure enough outages have been sampled). Each outage case is checked for predictive availability by the integrity check. If available, accumulators are incremented by the prior probability of the given outage. For each location, the total accuracy, integrity, and availability are computed by summing the products of the prior probability and the conditional probability for each performance measure. Recall measurement events are associated with time of day and the combination of satellites that are downed.

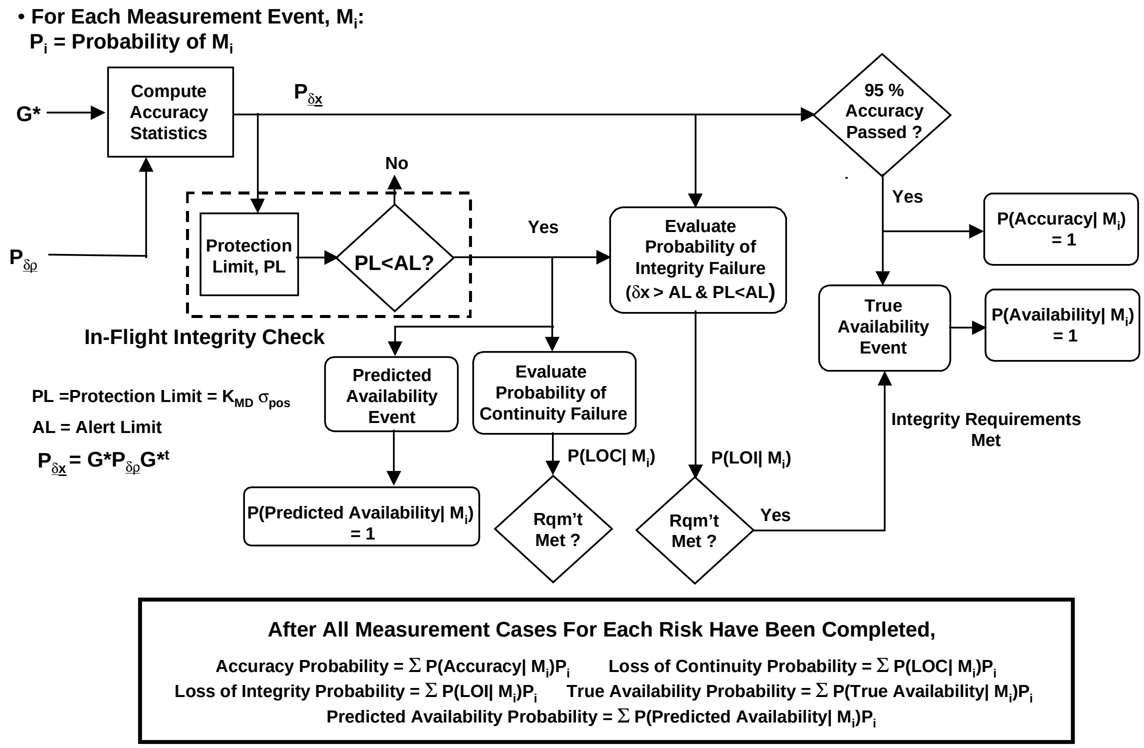

Figure D-5 GPS/WAAS Performance Evaluation

If a real Monte Carlo simulation were being done over time, the integrity check would be used to determine continuity failures over the required interval of time because the protection limit would change at a high rate as a result of the high-rate UDREs, GIVEs, and fault indicators from the WMS. (A NO during the flight operation would be considered a continuity failure.) Because this is a snapshot evaluation, the in-flight integrity check only assesses predictive availability at the beginning of the flight operation and continuity failures have to be assessed separately by

a. Calculating the failure probability over the mission time, $1 - e^{-\lambda dt}$ (where $\lambda = 1/MTBF$), for each remaining good satellite (summed with the WAAS ground segment continuity)

b. Checking to see if the in-flight integrity check fails with that satellite removed

If the in-flight integrity check fails, the failure probability is placed in the continuity histogram. Because the continuity requirement is separate from availability for WAAS (see Section 2.1 in the main report), the continuity histogram must show all probabilities less than the continuity requirement and all availabilities greater than their requirement for the particular mission to be acceptable. In general, the evaluation results for two GEOS showed that the continuity requirements would be violated during the en route and terminal phases because of their most demanding requirement ($1x10^{-6}$ per hour). The four- and five-GEOS cases generally passed whenever availability passed.

WAAS availability results cited in this report are based on predicted availability, which is identical to the procedure that aircraft apply to determine their WAAS availability according to the WAAS MOPS (RTCADO-229A). Because the same NSTB UDRE and GIVE data were used to generate predicted availability and true availability (which does not demand continuity to be satisfied), they are essentially equivalent if the AL is a tighter constraint on nominal position accuracy than is the 95-percent accuracy requirement. This is generally true for a well-designed system.

Finally, the GPS/WAAS simulation did not model for the fallback to GPS-SPS when all GEOS were lost (usually a very small probability). In this case, the availability of GPS-SPS multiplied by the probability of no GEOS was added to the simulation availability to include this effect.

D.4 REFERENCES

1. Amadi, et al., "Validation Analysis of the WAAS GIVE and UIVE Algorithms," *ION Proceedings, 53rd Annual Meeting*, July 1997.

2. Peck, et al., "User Differential Range Error Algorithms for the Wide-Area Augmentation System," *ION Proceedings, 53rd Annual Meeting*, July 1997.

3. Walter, et al., "Comparison of Stanford Grid Point Monitoring Algorithms to 3 out of 4 Monitoring," Stanford University WAAS Laboratory, unpublished memorandum, December 1998.

4. Klobuchar, et al., "Potential Ionospheric Limitations to Wide-Area Differential GPS", *ION GPS-93*, Salt Lake City, Utah, September 1993.

5. S. Pullen, et al., "A Preliminary Study of the Effect of Ionospheric Scintillation on WAAS User Availability in Equatorial Regions," *ION GPS-98*, pp.687-699, Nashville, Tennessee, September 1998.

6. Skone, et al., "Detailed Analysis of Auroral Zone WADGPS Ionospheric Grid Accuracies During Magnetospheric Substorm Event," *ION GPS-98*, pp. 701-710, Nashville, Tennessee, September 1998.

7. P. Eng, "WAAS Messaging System: Data Rate, Capacity, and Forward Error Correction," *Navigation: Journal of the ION*, Vol.44, No. 1, spring 1997.

8. S. Pullen, "GEO SV Probabilities and selective availability Error," E-mail to Larry Levy on 19 December 1998.

Appendix E

GPS/LAAS SIMULATION DESCRIPTION

The simulation for GPS/LAAS was provided through a modification of the GPS-SPS simulation. The primary differences are associated with the signal-in-space characteristics (due to the use of differential positioning techniques), and the computational details related to predictive availability, integrity, and continuity. The details with regard to GPS satellite downings and aircraft equipment models are identical. The need for the differences is in the method of positioning.

E.1 RELATIVE POSITIONING

The GPS/LAAS concept is illustrated in Figure E-1. Both the aircraft and the LAAS ground station (LGS) are using signal measurements to determine *slant range* (i.e., line-of-sight distance) from each in-view GPS satellite. These measurements allow the aircraft and the LGS to derive their positions relative to the satellite locations identified by messages provided in the satellite signals. The absolute positions of the aircraft and the LGS are limited by several error sources that do not limit a measure of the difference in their positions. For example, because the satellites are very far away (>10,000 nmi) and the aircraft and LGS are very near (<30 nmi), large errors in the locations of the satellites are almost absent in the measurement of *relative position* of the aircraft with respect to the LGS. Therefore, GPS satellite ephemeris errors do not significantly influence the relative position measurement. More importantly, in the near term, the *selective availability* feature of the GPS signals is also virtually eliminated in the relative positioning measurement. (Selective availability is a signal technique that causes the absolute position of civil GPS users to randomly wander producing an uncertainty of ~100 m.) The relative positioning process removes this limitation. That is, the absolute position wander at the aircraft is virtually identical to the wander at the LGS; therefore, its effect is removed in the relative position measurement. Furthermore, errors caused by signal refraction in the ionosphere are also virtually eliminated by the relative positioning process (i.e., refraction errors at the aircraft are virtually identical to refraction errors at the LGS). The proper removal of these errors requires that the update rate of the relative positioning corrections is fast enough to follow the error rates, which are dominated by the selective availability error rate. The 0.5-second correction rate of the GPS/LAAS operation is sufficient to essentially zero these three error contributors (i.e., selective availability, ephemeris, and ionosphere).

The functional implementation of the concept is shown in Figure E-2. The aircraft and LGS receive signals from all in-view GPS satellites (and GEOS when applicable), and the LGS determines which, if any, are not yet suitable for positioning service. The LGS then determines a correction for the measured slant range to each satellite by comparing them to ones computed from the known LGS location to each satellite location identified by the received satellite ephemeredes. These slant range corrections are sent to the aircraft, where they are applied to the measurements provided by the aircraft receiver. The corrected aircraft receiver measurements are then used to compute aircraft position. The aircraft position is thus transferred to the same absolute position domain as the LGS restricted only by the errors in the relative position measurement between the aircraft and the LGS.

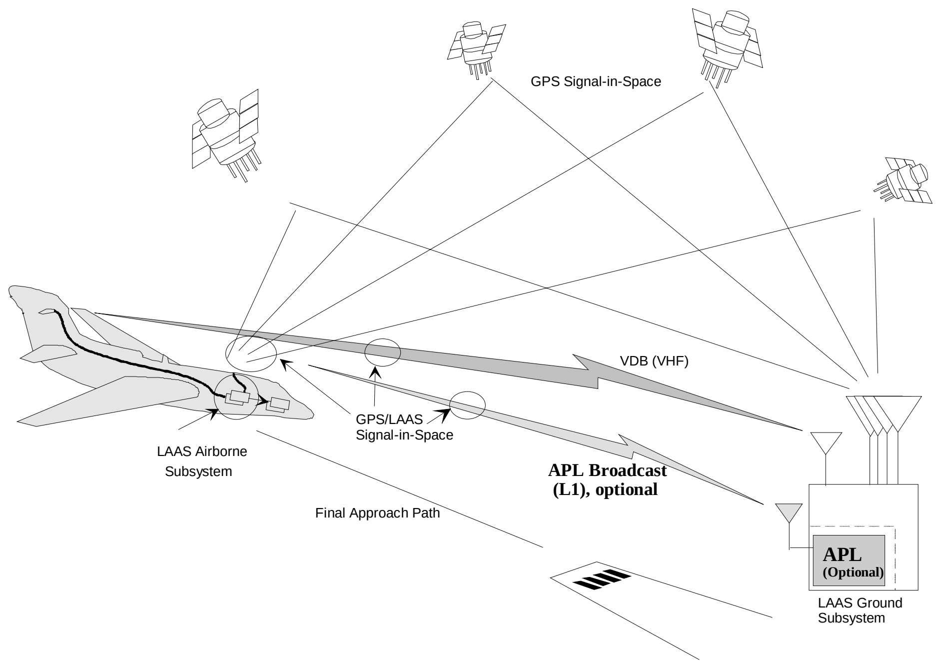

Figure E-1 GPS/LAAS Relative Positioning Concept (from GPS/LAAS MASPS-7, 7/22/98)

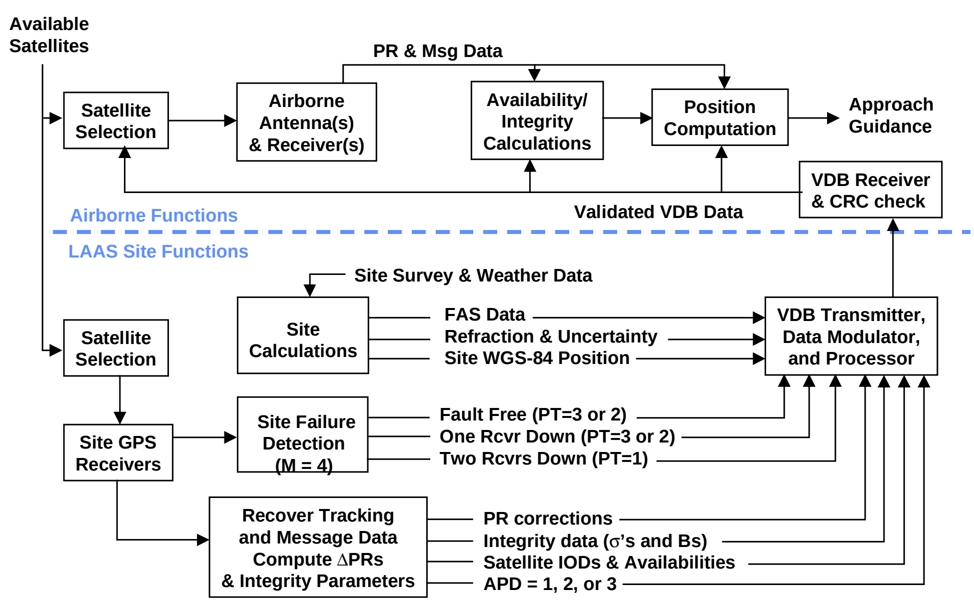

Figure E-2 GPS/LAAS Functional Block Diagram

In addition to the pseudorange correction data, the LGS transmits a set of data that characterizes the level of service available, integrity data used in the aircraft equipment to assess the accuracy of the position solution, and data that indicate satellite support status. The integrity data provide an uncertainty value for each satellite pseudorange correction and an estimated bias that might be attributed to each receiver measurement used in computing the correction. The bias values are used in the airborne computation to predict lateral and vertical protection limits for fault-free and single-measurement fault conditions. Finally, the LGS transmits the data defining the approach path to be used by the aircraft. The locations along the approach path are naturally known with very high position accuracy relative to the LGS.

E.2 SIMULATION

Figure E-3 shows how the GPS/LAAS simulation was accomplished. The GPS-SPS simulation provided all aspects of the GPS satellite selection process; they were discussed in Appendix C. The measurement error computation for the signal-in-space contribution is very different, but the avionics errors are directly from the GPS-SPS simulation. As shown, the lateral and vertical error distributions are computed from true sigma estimates from simulated models. These distributions are used to test the accuracy and integrity requirement at each measurement point (i.e., tests that the 95-percent accuracy and misleading information requirements are met). The probability of providing misleading information is computed from the area of the accuracy distribution beyond the alert limits. Combined signal-in-space (*ground* LGS computation), *airborne*, and *tropospheric* errors (producing σ_i) are used to compute predicted protection limits. The protection limits are compared with the alert limit requirements to test for predicted availability. Finally, continuity is tested.

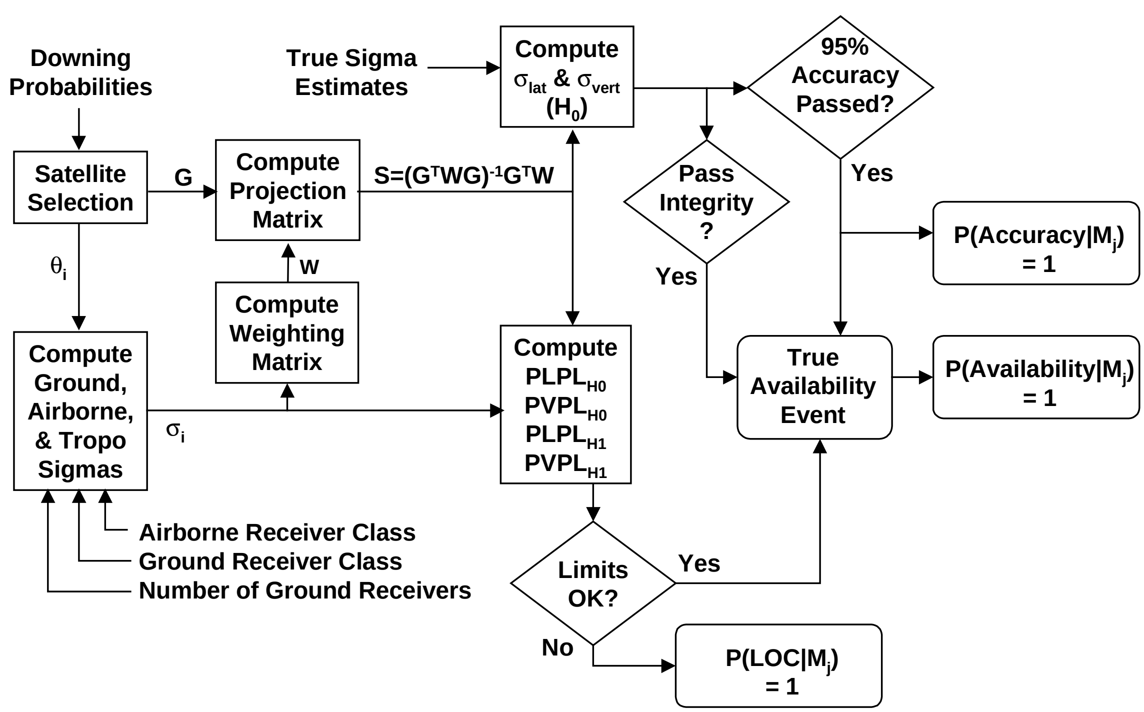

Figure E-3 GPS/LAAS Simulation Structure

Protection limits are defined for lateral and vertical position uncertainties, and they define the values that must not be exceeded for safe landing. The aircraft and, hence, the simulation computes a Predicted Lateral Protection Limit (PLPL) and a Predicted Vertical Protection Limit (PVPL). These values are computed under the assumption that all LGS reference receivers are providing unbiased range correction data (referred to as the H_0 hypothesis) and that one of the provided measurements may contain a bias error (referred to as the H_1 hypothesis). These numbers are tested against the specified limits to predict that the approach is available.

E.2.1 MEASUREMENT ERRORS

The pseudo-range measurement (the term *pseudo-range* is used for GPS slant range measurements to recognize that the measurement includes errors that will be corrected by the navigation processing before it represents measured range) errors for the GPS/LAAS signal-in-space are defined by:

$$\sigma_{pr\_gnd}(\theta_i) \leq \sqrt{\frac{(a_0 + a_1 e^{-\theta_i/\theta_0})^2}{M_i} + a_2{}^2 + \left(\frac{a_3}{\sin(\theta_i)}\right)^2}$$

where

M_i = number of ground reference receivers
i = i^{th} ranging source
θ_I = elevation angle for i^{th} ranging source

and a_0, a_1, a_2, a_3, and θ_0 are parameters defined as follows:

Class	θ_i (deg)	a_0 (m)	a_1 (m)	θ_0 (deg)	a_2 (m)	a_3 (m)
A	> 5	0.5	1.65	14.3	0.08	0.03
B	> 5	0.16	1.07	15.5	0.08	0.03
C	> 35	0.15	0.84	15.5	0.04	0.01
	≤ 35	0.24	0	–	0.04	0.01

This definition was taken directly from the GPS/LAAS MASPS. The ranging uncertainty equation is all inclusive, including receiver noise, multipath errors, and residuals of ionospheric, tropospheric, and satellite ephemeris errors. These and all signal measurement errors are based on the carrier range smoothing defined for the SPS simulation (Appendix C) Three classes of LGS receiver systems are defined, but only classes B and C will be used in the GPS/LAAS. Class B systems are being used currently, but they will eventually be replaced by class C systems. The class designation identifies an antenna/receiver design configuration. The class B system is based on choke ring antennas and current receivers. The class C system will use a specially designed multipath limiting antenna (MLA) with separate receivers for upper and lower elevation signal reception, and the receivers will be of an improved design. Additionally, a special configuration is planned for airports that require the highest service availability. The special station configuration will provide for improved MLA performance (~ square root of 2) and will use two receivers for each antenna aperture to gain the averaging improvements (square root of 2) that will halve measurement errors. As indicated, the measurement errors are a function of satellite elevation angle and the number of receivers used at the LGS. Errors computed from the equation are shown graphically in Figure E-4.

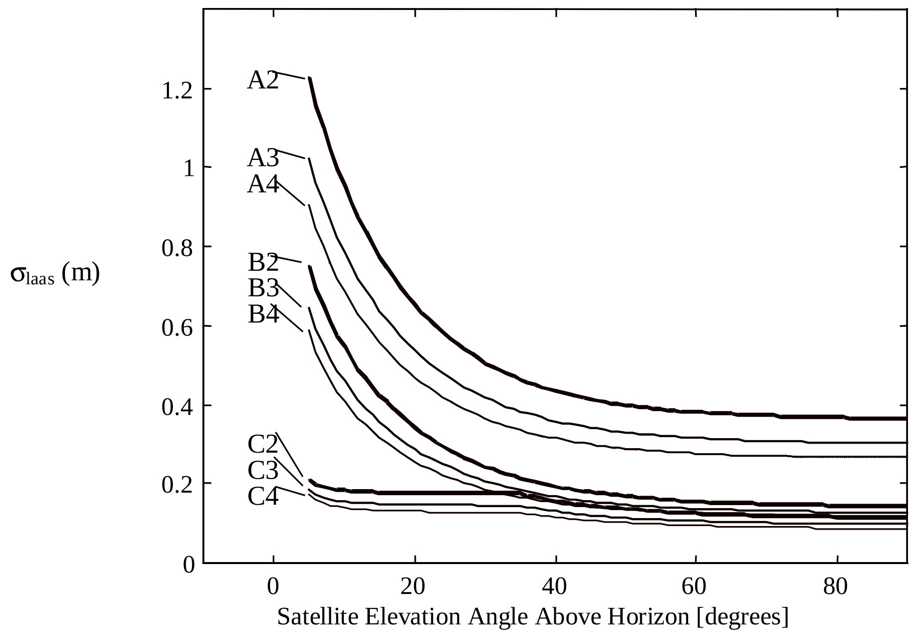

Figure E-4 GPS/LAAS Signal-in-Space Errors

Signal-in-space pseudo-range errors for GEOS are currently larger than GPS errors. The value used for this study include a scale factor of 1.91 on the GPS uncertainty (at the same elevation angle) with an added uncertainty of 0.15 m. Signal-in-space pseudo-range errors for APLs were set at 0.5 m. These numbers are in accordance with the LAAS MASPS.

Aircraft errors for the LAAS are defined for predicted performance by the following equations given in the LAAS MASPS (class B aircraft receivers are used in this study):

$$\sigma_{pr\_air,GPS}(\theta_i) \leq a_0 + a_1 e^{-(\theta_i/\theta_0)}$$

where i and θ_i are as defined for the LGS and a_0, a_1, and θ_0 are parameters defined as follows:

Class	θ_0 (deg)	a_0 (m)	a_1 (m)
A	19.6	0.16	0.23
B	27.7	0.0741	0.18

Aircraft measurement errors representing the actual receiver were based on the same signal conditions (GPS specification and aircraft antenna gain model), thermal noise, and multipath models defined for the SPS simulation. In either case, GEOS errors at the aircraft were not scaled (i.e., the uncertainty was the same as GPS, but the 0.15-m increase was still included). APL errors at the aircraft were set at 0.4 m.

Tropospheric errors are defined as

$$\sigma_{tropo}(\theta) = \sigma_N \Delta h \frac{10^{-6}}{\sin(\theta)}$$

where σ_N = refractivity uncertainty transmitted from LGS (= 10 in this study)

E.2.2 PREDICTED AVAILABILITY

As shown in Figure E-3, the measurement errors are processed through the geometry for each satellite coverage condition to compute distributions for lateral and vertical errors. These are used to compute PLPLs and PVPLs under the two measurement hypotheses:

$$\mathrm{PVPL}_{\mathrm{H1}} = \mathrm{K}_{\mathrm{ffd}}\sigma_{\mathrm{B,vert}} + \mathrm{K}_{\mathrm{md}}\sigma_{\mathrm{vert,H1}}$$

$$\mathrm{PLPL}_{\mathrm{H1}} = \mathrm{K}_{\mathrm{ffd}}\sigma_{\mathrm{B,lat}} + \mathrm{K}_{\mathrm{md}}\sigma_{\mathrm{lat,H1}}$$

$$\mathrm{PVPL}_{\mathrm{H0}} = \mathrm{K}_{\mathrm{ffmd}}\sqrt{\sum_{\mathrm{i=1}}^{\mathrm{N}} \mathrm{s}_{\mathrm{i,vert}}^{2}\sigma_{\mathrm{i}}^{2}}$$

$$\mathrm{PLPL}_{\mathrm{H0}} = \mathrm{K}_{\mathrm{ffmd}}\sqrt{\sum_{\mathrm{i=1}}^{\mathrm{N}} \mathrm{s}_{\mathrm{i,lat}}^{2}\sigma_{\mathrm{i}}^{2}}$$

where

K_{ffd} = multiplier, which determines the probability of fault-free detection given *M* reference receivers (Table E-1)

$$\sigma_{B,vert} = \sqrt{\sum_{i=1}^{N} s_{i,vert}^{2} \frac{\sigma_{pr\_gnd}^{2}[i]}{\left(M[i]-1\right)}}$$

$$\sigma_{B,lat} = \sqrt{\sum_{i=1}^{N} s_{i,lat}^{2} \frac{\sigma_{pr\_gnd}^{2}[i]}{\left(M[i]-1\right)}}$$

K_{ffmd} = multiplier which determines the probability of fault-free missed detection (Table E-2)

$$\sigma_{vert,H1}^{2} = \sum_{i=1}^{N} s_{i,vert}^{2}\sigma_{i,H1}^{2}$$

Table E-1 Fault-Free Detection Multipliers

Performance Type	K_{ffd}		
	M_m = 2	M_m = 3	M_m = 4
1	5.026	5.104	5.158
2	N/A	5.233	5.286
3	N/A	5.451	5.502

Table E-2 Missed Detection Multipliers

Performance Type	K_{ffmd}			K_{md}		
	M_m=2	M_m=3	M_m=4	M_m=2	M_m=3	M_m=4
1	5.762	5.810	5.847	2.935	2.898	2.878
2	6.598	6.641	6.673	4.305	4.279	4.265
3	6.598	6.641	6.673	4.305	4.279	4.265

$$\sigma_{lat,H1}^2 = \sum_{i=1}^{N} s_{i,lat}^2 \sigma_{i,H1}^2$$

$s_{i,lat}$ = $s_{i,2}$ = projection of the lateral component for i[th] ranging source (element of ***S*** in Figure E-3)

$s_{i,vert}$ = $s_{i,3}$ + $s_{i,1}$ * tan θ_{GS} = projection of the vertical component and translation of the along track errors into the vertical for i[th] ranging source (computed from elements of ***S*** in Figure E-3)

$$\sigma_i^2 = \sigma_{pr\_gnd,i}^2 + \sigma_{tropo,i}^2 + \sigma_{pr\_air,GPS,i}^2$$

$$\sigma_{i,H1}^2 = \frac{M_i \cdot \sigma_{pr\_gnd,i}^2}{M_i - 1} + \sigma_{pr\_air,GPS,i}^2 + \sigma_{tropo,i}^2$$

$\sigma_{tropo,i}$ = residual tropospheric error for satellite *i*

$\sigma_{pr\_air,GPS,i}$ = airborne noise term for satellite *i* (as defined above)

θ_{GS} = glide slope

Performance types shown in Tables E-1 and E-2 are approximately equivalent to the corresponding approach category (e.g., performance type 1 ≅ Category I).

At each step in the LAAS performance simulation, predictive availability is determined by testing the four H_0 and H_1 protection limits against the required alert limits. If the predicted protection limits are less than the alert limits, predictive availability is set to 1; otherwise, it is set to 0. The GPS downings use the procedures followed for the GPS-SPS simulation. However, the few GEOS runs assumed a GEOS with a zero failure rate.

E.2.3 ACCURACY AND INTEGRITY

As indicated in Figure E-3, the true sigma estimates are processed through the geometry for each satellite coverage condition to compute distributions for lateral and vertical errors. These estimated errors are based on the same LGS and tropospheric error estimates used to develop the σ_i in the predicted availability computation, but the airborne errors here are taken from the SPS simulation model. If the predicted availability test was passed, the 95-percent probabilities for lateral and vertical accuracy are tested against the accuracy requirements. If they both pass, the conditional probability for accuracy is set to 1. The same distributions are tested to determine if the probability of the position error being greater than the protection limits is less than the misleading information probability included in the integrity requirement. If that condition is satisfied the integrity test is passed.

E.2.4 CONTINUITY

Figure E-5 (taken from Appendix D of the LAAS MASPS) shows the proposed breakdown of the overall 8 x 10^{-6}/15-second continuity requirement. Some of the failure probability allocations shown are assumed (for the purposes of this report) to be achieved at the specified values and are not strongly a function of user geometry. These are

a. P_r(VDB failure) 2.0 x 10^{-7}/15 sec

b. P_r(ref. receiver failure) 1.3 x 10^{-6}/15 sec

c. P_r(ground mon. false alarm) 1.0 x 10^{-6}/15 sec

These three fixed probabilities add up to 2.5 x 10^{-6}/15 seconds, which becomes the base (minimum) continuity loss probability.

The remaining two sources, satellite loss and protection limit (> alert limit without configuration change), represent almost 70 percent of the total allocation and are geometry dependent, allowing estimation of the actual continuity loss probability given knowledge of the user satellite geometry and pseudo-range error standard deviation.

For continuity calculation, if the LAAS predictive availability test is passed, start with a base continuity loss probability of 2.5 x 10^{-6}/15 seconds from above and add the following:

a. Satellite loss probability – Compute the number of critical satellites N_c by computing $PVPL_{H0}$ and $PLPL_{H0}$ for each one-satellite-removed subset of the set of visible and healthy satellites. If either of these exceeds VAL or LAL, the satellite that was dropped is **critical** because its unexpected loss would cause an alert. For each critical satellite in the user constellation, a continuity loss probability equal to the probability of each satellite loss is accumulated.

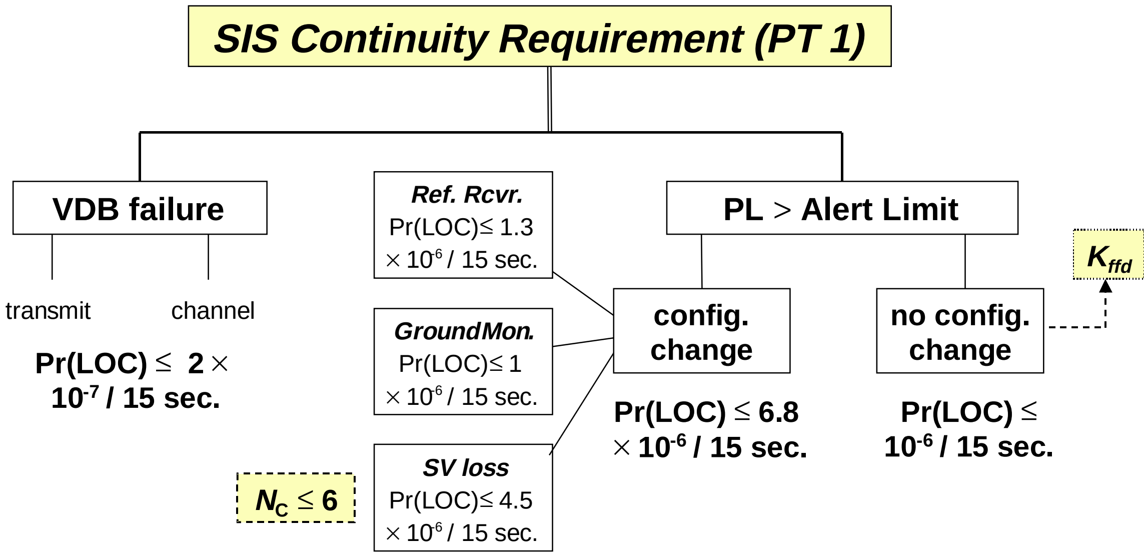

Figure E-5 Proposed LAAS MASPS PT 1 Continuity Allocation

b. PL > AL without configuration change (no satellite lost) – For the full set of visible and healthy satellites, compute the differences VAL – $PVPL_{H1}$ and LAL – $PLPL_{H1}$ to find the remaining margins in both protection levels against increases in B values that could cause the alert limits to be exceeded. Then, using the Gaussian cdf functions and assuming one independent B-value update (B values are highly correlated over 15 seconds) for each reference receiver, compute the probability of a B value exceeding the computed B-value threshold. This probability is then added to the total continuity loss probability from step a.

In Category II and III simulation runs, the resulting probability of loss of continuity is tested against the requirements. If the continuity test is passed, the predicted availability test was already passed. If the accuracy and integrity tests were passed, a true availability event is scored. In Category I simulation runs, loss of continuity is evaluated separately from availability.

E.2.5 IONOSPHERIC SCINTILLATION

Several GPS/LAAS simulation runs were made to assess the impact of ionospheric scintillation. The method used was developed for the SPS simulation and is described in Appendix C.

Appendix F

SPS AVAILABILITY RESULTS

Availability results for the SPS simulation cases analyzed during the study are given in the following tables. The run condition is indicated in the top line, the station designation is given in the first column, and flight phase data are arrayed in the second to fourth columns.

Timeframe 1, 24 SVs, SA on

Availability	Oceanic	Enroute	Terminal	NPA
NPR	0.980738	0.944987	0.87502	0.53215
HNL	0.994107	0.974177	0.938803	0.661072
FAI	0.996691	0.978716	0.954628	0.709592
SEA	0.987659	0.938832	0.888152	0.481277
LAX	0.980157	0.944506	0.906197	0.521968
ASE	0.988241	0.934803	0.884581	0.469454
FAR (Fargo, ND)	0.989894	0.936254	0.888363	0.496103
DFW	0.98017	0.924056	0.867069	0.485136
ORD	0.985959	0.937687	0.896235	0.446845
ATL	0.986106	0.934129	0.857106	0.43171
JFK	0.987453	0.935938	0.88579	0.418103
SJU	0.99549	0.978077	0.942078	0.672822
BIKF	0.994002	0.984802	0.964068	0.705856
Guam	0.99677	0.978352	0.954927	0.800539
Bermuda	0.981244	0.92918	0.872771	0.513518
Mean	0.988312067	0.950299733	0.905052533	0.556409667
High	0.99677	0.984802	0.964068	0.800539
Low	0.980157	0.924056	0.857106	0.418103

Timeframe 1, 24 SVs, SA on, 3 hr. MTTR

Availability	Oceanic	Enroute	Terminal	NPA
NPR	0.988157	0.960669	0.894839	0.560407
HNL	0.998068	0.987337	0.960011	0.69852
FAI	0.998758	0.983329	0.963103	0.736172
SEA	0.995197	0.956042	0.914008	0.506898
LAX	0.986062	0.960607	0.930031	0.553663
ASE	0.995446	0.952364	0.908788	0.497611
FAR (Fargo, ND)	0.996255	0.953013	0.91232	0.524955
DFW	0.987971	0.941769	0.891272	0.514198
ORD	0.992686	0.955684	0.92534	0.475893
ATL	0.994555	0.953954	0.884769	0.457738
JFK	0.995287	0.956673	0.916692	0.443905
SJU	0.99859	0.988994	0.959468	0.704135
BIKF	0.995657	0.989952	0.973183	0.734324
Guam	0.998943	0.985076	0.965147	0.826905
Bermuda	0.990345	0.947863	0.897614	0.542343
Mean	0.9941318	0.9648884	0.926439	0.5851778
High	0.998943	0.989952	0.973183	0.826905
Low	0.986062	0.941769	0.884769	0.443905

Timeframe 2, 24 SVs, SA off, All

Availability

	Oceanic	Enroute	Terminal	NPA
NPR	0.987343	0.975031	0.971318	0.902434
HNL	0.996832	0.992422	0.98703	0.955453
FAI	0.997461	0.996179	0.99392	0.964196
SEA	0.990839	0.983512	0.967073	0.909485
LAX	0.991355	0.977917	0.967886	0.926252
ASE	0.990441	0.983238	0.962949	0.904827
FAR (Fargo, ND)	0.991528	0.987615	0.97401	0.914207
DFW	0.982982	0.977241	0.964005	0.889732
ORD	0.988624	0.984056	0.973422	0.908488
ATL	0.98879	0.983541	0.970656	0.903514
JFK	0.99185	0.979274	0.963008	0.913728
SJU	0.997379	0.99355	0.988529	0.960754
BIKF	0.997797	0.993451	0.991007	0.974648
Guam	0.998505	0.996071	0.990561	0.968175
Bermuda	0.98704	0.980327	0.962053	0.897977
Mean	0.991917733	0.985561667	0.9751618	0.926258
High	0.998505	0.996179	0.99392	0.974648
Low	0.982982	0.975031	0.962053	0.889732

Timeframe 2, 24 SVs, SA off, All, 3 hr. MTTR

Availability

	Oceanic	Enroute	Terminal	NPA
NPR	0.993053	0.983666	0.982053	0.920527
HNL	0.999266	0.997351	0.994943	0.973232
FAI	0.999048	0.998558	0.997634	0.971135
SEA	0.996646	0.991445	0.978328	0.933171
LAX	0.996771	0.985041	0.978664	0.946717
ASE	0.996423	0.991296	0.974522	0.925576
FAR (Fargo, ND)	0.996966	0.99523	0.985272	0.935436
DFW	0.989238	0.98665	0.976874	0.911049
ORD	0.993876	0.991863	0.985158	0.93287
ATL	0.995767	0.993397	0.983781	0.928646
JFK	0.997317	0.987799	0.974742	0.940829
SJU	0.999411	0.997744	0.995501	0.975494
BIKF	0.999208	0.995452	0.994446	0.981653
Guam	0.999704	0.998661	0.994312	0.976754
Bermuda	0.994848	0.989977	0.974137	0.920436
Mean	0.9965028	0.992275333	0.984691133	0.944901667
High	0.999704	0.998661	0.997634	0.981653
Low	0.989238	0.983666	0.974137	0.911049

Timeframe 2, 30 SVs, SA off, All

Availability

	Oceanic	Enroute	Terminal	NPA
NPR	0.99992	0.999768	0.999619	0.998486
HNL	0.999975	0.999932	0.999875	0.999059
FAI	0.999978	0.999971	0.999937	0.999744
SEA	0.99997	0.999896	0.999831	0.999264
LAX	0.999844	0.999538	0.999403	0.997703
ASE	0.999954	0.999859	0.999751	0.998858
FAR (Fargo, ND)	0.999972	0.999944	0.999889	0.999452
DFW	0.999764	0.999484	0.996005	0.991982
ORD	0.999956	0.9999	0.999812	0.999052
ATL	0.999935	0.999666	0.999511	0.998366
JFK	0.999954	0.99984	0.999725	0.998427
SJU	0.999972	0.999941	0.999907	0.999527
BIKF	0.99997	0.99993	0.999889	0.999245
Guam	0.999982	0.999981	0.999978	0.999942
Bermuda	0.99996	0.999908	0.99977	0.998803
Mean	0.9999404	0.9998372	0.9995268	0.998527333
High	0.999982	0.999981	0.999978	0.999942
Low	0.999764	0.999484	0.996005	0.991982

Timeframe 2, 30 SVs, SA off, All, 3 hr. MTTR

Availability

	Oceanic	Enroute	Terminal	NPA
NPR	0.999994046	0.999976354	0.999959024	0.999645862
HNL	0.999999525	0.999995328	0.999989912	0.999716952
FAI	0.999999772	0.999999567	0.999995907	0.99997336
SEA	0.99999936	0.999991488	0.99998527	0.999919497
LAX	0.999984423	0.999889031	0.999873554	0.999295001
ASE	0.999997861	0.999987747	0.999976064	0.999810869
FAR (Fargo, ND)	0.999998888	0.999996943	0.999992272	0.999943982
DFW	0.999915024	0.999804099	0.996352558	0.992816768
ORD	0.999997285	0.999992437	0.999983326	0.999835873
ATL	0.99999556	0.999905069	0.999887286	0.999555036
JFK	0.999997785	0.999985021	0.999972414	0.999581202
SJU	0.999998949	0.999996017	0.999992887	0.999890525
BIKF	0.999998997	0.999994175	0.999989206	0.999735407
Guam	0.999999859	0.99999981	0.999999713	0.999997082
Bermuda	0.999998516	0.999993758	0.99997837	0.99970711
Mean	0.999991723	0.999967123	0.999728518	0.999294968
High	0.999999859	0.99999981	0.999999713	0.999997082
Low	0.999915024	0.999804099	0.996352558	0.992816768

Timeframe 2, 30 SVs, SA off, All, Increased iono noise

Availability

	Oceanic	Enroute	Terminal	NPA
NPR	0.99992	0.999768	0.999619	0.998486
HNL	0.999975	0.999932	0.999875	0.999059
FAI	0.999978	0.999971	0.999937	0.999744
SEA	0.99997	0.999896	0.999831	0.999264
LAX	0.999844	0.999538	0.999403	0.997703
ASE	0.999954	0.999859	0.999751	0.998858
FAR (Fargo, ND)	0.999972	0.999944	0.999889	0.999452
DFW	0.999764	0.999484	0.996005	0.991982
ORD	0.999956	0.9999	0.999812	0.999052
ATL	0.999935	0.999666	0.999511	0.998366
JFK	0.999954	0.99984	0.999725	0.998427
SJU	0.999972	0.999941	0.999907	0.999527
BIKF	0.99997	0.99993	0.999889	0.999245
Guam	0.999982	0.999981	0.999978	0.999942
Bermuda	0.99996	0.999908	0.99977	0.998803
Mean	0.9999404	0.9998372	0.9995268	0.998527333
High	0.999982	0.999981	0.999978	0.999942
Low	0.999764	0.999484	0.996005	0.991982

Timeframe 3, 24SVs, SA off, All, Autonav, Dual Frequency

Availability

	Oceanic	Enroute	Terminal	NPA
NPR	0.990997	0.986827	0.982043	0.974342
HNL	0.996895	0.995807	0.99502	0.991249
FAI	0.997654	0.997426	0.997002	0.995813
SEA	0.991899	0.989813	0.988385	0.978264
LAX	0.992115	0.988089	0.984183	0.97538
ASE	0.991358	0.990245	0.989488	0.978967
FAR (Fargo, ND)	0.992406	0.991169	0.990293	0.986456
DFW	0.986988	0.982445	0.981522	0.975604
ORD	0.992271	0.98844	0.987256	0.98269
ATL	0.990149	0.988605	0.987687	0.981985
JFK	0.992711	0.991488	0.989322	0.974026
SJU	0.997861	0.997138	0.996417	0.992493
BIKF	0.998011	0.997768	0.997677	0.992882
Guam	0.998871	0.998325	0.997297	0.995129
Bermuda	0.988042	0.986525	0.982473	0.975867
Mean	0.9932152	0.991340667	0.989737667	0.9834098
High	0.998871	0.998325	0.997677	0.995813
Low	0.986988	0.982445	0.981522	0.974026

Timeframe 3, 24 SVs, SA off, All, Autonav, Dual Frequency, 3 hr. MTTR

Availability

	Oceanic	Enroute	Terminal	NPA
NPR	0.996607	0.992813	0.988749	0.983366
HNL	0.999274	0.998788	0.998455	0.996834
FAI	0.99913	0.999044	0.998874	0.998415
SEA	0.997129	0.996167	0.995521	0.987167
LAX	0.9971	0.993403	0.989759	0.983887
ASE	0.99683	0.99634	0.996011	0.987489
FAR (Fargo, ND)	0.997368	0.996804	0.996422	0.994715
DFW	0.992952	0.988996	0.988588	0.98592
ORD	0.997409	0.993795	0.993257	0.991264
ATL	0.996385	0.995685	0.995278	0.992715
JFK	0.997697	0.997155	0.996144	0.98352
SJU	0.999627	0.999303	0.998998	0.997281
BIKF	0.999293	0.999205	0.999193	0.995225
Guam	0.999867	0.999624	0.999164	0.998232
Bermuda	0.995304	0.994608	0.990888	0.986069
Mean	0.9974648	0.996115333	0.995020067	0.9908066
High	0.999867	0.999624	0.999193	0.998415
Low	0.992952	0.988996	0.988588	0.983366

Timeframe 3, 30 SVs, SA off, All, Autonav, Dual Frequency

Availability

	Oceanic	Enroute	Terminal	NPA
NPR	0.999961	0.999913	0.999882	0.999747
HNL	0.999977	0.999974	0.999966	0.999917
FAI	0.999979	0.999977	0.999975	0.999964
SEA	0.999973	0.99997	0.999954	0.999883
LAX	0.999879	0.999842	0.99964	0.999501
ASE	0.999967	0.999952	0.999931	0.999838
FAR (Fargo, ND)	0.999982	0.999971	0.999967	0.999933
DFW	0.999936	0.999763	0.999585	0.999344
ORD	0.999976	0.999954	0.999938	0.999863
ATL	0.999945	0.99993	0.999892	0.999635
JFK	0.999962	0.999947	0.999921	0.999814
SJU	0.999979	0.999972	0.999963	0.999929
BIKF	0.999976	0.99997	0.999964	0.999923
Guam	0.999983	0.999982	0.999982	0.99998
Bermuda	0.999969	0.999954	0.99995	0.999865
Mean	0.999962933	0.999938067	0.999900667	0.999809067
High	0.999983	0.999982	0.999982	0.99998
Low	0.999879	0.999763	0.999585	0.999344

Timeframe 3, 30 SVs, SA off, All, Autonav, Dual Frequency, Iono Scintillation

Availability

	Oceanic	Enroute	Terminal	NPA
NPR	0.99996072	0.999912888	0.99988194	0.999746629
HNL	0.931655956	0.931653585	0.931645978	0.931600202
FAI	0.998817157	0.998815544	0.998589086	0.998557783
SEA	0.999973175	0.999969653	0.999954073	0.999883234
LAX	0.999879383	0.999842421	0.999639821	0.999500692
ASE	0.999966716	0.999951671	0.999931024	0.999838145
FAR (Fargo, ND)	0.99998155	0.999970697	0.999966531	0.99993255
DFW	0.999935936	0.999763149	0.999584892	0.999344398
ORD	0.99997567	0.999954033	0.999937754	0.999862915
ATL	0.99994527	0.99993042	0.999892255	0.999634676
JFK	0.999962226	0.999947333	0.999920669	0.999814158
SJU	0.930536435	0.930529199	0.930521577	0.930489419
BIKF	0.999058603	0.999052999	0.999046677	0.999003377
Guam	0.930539315	0.930538915	0.930538782	0.930536921
Bermuda	0.999968697	0.999954105	0.999949753	0.999865198
Mean	0.986010454	0.985985774	0.985933388	0.985840686
High	0.99998155	0.999970697	0.999966531	0.99993255
Low	0.930536435	0.930529199	0.930521577	0.930489419

Timeframe 3, 30 SVs, SA off, All, Autonav, Dual Frequency, 3 hr. MTTR

Availability

	Cat I
NPR	0.996232821
HNL	0.998204789
FAI	0.998746446
SEA	0.997127502
LAX	0.984213734
ASE	0.995551632
FAR (Fargo, ND)	0.998446051
DFW	0.989592667
ORD	0.993373667
ATL	0.99267662
JFK	0.991877096
SJU	0.998632889
BIKF	0.995239984
Guam	0.999956619
Bermuda	0.996926719
Mean	0.995119949
High	0.999956619
Low	0.984213734

Appendix G

GPS/WAAS AVAILABILITY RESULTS

Availability results for the GPS/WAAS simulation cases analyzed during the study are given in the following tables. The run condition is indicated to the right of each table, the station designation is given in the first column, and flight phase data are arrayed in the remaining columns. Additional special oceanic cases are included, for all others the oceanic data is blank.

Sites	Oceanic	Enroute	Terminal	NPA	Cat I
JFK		0.99998629	0.9999707	0.9998313	0.9956259
ATL		0.99998512	0.9999774	0.9998699	0.9953049
ORD		0.99998686	0.9999804	0.9999165	0.9959059
DFW		0.99998459	0.9999758	0.9998913	0.994531
SEA		0.99999289	0.9999929	0.9999925	0.9989389
LAX		0.9999929	0.9999928	0.9999923	0.9993219
ASE		0.99998507	0.9999783	0.9998388	0.9954329
FAI		0.99998909	0.9999864	0.9999178	
FAR		0.99998647	0.9999806	0.9998825	0.9956569
SJU		0.99999003	0.9999869	0.9999571	
High		0.9999929	0.9999929	0.9999925	0.9993219
Low		0.99998459	0.9999707	0.9998313	0.994531
Mean		0.99998793	0.9999822	0.999909	0.9963398

Nominal Stanford Processing
2 GEOS Availability

Sites	Oceanic	Enroute	Terminal	NPA	Cat I
JFK		0.99999909	0.9999991	0.9999991	0.9998831
ATL		0.99999909	0.9999991	0.9999991	0.9997881
ORD		0.99999909	0.9999991	0.9999991	0.9999261
DFW		0.99999909	0.9999991	0.9999991	0.9998981
SEA		0.99999909	0.9999991	0.9999991	0.9995911
LAX		0.99999909	0.9999991	0.9999991	0.9996261
ASE		0.99999909	0.9999991	0.9999991	0.9995821
FAI		0.99999908	0.9999991	0.9999988	
FAR		0.99999909	0.9999991	0.9999991	0.9998461
SJU		0.99999909	0.9999991	0.9999991	
High		0.99999909	0.9999991	0.9999991	0.9999261
Low		0.99999908	0.9999991	0.9999988	0.9995821
Mean		0.99999908	0.9999991	0.9999991	0.9997676

Nominal Stanford Processing
4 GEOS Availability

Sites	Oceanic	Enroute	Terminal	NPA	Cat I
JFK		0.99999909	0.9999991	0.9999991	0.9999601
ATL		0.99999909	0.9999991	0.9999991	0.9999481
ORD		0.99999909	0.9999991	0.9999991	0.9999491
DFW		0.99999909	0.9999991	0.9999991	0.9999601
SEA		0.99999909	0.9999991	0.9999991	0.9996101
LAX		0.99999909	0.9999991	0.9999991	0.9997281
ASE		0.99999909	0.9999991	0.9999991	0.9997771
FAI		0.99999908	0.9999991	0.9999988	
FAR		0.99999909	0.9999991	0.9999991	0.9999381
SJU		0.99999909	0.9999991	0.9999991	
High		0.99999909	0.9999991	0.9999991	0.9999601
Low		0.99999908	0.9999991	0.9999988	0.9996101
Mean		0.99999908	0.9999991	0.9999991	0.9998588

Nominal Stanford Processing
5 GEOS Availability

Raytheon Processing
2 GEOS Availability

Sites	Oceanic	Enroute	Terminal	NPA	Cat I
JFK		0.99998629	0.9999707	0.9998313	0.994043
ATL		0.99998512	0.9999774	0.9998699	0.991391
ORD		0.99998686	0.9999804	0.9999165	0.994172
DFW		0.99998459	0.9999758	0.9998913	0.992431
SEA		0.99999289	0.9999929	0.9999925	0.9979709
LAX		0.9999929	0.9999928	0.9999923	0.9985529
ASE		0.99998507	0.9999783	0.9998388	0.994925
FAI		0.99998909	0.9999864	0.9999178	
FAR		0.99998647	0.9999806	0.9998825	0.9951119
SJU		0.99999003	0.9999869	0.9999571	
High		0.9999929	0.9999929	0.9999925	0.9985529
Low		0.99998459	0.9999707	0.9998313	0.991391
Mean		0.99998793	0.9999822	0.999909	0.9948247

Raytheon Processing
4 GEOS Availability

Sites	Oceanic	Enroute	Terminal	NPA	Cat I
JFK		0.99999909	0.9999991	0.9999991	0.9993981
ATL		0.99999909	0.9999991	0.9999991	0.9993951
ORD		0.99999909	0.9999991	0.9999991	0.9995561
DFW		0.99999909	0.9999991	0.9999991	0.9988241
SEA		0.99999909	0.9999991	0.9999991	0.9990731
LAX		0.99999909	0.9999991	0.9999991	0.9994511
ASE		0.99999909	0.9999991	0.9999991	0.9992571
FAI		0.99999908	0.9999991	0.9999988	
FAR		0.99999909	0.9999991	0.9999991	0.9993551
SJU		0.99999909	0.9999991	0.9999991	
High		0.99999909	0.9999991	0.9999991	0.9995561
Low		0.99999908	0.9999991	0.9999988	0.9988241
Mean		0.99999908	0.9999991	0.9999991	0.9992887

Raytheon Processing
5 GEOS Availability

Sites	Oceanic	Enroute	Terminal	NPA	Cat I
JFK		0.99999909	0.9999991	0.9999991	0.9998521
ATL		0.99999909	0.9999991	0.9999991	0.9997571
ORD		0.99999909	0.9999991	0.9999991	0.9996121
DFW		0.99999909	0.9999991	0.9999991	0.9996771
SEA		0.99999909	0.9999991	0.9999991	0.9992881
LAX		0.99999909	0.9999991	0.9999991	0.9995551
ASE		0.99999909	0.9999991	0.9999991	0.9994591
FAI		0.99999908	0.9999991	0.9999988	
FAR		0.99999909	0.9999991	0.9999991	0.9995381
SJU		0.99999909	0.9999991	0.9999991	
High		0.99999909	0.9999991	0.9999991	0.9998521
Low		0.99999908	0.9999991	0.9999988	0.9992881
Mean		0.99999908	0.9999991	0.9999991	0.9995923

Solar Max
Nominal Stanford Processing
2 GEOS Availability

Sites	Oceanic	Enroute	Terminal	NPA	Cat I
JFK		0.99998629	0.9999707	0.9998313	0.990263
ATL		0.99998512	0.9999774	0.9998699	0.9635672
ORD		0.99998686	0.9999804	0.9999165	0.98275
DFW		0.99998459	0.9999758	0.9998913	0.987862
SEA		0.99999289	0.9999929	0.9999925	0.9968929
LAX		0.9999929	0.9999928	0.9999923	0.9971839
ASE		0.99998507	0.9999783	0.9998388	0.994282
FAI		0.99998909	0.9999864	0.9999178	
FAR		0.99998647	0.9999806	0.9998825	0.993692
SJU		0.99999003	0.9999869	0.9999571	
High		0.9999929	0.9999929	0.9999925	0.9971839
Low		0.99998459	0.9999707	0.9998313	0.9635672
Mean		0.99998793	0.9999822	0.999909	0.9883116

Sites	Oceanic	Enroute	Terminal	NPA	Cat I
JFK		0.99999909	0.9999991	0.9999991	0.9990911
ATL		0.99999909	0.9999991	0.9999991	0.9970071
ORD		0.99999909	0.9999991	0.9999991	0.9990151
DFW		0.99999909	0.9999991	0.9999991	0.9972751
SEA		0.99999909	0.9999991	0.9999991	0.9980211
LAX		0.99999909	0.9999991	0.9999991	0.9983511
ASE		0.99999909	0.9999991	0.9999991	0.9986391
FAI		0.99999908	0.9999991	0.9999988	
FAR		0.99999909	0.9999991	0.9999991	0.9988571
SJU		0.99999909	0.9999991	0.9999991	
High		0.99999909	0.9999991	0.9999991	0.9990911
Low		0.99999908	0.9999991	0.9999988	0.9970071
Mean		0.99999908	0.9999991	0.9999991	0.9982821

Solar Max
Nominal Stanford Processing
4 GEOS Availability

Sites	Oceanic	Enroute	Terminal	NPA	Cat I
JFK		0.99999909	0.9999991	0.9999991	0.9991611
ATL		0.99999909	0.9999991	0.9999991	0.9988211
ORD		0.99999909	0.9999991	0.9999991	0.9993261
DFW		0.99999909	0.9999991	0.9999991	0.9991411
SEA		0.99999909	0.9999991	0.9999991	0.9987221
LAX		0.99999909	0.9999991	0.9999991	0.9992371
ASE		0.99999909	0.9999991	0.9999991	0.9993301
FAI		0.99999908	0.9999991	0.9999988	
FAR		0.99999909	0.9999991	0.9999991	0.9991741
SJU		0.99999909	0.9999991	0.9999991	
High		0.99999909	0.9999991	0.9999991	0.9993301
Low		0.99999908	0.9999991	0.9999988	0.9987221
Mean		0.99999908	0.9999991	0.9999991	0.9991141

Solar Max
Nominal Stanford Processing
5 GEOS Availability

Sites	Oceanic	Enroute	Terminal	NPA	Cat I
JFK		0.99998629	0.9999707	0.9998313	0.8903057
ATL		0.99998512	0.9999774	0.9998699	0.705861
ORD		0.99998686	0.9999804	0.9999165	0.9420573
DFW		0.99998459	0.9999758	0.9998913	0.8727168
SEA		0.99999289	0.9999929	0.9999925	0.9648482
LAX		0.9999929	0.9999928	0.9999923	0.984258
ASE		0.99998507	0.9999783	0.9998388	0.987097
FAI		0.99998909	0.9999864	0.9999178	
FAR		0.99998647	0.9999806	0.9998825	0.981943
SJU		0.99999003	0.9999869	0.9999571	
High		0.9999929	0.9999929	0.9999925	0.987097
Low		0.99998459	0.9999707	0.9998313	0.705861
Mean		0.99998793	0.9999822	0.999909	0.9161359

Solar Max
Raytheon Processing
2 GEOS Availability

Sites	Oceanic	Enroute	Terminal	NPA	Cat I
JFK		0.99999909	0.9999991	0.9999991	0.9901361
ATL		0.99999909	0.9999991	0.9999991	0.8939302
ORD		0.99999909	0.9999991	0.9999991	0.9795381
DFW		0.99999909	0.9999991	0.9999991	0.9141082
SEA		0.99999909	0.9999991	0.9999991	0.9767741
LAX		0.99999909	0.9999991	0.9999991	0.9904381
ASE		0.99999909	0.9999991	0.9999991	0.9954121
FAI		0.99999908	0.9999991	0.9999988	
FAR		0.99999909	0.9999991	0.9999991	0.9953011
SJU		0.99999909	0.9999991	0.9999991	
High		0.99999909	0.9999991	0.9999991	0.9954121
Low		0.99999908	0.9999991	0.9999988	0.8939302
Mean		0.99999908	0.9999991	0.9999991	0.9669547

Solar Max
Raytheon Processing
4 GEOS Availability

Sites	Oceanic	Enroute	Terminal	NPA	Cat I
JFK		0.99999909	0.9999991	0.9999991	0.9923871
ATL		0.99999909	0.9999991	0.9999991	0.9274112
ORD		0.99999909	0.9999991	0.9999991	0.9875971
DFW		0.99999909	0.9999991	0.9999991	0.9652171
SEA		0.99999909	0.9999991	0.9999991	0.9818561
LAX		0.99999909	0.9999991	0.9999991	0.9930581
ASE		0.99999909	0.9999991	0.9999991	0.9973351
FAI		0.99999908	0.9999991	0.9999988	
FAR		0.99999909	0.9999991	0.9999991	0.9968061
SJU		0.99999909	0.9999991	0.9999991	
High		0.99999909	0.9999991	0.9999991	0.9973351
Low		0.99999908	0.9999991	0.9999988	0.9274112
Mean		0.99999908	0.9999991	0.9999991	0.9802085

Solar Max
Raytheon Processing
5 GEOS Availability

Sites	Oceanic	Enroute	Terminal	NPA	Cat I
JFK	0.9999802	0.99997529	0.9999597	0.9998193	0.990222
ATL	0.9999899	0.99998512	0.9999774	0.9998699	0.9952869
ORD	0.9999682	0.99996386	0.9999574	0.9998915	0.993534
DFW	0.9999897	0.99998459	0.9999758	0.9998913	0.994552
SEA	0.9999929	0.99999289	0.9999929	0.9999925	0.9987319
LAX	0.9999929	0.9999929	0.9999928	0.9999923	0.9991199
ASE	0.9999902	0.99998507	0.9999783	0.9998388	0.9954669
FAI	0.9999912	0.99998909	0.9999864	0.9999178	
FAR	0.9886055	0.98860155	0.9885957	0.9884735	0.9752661
SJU	0.9999915	0.99999003	0.9999869	0.9999561	
High	0.9999929	0.9999929	0.9999929	0.9999925	0.9991199
Low	0.9886055	0.98860155	0.9885957	0.9884735	0.9752661
Mean	0.9988492	0.99884604	0.9988403	0.9987643	0.9927725

Scintillation
Nominal Stanford Processing
2 GEOS Availability

Sites	Oceanic	Enroute	Terminal	NPA	Cat I
JFK	0.9999991	0.99999909	0.9999991	0.9999991	0.9995681
ATL	0.9999991	0.99999909	0.9999991	0.9999991	0.9998091
ORD	0.9999991	0.99999909	0.9999991	0.9999991	0.9989071
DFW	0.9999991	0.99999909	0.9999991	0.9999991	0.9998551
SEA	0.9999991	0.99999909	0.9999991	0.9999991	0.9995101
LAX	0.9999991	0.99999909	0.9999991	0.9999991	0.9996251
ASE	0.9999991	0.99999909	0.9999991	0.9999991	0.9996031
FAI	0.9999991	0.99999908	0.9999991	0.9999988	
FAR	0.9999921	0.99998209	0.9999821	0.9999301	0.9909231
SJU	0.9999991	0.99999909	0.9999991	0.9999991	
High	0.9999991	0.99999909	0.9999991	0.9999991	0.9998551
Low	0.9999921	0.99998209	0.9999821	0.9999301	0.9909231
Mean	0.9999984	0.99999738	0.9999974	0.9999922	0.9984751

Scintillation
Nominal Stanford Processing
4 GEOS Availability

Sites	Oceanic	Enroute	Terminal	NPA	Cat I
JFK	0.9999991	0.99999909	0.9999991	0.9999991	0.9998401
ATL	0.9999991	0.99999909	0.9999991	0.9999991	0.9999481
ORD	0.9999991	0.99999909	0.9999991	0.9999991	0.9997451
DFW	0.9999991	0.99999909	0.9999991	0.9999991	0.9999591
SEA	0.9999991	0.99999909	0.9999991	0.9999991	0.9995611
LAX	0.9999991	0.99999909	0.9999991	0.9999991	0.9996741
ASE	0.9999991	0.99999909	0.9999991	0.9999991	0.9996751
FAI	0.9999991	0.99999908	0.9999991	0.9999988	
FAR	0.9999961	0.99999609	0.9999961	0.9999711	0.9942361
SJU	0.9999991	0.99999909	0.9999991	0.9999991	
High	0.9999991	0.99999909	0.9999991	0.9999991	0.9999591
Low	0.9999961	0.99999609	0.9999961	0.9999711	0.9942361
Mean	0.9999988	0.99999878	0.9999988	0.9999963	0.9990798

Scintillation
Nominal Stanford Processing
5 GEOS Availability

Scintillation
Raytheon Processing
2 GEOS Availability

Sites	Oceanic	Enroute	Terminal	NPA	Cat I
JFK	0.9999802	0.99997529	0.9999597	0.9998193	0.98797
ATL	0.9999899	0.99998512	0.9999774	0.9998699	0.991295
ORD	0.9999682	0.99996386	0.9999574	0.9998915	0.991088
DFW	0.9999897	0.99998459	0.9999758	0.9998913	0.99248
SEA	0.9999929	0.99999289	0.9999929	0.9999925	0.9976279
LAX	0.9999929	0.9999929	0.9999928	0.9999923	0.9983999
ASE	0.9999902	0.99998507	0.9999783	0.9998388	0.994915
FAI	0.9999912	0.99998909	0.9999864	0.9999178	
FAR	0.9886055	0.98860155	0.9885957	0.9884735	0.9717431
SJU	0.9999915	0.99999003	0.9999869	0.9999561	
High	0.9999929	0.9999929	0.9999929	0.9999925	0.9983999
Low	0.9886055	0.98860155	0.9885957	0.9884735	0.9717431
Mean	0.9988492	0.99884604	0.9988403	0.9987643	0.9906899

Scintillation
Raytheon Processing
4 GEOS Availability

Sites	Oceanic	Enroute	Terminal	NPA	Cat I
JFK	0.9999991	0.99999909	0.9999991	0.9999991	0.9988781
ATL	0.9999991	0.99999909	0.9999991	0.9999991	0.9993961
ORD	0.9999991	0.99999909	0.9999991	0.9999991	0.9980951
DFW	0.9999991	0.99999909	0.9999991	0.9999991	0.9987651
SEA	0.9999991	0.99999909	0.9999991	0.9999991	0.9989211
LAX	0.9999991	0.99999909	0.9999991	0.9999991	0.9994211
ASE	0.9999991	0.99999909	0.9999991	0.9999991	0.9992981
FAI	0.9999991	0.99999908	0.9999991	0.9999988	
FAR	0.9999921	0.99998209	0.9999581	0.9999201	0.9796011
SJU	0.9999991	0.99999909	0.9999991	0.9999991	
High	0.9999991	0.99999909	0.9999991	0.9999991	0.9994211
Low	0.9999921	0.99998209	0.9999581	0.9999201	0.9796011
Mean	0.9999984	0.99999738	0.999995	0.9999912	0.996547

Scintillation
Raytheon Processing
5 GEOS Availability

Sites	Oceanic	Enroute	Terminal	NPA	Cat I
JFK	0.9999991	0.99999909	0.9999991	0.9999991	0.9994461
ATL	0.9999991	0.99999909	0.9999991	0.9999991	0.9998031
ORD	0.9999991	0.99999909	0.9999991	0.9999991	0.9987451
DFW	0.9999991	0.99999909	0.9999991	0.9999991	0.9996541
SEA	0.9999991	0.99999909	0.9999991	0.9999991	0.9992181
LAX	0.9999991	0.99999909	0.9999991	0.9999991	0.9995491
ASE	0.9999991	0.99999909	0.9999991	0.9999991	0.9995051
FAI	0.9999991	0.99999908	0.9999991	0.9999988	
FAR	0.9999961	0.99999609	0.9999711	0.9999711	0.9854591
SJU	0.9999991	0.99999909	0.9999991	0.9999991	
High	0.9999991	0.99999909	0.9999991	0.9999991	0.9998031
Low	0.9999961	0.99999609	0.9999711	0.9999711	0.9854591
Mean	0.9999988	0.99999878	0.9999963	0.9999963	0.9976725

Nominal Stanford Processing
3 GEOS Availability

Sites	Oceanic	Enroute	Terminal	NPA	Cat I
JFK		0.99999907	0.999999	0.9999985	0.9996041
ATL		0.99999906	0.999999	0.9999987	0.9992951
ORD		0.99999907	0.999999	0.9999988	0.9995561
DFW		0.99999906	0.999999	0.9999987	0.9995061
SEA		0.99999909	0.9999991	0.9999991	0.9991331
LAX		0.99999909	0.9999991	0.9999991	0.9996481
ASE		0.99999906	0.999999	0.9999986	0.9995751
FAI		0.99999524	0.9999926	0.9999239	
FAR		0.99999907	0.999999	0.9999987	0.9994891
SJU		0.99999908	0.9999991	0.999999	
High		0.99999909	0.9999991	0.9999991	0.9996481
Low		0.99999524	0.9999926	0.9999239	0.9991331
Mean		0.99999869	0.9999984	0.9999913	0.9994758

Sites	Oceanic	Enroute	Terminal	NPA	Cat I
JFK		0.99991982	0.9997389	0.9981262	0.9586582
ATL		0.9999063	0.9998169	0.9985724	0.9583492
ORD		0.99992642	0.9998515	0.9991124	0.9589282
DFW		0.9998991	0.9997969	0.9988196	0.9576032
SEA		0.99997901	0.9999761	0.9999265	0.9969409
LAX		0.99997927	0.999973	0.9998961	0.9975949
ASE		0.99990573	0.9998278	0.9982128	0.9584722
FAI		0.99994726	0.9999165	0.9991324	
FAR		0.99992093	0.9998528	0.9987172	0.9586882
SJU		0.99996115	0.9999254	0.9996222	
High		0.99997927	0.9999761	0.9999265	0.9975949
Low		0.9998991	0.9997389	0.9981262	0.9576032
Mean		0.9999345	0.9998676	0.9990138	0.9681544

3 year MTTR
Nominal Stanford Processing
2 GEOS Availability

Sites	Oceanic	Enroute	Terminal	NPA	Cat I
JFK		0.99999099	0.9999907	0.9999884	0.9997731
ATL		0.99999097	0.9999908	0.9999891	0.9996701
ORD		0.999991	0.9999909	0.9999898	0.9998231
DFW		0.99999096	0.9999908	0.9999894	0.9997331
SEA		0.99999709	0.9999971	0.9999971	0.9995371
LAX		0.99999709	0.9999971	0.9999971	0.9996071
ASE		0.99999097	0.9999909	0.9999885	0.9994891
FAI		0.99998376	0.9999825	0.9999511	
FAR		0.99999099	0.9999909	0.9999893	0.9997351
SJU		0.99999105	0.999991	0.9999906	
High		0.99999709	0.9999971	0.9999971	0.9998231
Low		0.99998376	0.9999825	0.9999511	0.9994891
Mean		0.99999149	0.9999913	0.999987	0.999671

3 year MTTR
Nominal Stanford Processing
4 GEOS Availability

Sites	Oceanic	Enroute	Terminal	NPA	Cat I
JFK		0.99999609	0.9999961	0.9999961	0.9999351
ATL		0.99999709	0.9999971	0.9999971	0.9999021
ORD		0.99999609	0.9999961	0.9999961	0.9999121
DFW		0.99999709	0.9999971	0.9999971	0.9999121
SEA		0.99999909	0.9999991	0.9999991	0.9995761
LAX		0.99999909	0.9999991	0.9999991	0.9997071
ASE		0.99999709	0.9999971	0.9999971	0.9997451
FAI		0.99998376	0.9999825	0.9999511	
FAR		0.99999709	0.9999971	0.9999971	0.9998981
SJU		0.99999609	0.9999961	0.9999961	
High		0.99999909	0.9999991	0.9999991	0.9999351
Low		0.99998376	0.9999825	0.9999511	0.9995761
Mean		0.99999585	0.9999957	0.9999926	0.9998235

3 year MTTR
Nominal Stanford Processing
5 GEOS Availability

Sites	Oceanic	Enroute	Terminal	NPA	Cat I
JFK	0.9999902	0.99998629	0.9999707	0.9998313	0.9954589
ATL	0.9999899	0.99998512	0.9999774	0.9998699	0.9952049
ORD	0.9999902	0.99998686	0.9999804	0.9999165	0.9953979
DFW	0.9999897	0.99998459	0.9999758	0.9998913	0.994189
SEA	0.9999929	0.99999289	0.9999929	0.9999925	0.9999549
LAX	0.9999929	0.9999929	0.9999928	0.9999923	0.9999209
ASE	0.9999902	0.99998507	0.9999783	0.9998388	0.9952869
FAI	0.9999912	0.99998909	0.9999864	0.9999188	0.9952709
FAR	0.9999904	0.99998647	0.9999806	0.9998825	0.9955229
HNL	0.9999914	0.99998995	0.9999875	0.9999555	0.9623862
KEF	0.9999914	0.9999905	0.9999887	0.9999347	
SJU	0.9999915	0.99999003	0.9999869	0.9999571	
NPR	0.9999903	0.99998733	0.9999811	0.999894	
GUM	0.9999917	0.99999091	0.9999883	0.9999726	
BDA	0.9999896	0.99998552	0.9999784	0.9998679	
High	0.9999929	0.9999929	0.9999929	0.9999925	0.9999549
Low	0.9999896	0.99998459	0.9999707	0.9998313	0.9623862
Mean	0.9999909	0.99998823	0.9999831	0.9999144	0.9928594

Alaska/Hawaii WRSs added
Nominal Stanford Processing
2 GEOS Availability

Sites	Oceanic	Enroute	Terminal	NPA	Cat I
JFK	0.9999991	0.99999909	0.9999991	0.9999991	0.9998701
ATL	0.9999991	0.99999909	0.9999991	0.9999991	0.9997121
ORD	0.9999991	0.99999909	0.9999991	0.9999991	0.9998481
DFW	0.9999991	0.99999909	0.9999991	0.9999991	0.9998761
SEA	0.9999991	0.99999909	0.9999991	0.9999991	0.9999971
LAX	0.9999991	0.99999909	0.9999991	0.9999991	0.9999971
ASE	0.9999991	0.99999909	0.9999991	0.9999991	0.9995581
FAI	0.9999991	0.99999908	0.9999991	0.9999988	0.9996931
FAR	0.9999991	0.99999909	0.9999991	0.9999991	0.9995961
HNL	0.9999991	0.99999908	0.9999991	0.999999	0.9824121
KEF	0.9999991	0.99999908	0.9999991	0.9999989	
SJU	0.9999991	0.99999909	0.9999991	0.9999991	
NPR	0.9999991	0.99999907	0.999999	0.9999978	
GUM	0.9999979	0.99999705	0.9999944	0.9999788	
BDA	0.9999991	0.99999909	0.9999991	0.9999991	
High	0.9999991	0.99999909	0.9999991	0.9999991	0.9999971
Low	0.9999979	0.99999705	0.9999944	0.9999788	0.9824121
Mean	0.999999	0.99999895	0.9999988	0.9999976	0.998056

Alaska/Hawaii WRSs added
Nominal Stanford Processing
4 GEOS Availability

Sites	Oceanic	Enroute	Terminal	NPA	Cat I
JFK	0.9999991	0.99999909	0.9999991	0.9999991	0.9999511
ATL	0.9999991	0.99999909	0.9999991	0.9999991	0.9999381
ORD	0.9999991	0.99999909	0.9999991	0.9999991	0.9999371
DFW	0.9999991	0.99999909	0.9999991	0.9999991	0.9999451
SEA	0.9999991	0.99999909	0.9999991	0.9999991	0.9999971
LAX	0.9999991	0.99999909	0.9999991	0.9999991	0.9999981
ASE	0.9999991	0.99999909	0.9999991	0.9999991	0.9996521
FAI	0.9999991	0.99999908	0.9999991	0.9999988	0.9996931
FAR	0.9999991	0.99999909	0.9999991	0.9999991	0.9997481
HNL	0.9999991	0.99999909	0.9999991	0.9999991	0.9856591
KEF	0.9999991	0.99999908	0.9999991	0.9999989	
SJU	0.9999991	0.99999909	0.9999991	0.9999991	
NPR	0.9999991	0.99999907	0.999999	0.9999978	
GUM	0.9999979	0.99999705	0.9999944	0.9999788	
BDA	0.9999991	0.99999909	0.9999991	0.9999991	
High	0.9999991	0.99999909	0.9999991	0.9999991	0.9999981
Low	0.9999979	0.99999705	0.9999944	0.9999788	0.9856591
Mean	0.999999	0.99999895	0.9999988	0.9999976	0.9984519

Alaska/Hawaii WRSs added
Nominal Stanford Processing
5 GEOS Availability

Sites	Oceanic	Enroute	Terminal	NPA	Cat I
JFK	0.9999902	0.99998629	0.9999707	0.9998313	0.9956259
ATL	0.9999899	0.99998512	0.9999774	0.9998699	0.9953049
ORD	0.9999902	0.99998686	0.9999804	0.9999165	0.9959059
DFW	0.9999897	0.99998459	0.9999758	0.9998913	0.994531
SEA	0.9999929	0.99999289	0.9999929	0.9999925	0.9989389
LAX	0.9999929	0.9999929	0.9999928	0.9999923	0.9993219
ASE	0.9999902	0.99998507	0.9999783	0.9998388	0.9954329
FAI	0.9999912	0.99998909	0.9999864	0.9999178	
FAR	0.9999904	0.99998647	0.9999806	0.9998825	0.9956569
HNL	0.9995554	0.99953596	0.9995135	0.9991795	
KEF	0.9999914	0.9999905	0.9999887	0.9999347	
SJU	0.9999905	0.99999003	0.9999869	0.9999571	
NPR	0.9999883	0.99998433	0.9999771	0.999884	
GUM	0.9996327	0.99948691	0.9993043	0.9986656	
BDA	0.9999896	0.99998552	0.9999784	0.9998679	
High	0.9999929	0.9999929	0.9999929	0.9999925	0.9993219
Low	0.9995554	0.99948691	0.9993043	0.9986656	0.994531
Mean	0.9999377	0.99992417	0.9999056	0.9997748	0.9963398

Nominal Stanford Processing
2 GEOS Availability
As before, but with Oceanic mission
and Non-CONUS sites added

Sites	Oceanic	Enroute	Terminal	NPA	Cat I
JFK	0.9994903	0.9983853	0.9939163	0.9540903	
ATL	0.9994193	0.9980513	0.9958433	0.9651083	
ORD	0.9995153	0.9985483	0.9966983	0.9784463	
DFW	0.9993613	0.9978983	0.9953733	0.9712373	
SEA	0.9994303	0.9982113	0.9964233	0.9659863	
LAX	0.9995123	0.9983673	0.9945103	0.9473423	
ASE	0.9995033	0.9980373	0.9961133	0.9562273	
FAI	0.9997913	0.9991863	0.9984263	0.9790843	
FAR	0.9995723	0.9984373	0.9967543	0.9687093	
HNL	0.9998413	0.9994323	0.9987273	0.9895843	
KEF	0.9998353	0.9995873	0.9990753	0.9836543	
SJU	0.9998673	0.9994553	0.9985723	0.9911833	
NPR	0.9995453	0.9986813	0.9968993	0.9731613	
GUM	0.9999343	0.9997043	0.9989523	0.9947623	
BDA	0.9993373	0.9981663	0.9961203	0.9648473	
High	0.9999343	0.9997043	0.9990753	0.9947623	
Low	0.9993373	0.9978983	0.9939163	0.9473423	
Mean	0.9995971	0.99867663	0.996827	0.9722283	

No WAAS, GPS only
2 GEOS Availability

Appendix H

GPS/LAAS AVAILABILITY RESULTS

Availability result for the GPS/LAAS simulation cases analyzed during the study are given in the following tables. The run condition is indicated on the top lines, the station designation is given in the first column, and flight phase data are arrayed in the data columns.

	Timeframe 1	Timeframe 1	Timeframe 1
	24 SVs	24 SVs, 2 APLs	24 SVs, 2 APLs, 3 hr MTTR
Availability			
	Category I	**Category I**	**Category I**
HNL	0.999870256	0.999994186	0.999998956
FAI	0.999410817	0.999955058	0.999963434
SEA	0.999235893	0.999781206	0.999885041
LAX	0.999300547	0.999598445	0.999805375
ASE	0.999249042	0.999663616	0.999805457
FAR (Fargo, ND)	0.999409023	0.999961073	0.999911854
DFW	0.999447494	0.999836827	0.999912892
ORD	0.999700344	0.999955576	0.999992098
ATL	0.999623208	0.999834381	0.999939463
JFK	0.999479272	0.999654692	0.999831055
SJU	0.999876205	0.999998766	0.999999326
Guam	0.999883788	0.99999927	0.999999946
Mean	0.999540491	0.999852758	0.999920408
High	0.999883788	0.99999927	0.999999946
Low	0.999235893	0.999598445	0.999805375

	Timeframe 1	Timeframe 1
	30 SVs	30 SVs, 2 APLs
Availability		
	Category I	**Category I**
HNL	0.999995846	0.999999889
FAI	0.999994989	0.999998127
SEA	0.999995034	0.999998351
LAX	0.999989782	0.999998364
ASE	0.999992771	0.999998145
FAR (Fargo, ND)	0.999992297	0.999996441
DFW	0.999988226	0.999997223
ORD	0.999991871	0.999996341
ATL	0.999985993	0.999997234
JFK	0.999996024	0.999998227
SJU	0.999998115	0.999999898
Guam	0.999997928	0.999999959
Mean	0.99999324	0.999998183
High	0.999998115	0.999999959
Low	0.999985993	0.999996341

Timeframe 2

24 SVs

Availability

	Category I	Category II	Category III
HNL	0.999950032	0.999639335	0.998446641
FAI	0.999881153	0.998008614	0.995503418
SEA	0.999908584	0.998196732	0.997289875
LAX	0.999506852	0.999002656	0.997646144
ASE	0.999915313	0.998719218	0.997406709
FAR (Fargo, ND)	0.999920351	0.999012434	0.99750945
DFW	0.999904501	0.998392008	0.996386051
ORD	0.999922867	0.998702668	0.990577095
ATL	0.999908645	0.998908608	0.990835098
JFK	0.999813974	0.999058112	0.996762299
SJU	0.999950053	0.999351404	0.998431572
Guam	0.999963298	0.999496652	0.998496849
Mean	0.999878802	0.998874037	0.996274267
High	0.999963298	0.999639335	0.998496849
Low	0.999506852	0.998008614	0.990577095

Timeframe 2

24 SVs, 2 APLs

Availability

	Category I	Category II	Category III
HNL	0.999998987	0.99996475	0.999933713
FAI	0.999985209	0.999150794	0.998114962
SEA	0.999986238	0.998837765	0.998275802
LAX	0.999790999	0.999250011	0.999029602
ASE	0.999981325	0.999055207	0.9986379
FAR (Fargo, ND)	0.999985098	0.999257203	0.998859447
DFW	0.999982358	0.999421284	0.999288223
ORD	0.999990696	0.999506533	0.999168789
ATL	0.999976124	0.999651143	0.99939798
JFK	0.999855693	0.999383949	0.998756333
SJU	0.999999536	0.999966261	0.999925421
Guam	0.999999677	0.999987516	0.999944942
Mean	0.999960995	0.999452701	0.999111093
High	0.999999677	0.999987516	0.999944942
Low	0.999790999	0.998837765	0.998114962

Timeframe 2

24 SVs, 2 APLs, LAAS system accuracy doubled

Availability

	Category I	Category II	Category III
HNL	0.999999694	0.999998775	0.999996597
FAI	0.999997549	0.999980898	0.999960088
SEA	0.999998063	0.999982649	0.999966065
LAX	0.999999004	0.999727197	0.99959545
ASE	0.999998892	0.999974295	0.999893238
FAR (Fargo, ND)	0.999997196	0.999980606	0.999962976
DFW	0.999996818	0.999977269	0.999956102
ORD	0.999999025	0.99998226	0.999968066
ATL	0.999996635	0.999971955	0.999947189
JFK	0.999993928	0.999851185	0.999710152
SJU	0.999999896	0.999999463	0.999998777
Guam	0.999999915	0.999999669	0.999999327
Mean	0.999998051	0.999952185	0.999912836
High	0.999999915	0.999999669	0.999999327
Low	0.999993928	0.999727197	0.99959545

Timeframe 2

24 SVs, 4 GEOSs

Availability

	Category I	Category II	Category III
HNL	0.999999049	0.999894363	0.999657124
FAI	0.999999424	0.999941952	0.999635171
SEA	0.999999996	0.999952635	0.999744396
LAX	1	0.999839094	0.999750443
ASE	0.999993682	0.99939234	0.998866095
FAR (Fargo, ND)	0.999991019	0.999404255	0.999089272
DFW	0.999991667	0.999351336	0.998201664
ORD	0.999992425	0.99963196	0.999465465
ATL	0.999991822	0.999819946	0.999509473
JFK	0.999993898	0.999917397	0.999845307
SJU	0.999999872	0.999971872	0.999950338
Guam	1	0.999984803	0.999961931
Mean	0.999996071	0.999758496	0.999473057
High	1	0.999984803	0.999961931
Low	0.999991019	0.999351336	0.998201664

Timeframe 2

24 SVs, 4 GEOSs, LAAS system accuracy doubled

Availability

	Category I	Category II	Category III
HNL	0.99999984	0.999998397	0.999995484
FAI	0.999999921	0.999998052	0.999996258
SEA	0.999999999	0.999999956	0.999999935
LAX	1	0.999999997	0.999999997
ASE	0.999999991	0.999990962	0.999982653
FAR (Fargo, ND)	0.999999922	0.999984536	0.999977588
DFW	0.999999964	0.999988193	0.999979521
ORD	0.99999996	0.999987916	0.999979521
ATL	0.999999934	0.99998932	0.99998437
JFK	0.999999981	0.999993384	0.999982562
SJU	1	0.999999782	0.999999497
Guam	1	1	1
Mean	0.999999959	0.999994208	0.999989782
High	1	1	1
Low	0.99999984	0.999984536	0.999977588

Timeframe 2

24 SVs, 4 GEOSs, LAAS system accuracy doubled, Iono scintillation

Availability

	Category I	Category II	Category III
HNL	0.930555406	0.930554064	0.930551353
FAI	0.999996162	0.999979991	0.999903674
SEA	0.999999992	0.999999798	0.999999144
LAX	1	0.999999997	0.999999997
ASE	0.999999991	0.999990842	0.999980168
FAR (Fargo, ND)	0.998627154	0.991975414	0.982569835
DFW	0.999999964	0.999988193	0.999979521
ORD	0.999999957	0.99998465	0.999857423
ATL	0.999999934	0.99998932	0.999984361
JFK	0.999999977	0.999988278	0.999947605
SJU	0.999999999	0.999999661	0.999995701
Guam	0.931228688	0.931228688	0.931228688
Mean	0.988367269	0.987806575	0.986999789
High	1	0.999999997	0.999999997
Low	0.930555406	0.930554064	0.930551353

Timeframe 2

24 SVs, 4 GEOSs, 2 APLs

Availability

	Category I	Category II	Category III
HNL	0.999999782	0.999989234	0.99998338
FAI	0.999999996	0.999982069	0.999964526
SEA	0.999999998	0.999997182	0.999995222
LAX	1	0.999989245	0.999980264
ASE	0.999999907	0.999704135	0.999334271
FAR (Fargo, ND)	0.999999904	0.999890164	0.999577729
DFW	0.999999829	0.99971342	0.999583761
ORD	0.999999921	0.999940743	0.99980405
ATL	0.999999841	0.999953631	0.999822733
JFK	0.999999939	0.999962048	0.999950105
SJU	0.999999982	0.999999706	0.999999542
Guam	1	0.999999785	0.999999672
Mean	0.999999925	0.99992678	0.999832938
High	1	0.999999785	0.999999672
Low	0.999999782	0.999704135	0.999334271

Timeframe 2

24 SVs, 4 GEOSs, 2 APLs, LAAS system accuracy doubled

Availability

	Category I	Category II	Category III
HNL	0.999999965	0.999999714	0.999999561
FAI	1	0.999999993	0.999999991
SEA	1	0.999999978	0.999999977
LAX	1	0.999999999	0.999999999
ASE	0.999999999	0.999999838	0.999999802
FAR (Fargo, ND)	0.999999984	0.999999863	0.999999738
DFW	0.999999999	0.999999578	0.999998549
ORD	0.999999999	0.999999819	0.999999721
ATL	1	0.999999617	0.999997551
JFK	1	0.999999826	0.999999806
SJU	1	0.999999981	0.999999966
Guam	1	1	1
Mean	0.999999995	0.999999851	0.999999555
High	1	1	1
Low	0.999999965	0.999999578	0.999997551

Timeframe 2

24 SVs, 4 GEOSs, 2 APLs, LAAS system accuracy doubled, Iono scintillation

Availability

	Category I	Category II	Category III
HNL	0.938584358	0.935834416	0.935834273
FAI	0.999999997	0.99999992	0.999999316
SEA	1	0.999999904	0.999999758
LAX	1	0.999999999	0.999999999
ASE	0.999999999	0.999999837	0.999999791
FAR (Fargo, ND)	0.999431469	0.996298147	0.991737796
DFW	0.999999999	0.999999578	0.999998549
ORD	0.999999998	0.999999457	0.999999006
ATL	1	0.999999617	0.999997551
JFK	0.999999999	0.999999675	0.999999575
SJU	1	0.999999968	0.99999966
Guam	0.945792337	0.945792337	0.945792337
Mean	0.990317346	0.989826904	0.989446468
High	1	0.999999999	0.999999999
Low	0.938584358	0.935834416	0.935834273

Timeframe 2

30 SVs

Availability

	Category I	Category II	Category III
HNL	0.99998655	0.999970363	0.999810917
FAI	0.99998012	0.999960007	0.999928941
SEA	0.999987935	0.99997579	0.999961377
LAX	0.99998564	0.99970138	0.999076681
ASE	0.999987782	0.999955786	0.999928381
FAR (Fargo, ND)	0.999987487	0.999960986	0.999939295
DFW	0.999985613	0.999964545	0.999924206
ORD	0.99998497	0.999961432	0.999940719
ATL	0.999987005	0.999901133	0.999861753
JFK	0.99998715	0.999970801	0.999941872
SJU	0.999985139	0.999977196	0.99996253
Guam	0.99998244	0.99997425	0.999950766
Mean	0.999985653	0.999939472	0.999852287
High	0.999987935	0.999977196	0.99996253
Low	0.99998012	0.99970138	0.999076681

Timeframe 2

30 SVs, LAAS system accuracy doubled

Availability

	Category I	Category II	Category III
HNL	0.999999968	0.999999517	0.999998874
FAI	0.999999958	0.999999658	0.999999119
SEA	0.99999992	0.999998452	0.999995697
LAX	0.999999666	0.99999675	0.999988778
ASE	0.999999815	0.999998693	0.999993984
FAR (Fargo, ND)	0.999999935	0.999999514	0.999997714
DFW	0.999997698	0.999997025	0.999995184
ORD	0.999999875	0.999996345	0.999994206
ATL	0.999999844	0.99999815	0.999988748
JFK	0.999999864	0.999998427	0.999997264
SJU	0.999999986	0.999999692	0.999999237
Guam	0.999999996	0.999999882	0.999999754
Mean	0.99999971	0.999998509	0.999995713
High	0.999999996	0.999999882	0.999999754
Low	0.999997698	0.999996345	0.999988748

Timeframe 2

30 SVs, 2 APLs

Availability

	Category I	Category II	Category III
HNL	0.999999996	0.999999569	0.999999355
FAI	0.999999975	0.999987874	0.999978396
SEA	0.999999934	0.999993332	0.999986479
LAX	0.999999773	0.999993475	0.999986496
ASE	0.999999849	0.999989102	0.99998098
FAR (Fargo, ND)	0.999999951	0.999994298	0.999982221
DFW	0.999997899	0.99999366	0.999989869
ORD	0.999999884	0.999991201	0.999979218
ATL	0.999999883	0.999990799	0.999988784
JFK	0.999999821	0.999994944	0.999986302
SJU	0.999999981	0.999999632	0.999999194
Guam	1	0.999999789	0.999998554
Mean	0.999999746	0.999993973	0.999987987
High	1	0.999999789	0.999999355
Low	0.999997899	0.999987874	0.999978396

Timeframe 2

30 SVs, 2 APLs, LAAS system accuracy doubled

Availability

	Category I	Category II	Category III
HNL	0.999999999	0.999999996	0.999999993
FAI	1	0.999999954	0.999999925
SEA	0.999999998	0.999999899	0.999999771
LAX	0.999999962	0.999999724	0.999999606
ASE	0.999999996	0.999999798	0.999999653
FAR (Fargo, ND)	0.999999998	0.999999901	0.999999836
DFW	0.999999997	0.999997849	0.999997811
ORD	0.999999997	0.999999862	0.999999766
ATL	0.999999994	0.999999803	0.999999686
JFK	0.999999997	0.999999739	0.999999623
SJU	0.999999999	0.99999998	0.999999977
Guam	1	1	0.999999999
Mean	0.999999995	0.999999709	0.999999637
High	1	1	0.999999999
Low	0.999999962	0.999997849	0.999997811

Timeframe 2

30 SVs, 4 GEOSs, LAAS system accuracy doubled

Availability

	Category I	Category II	Category III
HNL	1	0.999999928	0.999999892
FAI	1	0.999999993	0.999999972
SEA	1	0.999999999	0.999999998
LAX	1	1	1
ASE	1	0.99999992	0.999999779
FAR (Fargo, ND)	1	0.999999905	0.99999976
DFW	1	0.999999923	0.999999868
ORD	1	0.999999905	0.999999759
ATL	1	0.999999895	0.999999822
JFK	1	0.999999939	0.999999863
SJU	1	0.999999998	0.999999982
Guam	1	1	1
Mean	1	0.999999951	0.999999891
High	1	1	1
Low	1	0.999999895	0.999999759

Timeframe 2

30 SVs, 4 GEOS, 2 APLs

Availability

	Category I	Category II	Category III
HNL	1	0.99999997	0.999999925
FAI	1	0.999999793	0.999999634
SEA	1	0.999999886	0.9999998
LAX	1	0.999999894	0.999999819
ASE	0.999999998	0.999997294	0.99998894
FAR (Fargo, ND)	1	0.999999563	0.999998865
DFW	0.999999998	0.999996304	0.999993149
ORD	0.999999999	0.999997173	0.999985998
ATL	0.999999998	0.999993565	0.999992312
JFK	0.999999999	0.999998434	0.999995029
SJU	1	0.999999993	0.999999942
Guam	1	0.999999998	0.999999982
Mean	0.999999999	0.999998489	0.999996116
High	1	0.999999998	0.999999982
Low	0.999999998	0.999993565	0.999985998

Appendix I

UNINTENTIONAL INTERFERENCE RISK EVALUATION

I.1 INTRODUCTION

Because there are very few confirmed reports of GPS outages caused by unintentional interference, this portion of the study was based on evaluating the potential impact on GPS reception. All potential RFI sources listed in Reference 1 were carefully considered, including mobile satellite communications, unlicensed consumer transmitters, equipment failures, and harmonics from amateur radio, onboard aircraft equipment, onboard passenger equipment, broadcast radio, civil aviation radar, aviation VHF and UHF communications, OTH military radar, commercial VHF and UHF communications, and broadcast television. Previous work (References 1 through 7) was reviewed to determine the potential impact of these sources.

Of all the possible sources, only three were considered to pose enough of a threat to warrant further investigation; commercial VHF radio, broadcast television, and OTH military radar. It is unlikely that OTH radars pose a significant risk due to the absence of interference reports, the small number of installed systems, and their narrow antenna beam width. Lack of detailed technical information, however, precluded quantitative evaluation to confirm this.

A mathematical simulation was developed and run to determine the potential impact of commercial VHF and television transmissions on GPS reception. For both cases, a standard link budget equation was used along with models of typical transmit and receive antennas, assumed distributions of transmitter radiated harmonic levels, and aircraft trajectories for en route and approach phases of flight. Simulation results in the form of predicted maximum interference level contours were then compared to the WAAS MOPS interference levels (Reference 8) to determine the likelihood of outage that would be experienced by a GPS receiver just meeting the specification.

For all simulations, a GPS receive antenna pattern, based on gain measurements made by Patuxent River NAWC on moderate sized aircraft (Reference 1) and shown in Figure I-1, was used. While larger attenuation values are reflected in the NAWC data, it seemed appropriate for the simulations to limit attenuation at large depression angles (exceeding 50 degrees) to 20 dB. Larger values could not be assured due to the lack of measured patterns on widebody aircraft, the impact of such structures on antenna gain, and the variety of mounting locations.

I.2 COMMERCIAL VHF INTERFERENCE

Because information on out-of-band emissions of typical commercial VHF transmitters was not readily available, simulation was based on maximum transmit power and out-of-band emissions permitted by regulation. This gave a worst-case result.

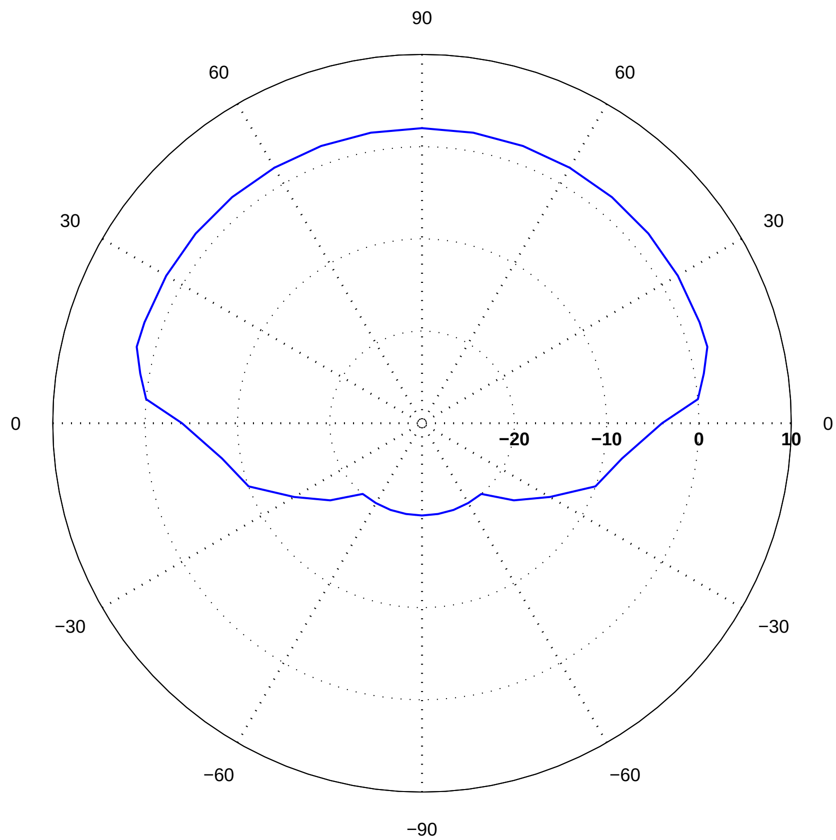

Figure I-1 GPS Receive Antenna Gain (dBi) Elevation Pattern Used for All Interference Simulations

Considering even this worst-case situation, a quick calculation showed that VHF transmitters pose no threat to en route aircraft because of the low transmit power (0.15 mW maximum allowable radiated harmonic level), large propagation loss guaranteed by altitude (7000 feet and 30,000 feet assumed for GA and transport aircraft, respectively), and shielding of the receive antenna by the aircraft. VHF-caused interference is only a concern to aircraft on approach where transmitters can be relatively close and interference can arrive at angles near (instead of far below) the horizon where the aircraft body provides less attenuation.

Simulation runs were performed for an aircraft on the typical approach path shown in Figure I-2. Two transmitter types were considered—fixed and mobile—each operating at maximum authorized power (150 and 60 watts, respectively). Transmitted harmonic levels were at the FCC specification, 60 dB below carrier power. An omni-directional antenna with 2-dBi gain was assumed at a height of 10 and 100 feet above the ground for the mobile and fixed cases, respectively. Based on the assumed transmit waveform of narrowband FM with a 20-kHz bandwidth and located at 157.42 MHz, the WAAS MOPS interference level was -110 dBm. (The tenth harmonic of this signal is 200 kHz wide and located at the GPS L_1 frequency.)

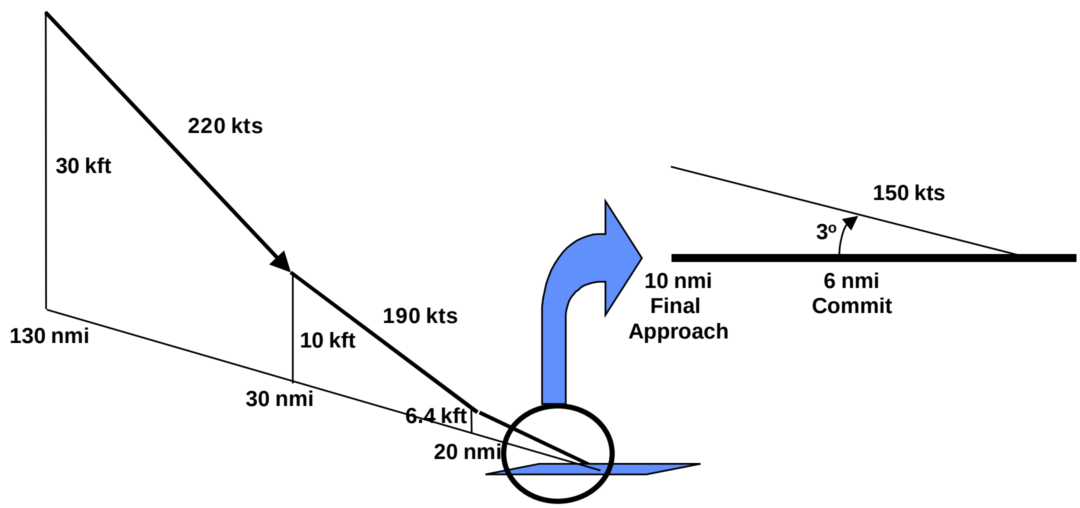

Figure I-2 Approach Scenario Used for Interference Simulations

Each simulation run consisted of setting the transmitter location, flying the aircraft on the standard approach past the transmitter, and computing the maximum received interference level seen at the input of the GPS receiver during an approach. Simulations were run for several hundred different transmitter locations; contours of the maximum interference level relative to the level permitted by the WAAS MOPS were plotted.

The simulation results are shown in Figure I-3 for both cases. The axes give the range with respect to the aircraft touchdown point, with the aircraft approaching from the right. The contours show the transmitter locations that cause the indicated maximum received interference level, relative to the specification interference level of the WAAS MOPS, at some point during the approach. (Only half of the contour is shown; the actual coverage area is symmetrical about the approach path, or the downrange axis.) For example, in the mobile case, the interference level seen by the approach aircraft's GPS receiver will not exceed the WAAS MOPS level, as long as the VHF transmitter remains at least 1 nmi from the approach path or at least 3.5 nmi away from the touchdown point.

Figure I-3 shows the transmitter exclusion area needed around airports to guarantee that worst-case VHF transmitters do not interfere with GPS reception of landing aircraft. This area is computed based on a GPS receiver that just meets the WAAS specs and on transmitters operating at maximum authorized power and maximum authorized out-of-band emission levels. Although the exclusion area is relatively large, a 20-dB improvement in the interference suppression performance of the GPS receiver removes the mobile threat and reduces the keep-out area of fixed transmitters to a small and manageable size.

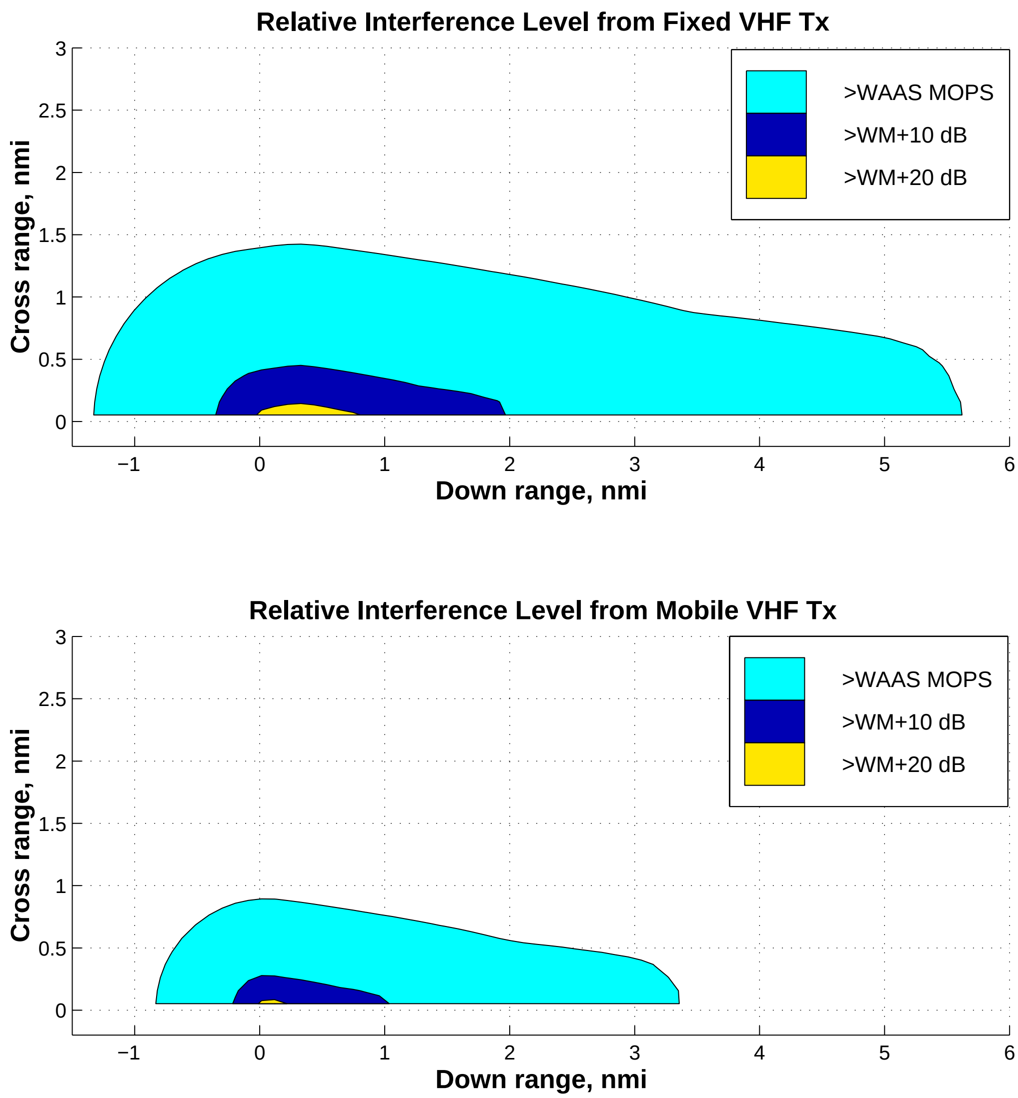

Figure I-3 Simulation Results for VHF Interference

The need for a large exclusion area does not seem consistent with operating experience: No GPS outages due to VHF transmitters have been reported, even though it is likely that large numbers of VHF transmitters (particularly mobile ones) frequently operate within the areas shown. There are several reasons for this discrepancy:

a. Based on the experience of JHU/APL and others (Reference 9 and 10), several currently available GPS receivers outperform the specification (by as much as 20 dB) for this type of interference.

b. VHF transmitters often do not transmit at the maximum allowed power.

c. It is expected that VHF transmitters suppress their tenth harmonics more than the 60 dB required by regulation (>80 dB could be expected).

d. Given the operating band assigned to commercial VHF, it is unlikely that the harmonics will fall in the L_1 band.

For these reasons, commercial VHF transmissions probably do not pose an operationally significant threat. However, it would be beneficial to increase regulation of the allowed out-of-band emission power (from 60 to 80 dB below carrier power) and to restrict placement of fixed VHF transmit antennas near runways. These two actions would eliminate the potential for problems without requiring increased interference mitigation in GPS receivers.

I.3 TELEVISION STATION INTERFERENCE

The high-power transmissions, relatively lenient out-of-band suppression requirement,[1] and the lack of monitoring makes television harmonic emissions a significant potential threat to GPS.[2] Three television channels in particular have harmonics that fall in the GPS L_1 band: Channel 23 (second harmonic) and channels 66 and 67 (third harmonic). Field measurements made by JHU/APL[3] and others (Reference 3) indicate that out-of-band emissions of many stations are far lower than the permitted maximum level. However, JHU/APL-collected data also show that some stations do worse. In two cases, third harmonics 13 and 16 dB higher than allowed by regulation were observed. And while stations are motivated (to produce good picture quality) to keep harmonics below the mandated levels, this does not guarantee the 60-dB suppression requirement will be met: According to discussions with station engineers, they do not perform (nor are they required to perform) specific monitoring to ensure they are meeting out-of-band emission regulations. The potential for television stations to interfere with GPS could become greater as HDTV becomes more widespread. (With HDTV, stations will be driven to maximize output power to ensure coverage in the fringe areas, and they will be less concerned about distortions that create out-of-band harmonics because that is not expected to produce noticeable impact on coverage area or picture quality.)

For the simulation, a television station interference model was devised based on the distribution of transmitter powers from the FCC television station database and the JHU/APL-measured carrier-to-harmonic power ratio (CHR) data. Simply using a worst-case model (as was done for the VHF case) consisting of the highest transmit power and lowest measured (or permitted) CHR would have yielded an overly pessimistic result. By using actual data (the CHR sample data set is admittedly small) in the form of a histogram (or distribution) of radiated harmonic levels, it was hoped that more realistic results would be obtained. Figure I-4 shows the distributions of transmitter power and CHR used for the simulation model. These are summarized in the harmonic effective radiated power levels shown in Table I-1.

---

[1] The FCC requires out-of-band emissions be limited to levels 60 dB below carrier power. A 5-MW transmitter operating within regulations, for example, is permitted to radiate 5 watts in the L_1 band, which would disrupt GPS reception over a very large area.

[2] Several years ago, a channel 23 station in Florida was reported to be disrupting GPS reception.

[3] Measurements of television stations 20, 24, 32, 45, 54, and 67 in the Baltimore-Washington D.C. area were made in November 1998. Data were collected from multiple ranges for some stations to sample antenna pattern variation. The picture and audio carriers were measured separately to provide a larger sample size: For some of these stations, separate transmit tubes are used for the carriers, resulting in two different out-of-band interference characteristics for each transmitter.

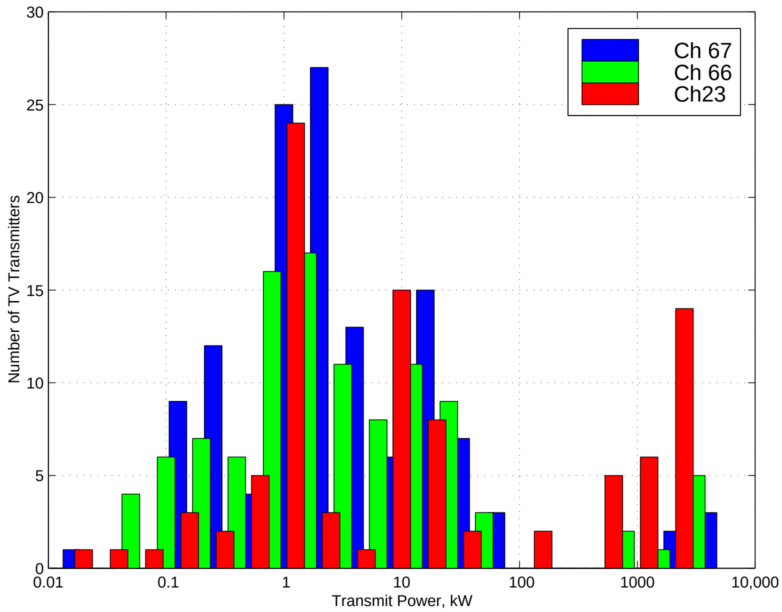

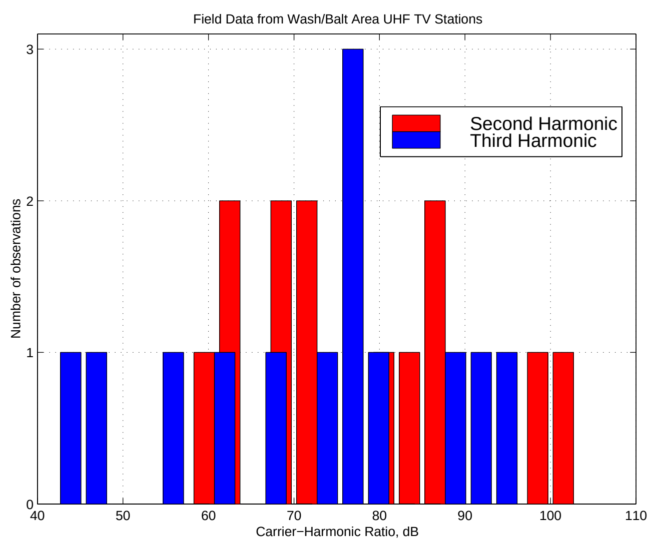

Figure I-4 Distributions of Television Transmitter Power and Measured Carrier-Harmonic Power Ratio Used for the Interference Simulation

Table I-1 Effective Radiated Harmonic Power Levels Used in Television Interference Simulations

Channel	99 Percentile	90 Percentile	50 Percentile
23	50 dBm	27 dBm	-3 dBm
66	32 dBm	9 dBm	-11 dBm
67	29 dBm	5 dBm	-12 dBm

The maximum permitted interference levels are different for each of the channels and the type of signaling used (analog, as is currently used, or digital, for HDTV). These differences are because of the dependence of the WAAS MOPS specification on interference bandwidth and frequency relative to L_1. The harmonic frequencies of the three channels are different, and the HDTV spectrum is much broader and less peaked than that of the current analog signaling. Table I-2 summarizes the WAAS MOPS values, for en route operations, used to estimate impact on GPS reception.

Table I-2 Maximum Interference Levels Permitted by WAAS MOPS

Channel	HDTV Signaling	Analog Signaling	
		Picture Carrier	Audio Carrier
23	-97 dBm	-116 dBm	-106 dBm
66	-99 dBm	-105 dBm	-114 dBm
67	-97 dBm	-113 dBm	-104 dBm

A television transmit antenna pattern was needed for the simulations. Station antennas are designed according to their assigned coverage areas, relative station location, and tower height. The elevation pattern typically contains a single high-gain lobe directed at, or slightly below, the horizon. The azimuth pattern can be directional or omni-directional according to the particular application. The gain pattern of a TWSC-24 omni-directional (in azimuth) transmit antenna was obtained from Harris Corporation and used for the simulation;[4] discussion with their engineers indicated that this is representative of television antennas generally in use. The elevation gain pattern used for the simulation is shown in Figure I-5. Antenna heights used were 600, 900, and 1200 feet above local terrain.

[4] This pattern is valid for the station frequency and not the second or third harmonics that are really the frequencies of interest. Because no specific pattern data were available at those frequencies, some antenna simulation and modeling was performed at the harmonics. The results suggested that the patterns at the harmonic are similar with regard to near-horizon coverage. For simplicity, the fundamental pattern was used for the interference simulation.

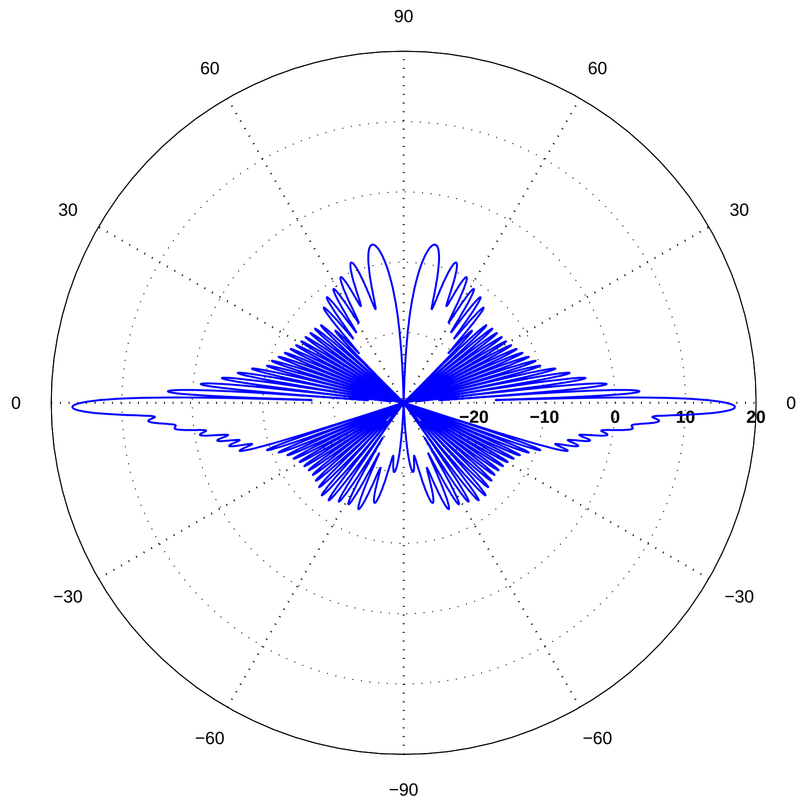

Figure I-5 Television Antenna Gain (dBi) Elevation Pattern Used for Simulations

Simulation runs were made for transport and general aviation aircraft en route and on approach. Similar to the VHF interference cases, each simulation run consisted of setting the transmitter location, "flying" the aircraft past the transmitter, and computing the maximum received interference level seen at the input of the GPS receiver during each flight. This process was repeated for several hundred different transmitter locations. Finally, contours of the maximum interference level relative to the specification level permitted by the WAAS MOPS were examined.

For the en route cases, it was found that the received interference level rarely exceeded the WAAS MOPS specification levels for GA (7000-foot altitude) aircraft and never for air transport (30,000-foot altitude). This is not a surprising result. Far away from the transmitter, propagation loss attenuates the interference sufficiently; at close range, the elevation angle between aircraft and transmitter results in a smaller amount of radiated interference (due to the transmit antenna pattern) and greater receive antenna attenuation (due to shielding by the aircraft).

Because there is so little effect for GA aircraft, probability of interference level is presented instead of a coverage contour for the en route case. Figure I-6 shows this result for the 1 percent worst-case transmitter[5] for the three channels with a transmit antenna height of 1200 feet.

[5] That is, the radiated harmonic levels of 99 percent of the stations are estimated to be below this value.

(The results are fairly insensitive to antenna height.) These curves apply to HDTV signals and the picture carrier of analog television signals. (Probability of interference level due to the audio carrier looks the same with the horizontal scale shifted to the right 7 dB.)

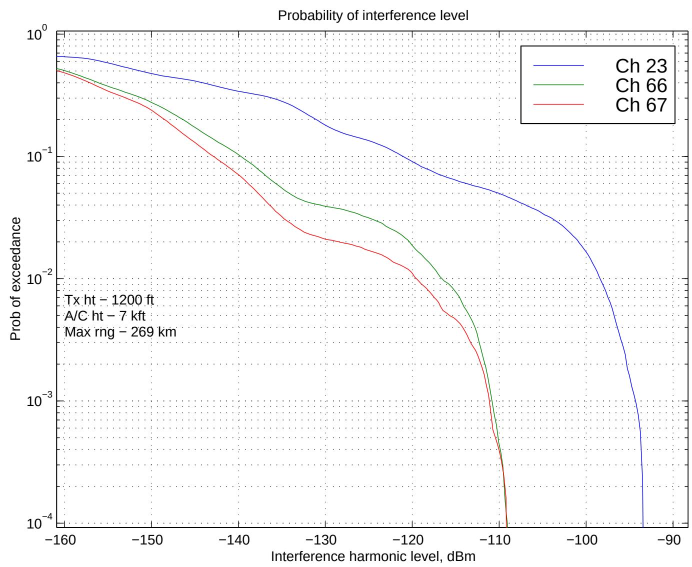

Figure I-6 Probability of Received Interference Level, En Route GA Aircraft

The curves represent the likelihood that an en route GA aircraft will experience a GPS outage (defined as received interference level exceeding the WAAS MOPS value), given that the aircraft is equally likely to be at any location within the radio horizon of the transmit antenna. As shown, received interference from channel 66 and 67 stations is expected to never exceed the permitted level for HDTV signaling (-99 and -97 dBm). Channel 23 interference exceeds the permitted level (-97 dBm) over 0.5 percent of the area. However, only 4 dB of additional interference suppression would overcome this interference. Because both the analysis and WAAS specification are conservative, television emissions are not expected to be a problem for any en route aircraft.

The simulation results for an aircraft on approach are shown in Figure I-7 in the form of interference level contours for a channel 23 station. Two cases are shown: the 99-percent worst-case transmitter (i.e., one whose transmitted harmonic levels are in the top 99 percentile represented by the FCC database combined with the APL-measured carrier-harmonic ratio data), and the 90-percent worst-case transmitter. (These effective radiated power levels are 50 and 27 dBm, as shown in Table I-1). Contour levels are shown relative to the WAAS requirement for NPA (these levels are 3 dB higher than for the en route case), assuming HDTV transmissions.

The results show that to avoid interference above the WAAS specification, the 99-percent worst-case channel 23 transmitter would have to be located more than 72 nmi away from the airport. However, all but the worst 10 percent of transmitters could be located as close as 8 nmi from the airport.

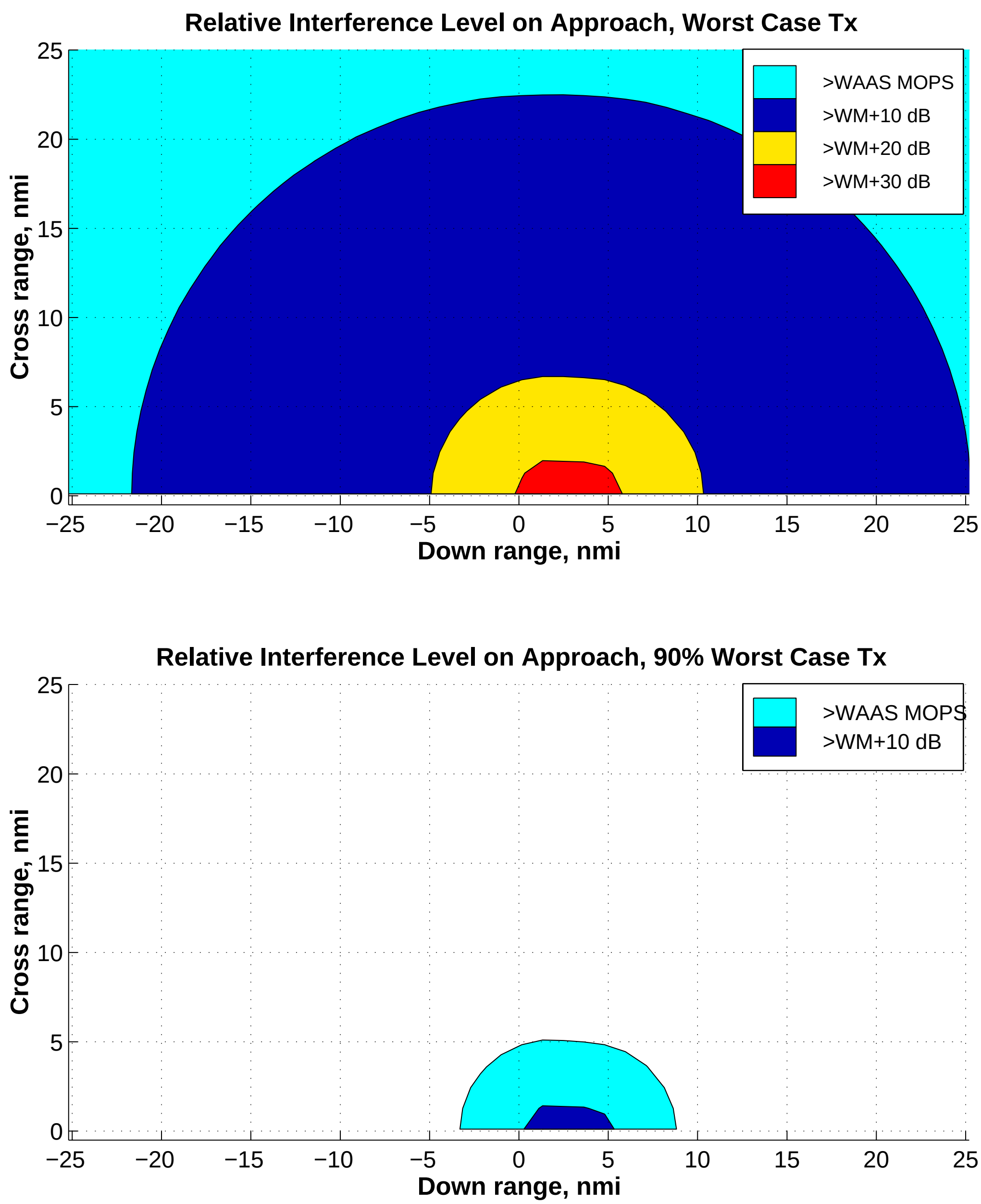

Figure I-7 Simulation Results for Television Interference

A combination of mitigation strategies would be the most effective way to eliminate the risk of television interference. By itself, transmitter location is not a practical solution. However, adding only a modest (10 dB) amount of interference suppression (through increasing the WAAS MOPS levels and/or adding interference suppression processing in the receiver) reduces the threat radius down to a range where siting restrictions are easily enforceable for most (say, 90 percent) of the transmitters. The highest power transmitters can be handled by RFI monitoring, both initially (during GPS approach certification) and after transmitter maintenance periods that can change out of band emissions levels (e.g., transmit tube replacement).

Note that the contours presented are based on a limited data set. Although they represent our best judgement with the available data, actual interference zones could be larger or smaller. However, it is clear that television harmonics can deny GPS to aircraft on approach. Fortunately, it is also clear that the risk of television interference can be made operationally insignificant by taking the simple mitigation steps described above.

I.4 REFERENCES

1. RTCA/DO-235, “Assessment of Radio Frequency Interference,” 27 January 1997.

2. RTCA/DO-119, “Potential Interference to Aircraft Electronic Equipment From Devices Carried Aboard,” 16 September 1988.

3. Volpe National Transportation Systems Center, et al, “Measurement of Television Interference to GPS,” 10 October 1995.

4. “ARTCC RF Environment Survey Summary,” Zeta Associates Z00425/95, September 1995.

5. Volpe National Transportation Systems Center, “VHF Transceiver Emissions in the GPS L1 Band,” 27 February 1995.

6. M. Johnson, “Interference to GNSS Receivers in the Civil Aviation Environment,” *Proceedings of ION GPS 94 Conference*, September 1994.

7. GPS Joint Program Office, “Report on GPS Issues with Inmarsat MSS Proposal,” JPO Web site, 2 November 1998.

8. RTCA/DO-229A, “Minimum Operational Performance Standards for Global Positioning System/Wide Area Augmentation System Airborne Equipment,” 8 June 1998.

9. Winer, B., et al., “GPS Receiver Laboratory RFI Tests”

10. Shallberg, K. W., et al., “WAAS Reference Receiver Measurement Performance and Tolerance in the Presence of RF Interference”

Appendix J

JAMMER DETECTION

A possible mitigation factor often cited against both unintentional and intentional interference is to provide a means for emitter detection and location. Because detection must be available at all times, it is assumed that the detection device would be located in the airport area at the highest possible location, most likely the airport tower.

A short study was conducted to determine the sensitivity of low-cost off-the-shelf devices. Assuming a 1-watt emitter, Figure J-1 plots the detection range and beamwidth of a detector versus detector antenna diameter. The figure shows that for reasonably sized antennas (<1 m), a low-power emitter can be detected to well over 100 miles. To maintain a reasonably sized beamwidth for location purposes, an antenna diameter of 0.5 meter could be selected. A complete system design was not pursued, but this example illustrates that technology is readily available to detect low power signals at a large distance.

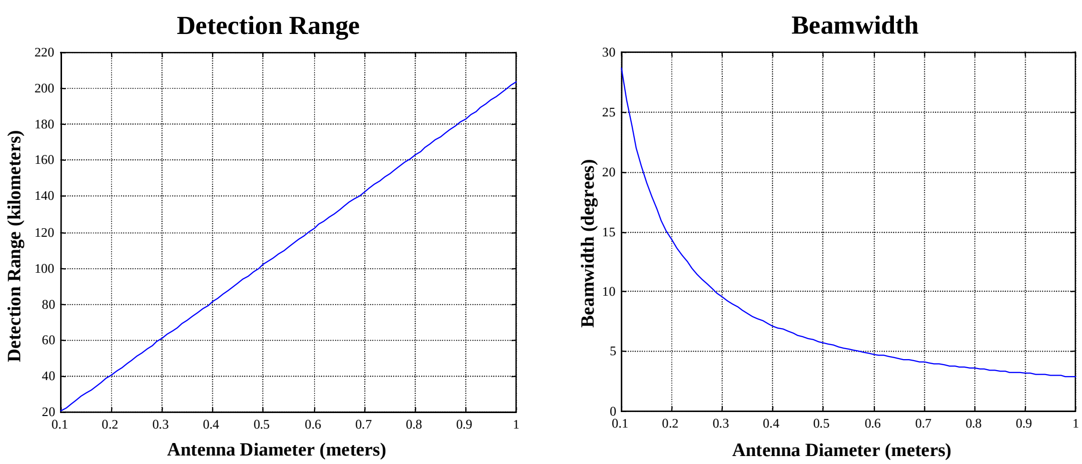

Figure J-1 Detector Sensitivity and Beamwidth for a 1-Watt Emitter

The principal limitation of the detector will be line-of-sight limit due to the radar horizon. Figure J-2 illustrates this problem. Assuming a detector at the top of the control tower, a ground emitter is seen out to a range of, for example, 17.4 nmi if the tower has a height of 200 feet. A ground emitter, on the other hand, could be at considerably greater distance and still be visible at the aircraft. For example, if the aircraft is at an initial approach altitude of 3000 feet and approximately 10 nmi from the tower, the ground emitter could be up to 67 nmi from the aircraft and thus undetected.

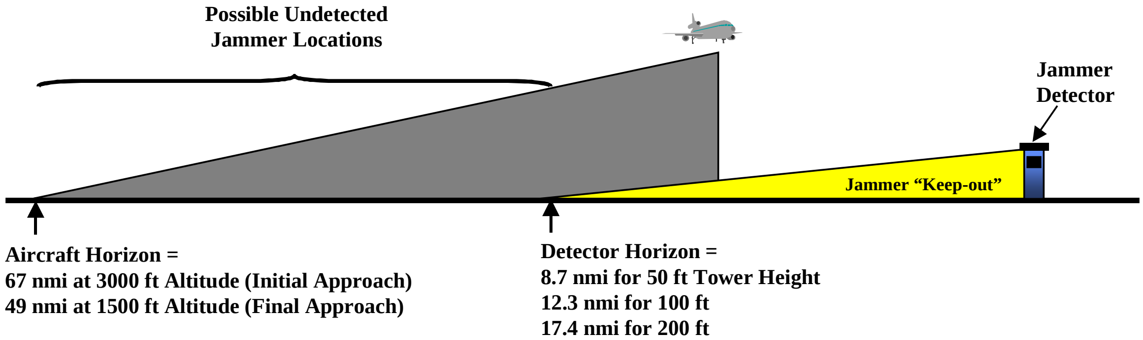

Figure J-2 Detector Line-of-Sight Limit

One conclusion of this study is that the most effective approach for emitter detection is to provide a means for aircraft to alert a central location that a GPS outage has occurred. If multiple aircraft raise the alert, it is clear an emitter is present. To locate the emitter will require an airborne device to triangulate on the source and thus locate it. This could be deployed, for example, by a helicopter or small aircraft provided by the appropriate government agency.

Appendix K

ANSWERS TO SOW STUDY QUESTIONS

The SOW for the GPS risk study included a set of questions that were to be answered by the study. While many of the questions are implicitly answered within the main report text, this appendix will attempt to provide brief direct responses to those questions. The questions addressed technical, operational, and institutional areas.

K.1 TECHNICAL

a. What are the strengths and weaknesses of the GPS control segment? What is being done to address weaknesses? Is there civil assistance and/or participation?

The GPS control segment is a very strong element of the current system, and the DOD is making investments in this area. It has excellent security characteristics, a well-disciplined and dedicated staff, and is tightly managed. It has been in operation since 1978 with a strong legacy of successful operation. The GPS JPO is currently pursuing several control segment improvements that will not only improve accuracy when selective availability is removed, but also improve robustness of the system. These improvements include improved filtering at the MCS, more frequent uploads, and the addition of six monitor stations that are presently operated by the National Imagery and Mapping Agency (NIMA). These new stations will provide greater visibility to the constellation and improved orbital error estimation due to both the increased number of stations and the location of stations at higher latitude. Addition of the satellite cross-link capabilities in the Autonomous Navigation (AUTONAV) program will make the GPS control segment even more robust. It would benefit from more process automation and quality monitoring capabilities. The GPS operators are sensitive to the civil needs, but the degree of civil participation should be improved with regard to policy development and is one of the key recommendations. Assuming civil requirements are clearly established, there should not be a strong need for assistance in daily operations.

b. What are the strengths and weaknesses of the GPS constellation? What is being done to address weaknesses? Is there civil assistance and/or participation?

The current constellation provides excellent coverage geometry for most applications. However, this study indicates that a 30-satellite GPS constellation might reduce the cost of planned GPS augmentations. DOD requirements are readily met with the existing constellation. Therefore, there is no DOD incentive to add satellites. Clearly, the push for more satellites would need to come from DOT, but there is no clear civil assistance or participation in this regard, nor is it clear how such assistance or participation would occur.

c. What are the strengths and weaknesses of the GPS signal(s) in space? Again, what correctives are DOD planning and has it had civil input?

The greatest weaknesses with GPS signals are the low power levels, use of the selective availability signal structure, and lack of a second civil frequency. There appears to be an understanding that all of these weaknesses are being addressed. However, a committed plan with specific details for implementing these improvements is lacking.

d. What GPS failure modes must augmentation systems address? Can they be adequately addressed to meet operational requirements for civil aviation? Are the present specifications for aviation augmentation of GPS sufficiently comprehensive to meet operational requirements?

The primary failure mode for GPS is the sudden loss of valid navigational signals. Complete loss of signals from a single satellite is seldom a problem because normally there are sufficient satellites to maintain acceptable service. In the event a single signal loss caused a problem, the condition would be evident and the pilot would be immediately alerted (i.e., it is not a loss of integrity) via the proposed WAAS/LAAS designs. Corrupted navigational signals could be a problem, but large sudden changes are readily detected within the navigation equipment. Moderate to small changes are detected within the WAAS and LAAS ground equipment and timely alerts can be provided. The current augmentations should be able to adequately address loss or corruption of GPS navigational signals. Current specifications for aviation augmentation are still being formulated; they may not yet be sufficiently comprehensive. It is the view of this study that the occurrence and nature of soft failures have not been adequately characterized and as a result, RAIM, WAAS, and LAAS designs may be overly conservative.

e. What are the certification criteria for aviation acceptance of GPS and GPS augmented services? Do these criteria have widespread understanding and acceptance?

The certification criteria for GPS and augmented GPS services have not been fully defined, but should be generally the same as those for any radio-navigation service. GPS signals provide measurements of distance and velocity along lines of sight to satellites at positions that are provided by a message included with the signals. The only difference between GPS positioning and other similar services is the movement of the signal reference positions. However, because satellite positions are known at the time of each position computation, the motion is transparent to the user. Although the GPS methodology may not be familiar to the civil aviation community and the integrity processes are different, it should not be difficult to gain widespread understanding and acceptance, if it is not already in place.

f. Is the FAA labor force sufficiently trained to transition to operation and maintenance of GPS augmented radio-navigation systems? If not, are plans in place for a smooth and expeditious transition? Are these clearly understood by FAA management, the labor force, and the affected unions?

It is unlikely that a substantial labor force is sufficiently trained for this transition, but there should be adequate time to provide the necessary training as the system evolves. However, there will be difficulties with a workforce that needs to divide its time between new and old systems. The transition plans reviewed during this study did not adequately address this area, and it is not apparent that these issues are clearly understood by all parties.

g. Is there indeed a valid threat to reliance on access to GPS for civil aviation? Can this threat be mitigated?

A large number of potential GPS vulnerabilities were investigated and for the most part are adequately addressed within the current DOD structure. It is clear that signal interference is the largest area of concern. With regard to unintentional interference, current FCC requirements do not ensure sufficient protection of GPS navigation signals. It is recommended that the current spectrum control practices be expanded to include protection for the GPS signals. Theoretical investigations suggest that television transmissions (particularly channel 23) should represent the greatest threat. However, there is little evidence of any significant current problems resulting from any offboard emitters. Most interference difficulties experienced thus far have been the result of onboard interference, and these are necessarily resolved during certification. While it is not possible to rule out future interference from offboard emitters, it should not be difficult to remedy such problems, and the introduction of a second civil frequency would further reduce concerns with regard to unintentional interference.

Intentional interference (i.e., jamming) is more problematic. Although there is a potential to jam civil GPS signals, the specific threats are difficult to define. Jamming will not itself pose a direct safety risk, but it can create considerable disruption. It will be necessary to define a specific civil threat environment before this issue can be adequately addressed. However, the jamming vulnerability can be reduced to a level that significantly decreases the threat, and some steps are absolutely required. First, enforcement procedures should be established as outlined in the recommendations of the report. Beyond that, numerous antenna and receiver techniques and navigation sensor integration techniques can further reduce this vulnerability.

Although there has been concern expressed about the ionosphere during peak solar activity periods, this problem has not been found to pose a significant threat. The higher refraction errors did not significantly change system availability. Scintillation effects are more difficult to characterize, but they are restricted to limited areas and directions.

h. Does DOD, DOT, and/or the FAA have a clear vision for a viable end-state satellite navigation capability? Has this vision been clearly articulated? Is there a strategy for achieving the desired end state?

It is fair to say that there is no clear *common* vision for a viable end-state satellite navigation capability. Certainly no such vision has been articulated; therefore, any current strategy must be suspect. However, those general plans that have been presented and some specific recommendations for the future do appear to be on the right track. What is sorely needed is a definitive national GPS plan and management commitment to establish a final configuration that is responsive to the full range of DOD and DOT requirements.

K.2 OPERATIONAL

a. What are the accepted ICAO and FAA definitions for navigation service requirements?

There appears to be a generally accepted set definitions for navigation service, although the difficulty attempting to gain a clear understanding of these definitions (they tended to change with time over the period of this study) might suggest there could still be some underlying disagreements. The precise definitions needed for consistent engineering analysis were not documented. The definitions used in this study were based on consultation with the FAA and guided by published definitions given in WAAS and LAAS documentation.

b. Have the definitions of navigation service been quantified? Are they captured in NAS-level system specifications?

Considerable time was devoted to a continual refinement of the navigation service criteria used in this study. The assessments of service required precise quantification, and that was finally achieved. However, it is not clear that there is universal agreement with regard to these quantified definitions. Because many specifications are still in the formative stage, it is not certain that they are yet captured.

c. What is the impact of radio-navigation on other air traffic control functions, i.e., the provision of surveillance and communications? Is there overlap? Does GPS and its augmentations (operational and technical) alter this relationship?

Apart from the different means for providing navigation input to the surveillance and communications functions, there has been no indication that current surveillance and communication functions would be altered. Both GPS augmentations will naturally add new communication requirements, but they are understood to be independent of current links. Initiatives are in place to exploit GPS for surveillance.

d. **Are there operational augmentations to GPS service that can satisfy NAS and user requirements? For example, can procedural steps be implemented to address GPS (or augmented GPS) shortcomings?**

Final assessment results did not assume any more operational constraints than those defined within the two augmentations (WAAS and LAAS). However, it is reasonable to expect that operational augmentations to further enhance system performance will evolve naturally. For example, time periods when GPS availability is relatively poor are highly predictable and could be used to modify operations.

e. **Have the DOT and FAA thoroughly assessed the projected growth in demand in NAS operations and factored in the impact of GPS and GPS-related services? Has the user community been consulted in these projections?**

The study did not assess projected growth in demand. However, this factor was noted as an important reason for establishing GPS services in planning documents. It is not clear to what extent the community has been consulted in these projections.

f. **Has the FAA assessed the steps necessary to introduce GPS and GPS-related services into the NAS? Is there a comprehensive set of operational requirements for implementation of GPS and GPS-related services? Have these requirements been properly planned for cost and schedule? Has the FAA operational community committed to these plans? Have NAS users?**

Certainly the FAA has preliminarily assessed the steps necessary for introducing GPS and GPS-related services into the NAS. However, until the planning has reached a greater level of detail and specificity, the assessment cannot be complete. Similarly, the current operational requirements cannot be considered comprehensive. Costs and schedules are not yet adequately planned and there is no large-scale commitment.

g. **In light of the study recommendations, has the FAA thoroughly planned for the impact of GPS and GPS-related services on the present inventory of radio-navigation aids? Are planning horizons adequate? Are they consistent with the budgetary cycle? Have user fiscal constraints been considered?**

These questions presuppose a level of planning that has not yet been apparent. Indeed, the need for a more complete and detailed plan is a primary recommendation. The study has only been able to address whether an improved GPS and the currently defined augmentations of GPS can meet the quantitative requirements established as the basis for the study.

h. **Have operational benefits from GPS and GPS-related services been captured? Has user input been incorporated? Are they valid and realistic? Are they quantified?**

This study was primarily concerned with ensuring that current capabilities could be maintained with a GPS-based system. Most of the benefits would be expected to apply to service extensions or more cost-effective operations, and these were not directly considered. However, there does appear to be a valid expectation that qualitative operational benefits will be achieved.

K.3 INSTITUTIONAL

a. What are the arrangements for DOD and DOT day-to-day oversight, control, and management of GPS?

While some general policy guidance has been established, no procedures suitable to the management of a truly national GPS seem to exist.

b. (question removed from SOW)

c. What is the U.S. Government's mechanism for addressing navigation, positioning, and timing requirements for all users and modes of transportation?

There is no definition of all users and modes of transportation to be unambiguously addressed. In any event, there is no clearly defined mechanism for addressing the full range of requirements.

d. How does the U.S. Government address international issues regarding GPS and other satellite navigation systems and augmentations? Is U.S. policy consistent in this regard? Is it timely and thoroughly coordinated?

The Government has made GPS available for global civil use. It cannot assume the responsibility for meeting operational service requirements for other nations, but it has not objected to making a significant portion of its required civil GPS services available. Naturally, the Government would object to alternative system concepts that would interfere with its intended uses for GPS, but it would not otherwise object to any other legitimate satellite navigation systems and augmentations established by other nations. Certainly, the Government would prefer that the alternatives instituted by other nations would be compatible with U.S. GPS avionics (i.e., U.S. aircraft could be supported in that airspace without the need for additional equipment). The Government has already indicated its willingness to support international cooperation with regard to the use of satellite navigation systems and augmentations. U.S. policy is consistent in this regard. It is difficult to assess timeliness and thorough coordination without reference to specific issues.

e. (question removed from SOW)

f. What is DOD policy regarding civil access to GPS performance monitoring, anticipated GPS failure modes and their effects, and plans for service improvement?

DOD policy regarding failure modes and their effects is sufficient to protect DOD applications. A key recommendation of this study is to establish a coordinated DOD/DOT policy to also protect the joint applications. This is just one of the details that must be worked out to implement a joint plan. Service improvements are already being identified, but the details associated with these are also subject to a committed U.S. Government plan.

g. (question removed from SOW)

h. Are DOT and FAA properly organized to address GPS issues – institutional, operational, and technical?

They are certainly more able to address these issues than anyone else. They have enlisted external expertise to help fill those GPS-unique technological areas where needed, and they are reaching out to the user community for additional support. They probably will need to extend these efforts and increase the level of coordination with the DOD before an acceptable national plan can be developed.

i. What is U.S. Government's long-term commitment to sustainment (and improvement) of GPS? Are there competing military technologies that could draw resources from a commitment to GPS?

The DOD is very committed to maintaining and improving GPS to meet its current and projected needs. Due to the increasing dependence of military systems on the GPS, it is expected that no competing military technology will be allowed to draw down this commitment. However, it must be recognized that the NAS requirements addressed in this study will require some capabilities that are not central to the DOD requirements. Therefore, an additional commitment from the Government will be needed to ensure these are adequately maintained and improved.